Development of Surface Plasmon Resonance Biosensor Using Self-Assembled Monolayer

A thesis submitted
for
the degree of Doctor of Philosophy

by

Suherman

in the

Division of Environmental Materials Science
Graduate School of Environmental Science
HOKKAIDO UNIVERSITY
February 2015

Acknowledgement

Bismillahirrahmaannirrahiim,

First of all, I would like to express my best gratitude to my supervisor Associate Professor Toshikazu Kawaguchi for the remarkable support of my Ph.D study and research, for his best guidance, for his patience, motivation, enthusiasm, immense knowledge and all kind of help during my Ph.D study. This expression also addresses to Kawaguchi sensei kindness to my family during our stay in Sapporo for 3,5 years.

My sincere thanks also go to Professor Katsuaki Shimazu and Professor Ichizo Yagi for all support, facilitation and opportunities for working in Shimazu/Yagi laboratory with comfortable environments.

Besides my advisor, I would like to thank to the rest of my thesis committee members: Professor Sunitz Tanaka, Professor Masatoshi Osawa, and Professor Ichizo Yagi for their encouragement, positive opinions, insightful comments, hard questions, and their appreciation to my works.

I would like to thank to Dr. Kou Nakata and Dr. Masaru Kato, Assistant professors for their support for me throughout my Ph.D works, and for their informed guidance and advice during laboratory activities. They always offered me good advice and brought previously unrecognized aspects of each situation to my attention.

I warmly thank to the members of Shimazu/Yagi group for their kind helps and cooperation during my work, also for all assistances for my family during their stay in Sapporo. Also special thanks to all Indonesian community living in Sapporo for

wonderful friendship and togetherness.

My highest appreciation goes to the HSF (Hitachi Scholarship Foundation) for their supports and facilitation during Ph.D course, also to USHIO INC. and Yabegawa Electric Industry Co. Ltd. for remarkable cooperation.

Last but not least, I would like to thank to my family: my beloved wife Rizki Suherman and our incredible kids Aziz, Lila, Aura and Yukiko, for all spirits and compassions. Finally, my greatest regards to Almighty Allah SWT for bestowing upon me the courage and patience to face the complexities of life and complete this project successfully. *Alhamdulillah.*

Sapporo

February 4, 2015

Suherman

Table of contents

Title: Development of Surface Plasmon Resonance Biosensor Using Self-Assembled Monolayer

Chapter 1: Introduction **7**

1.1 Recent environmental challenge 7

1.2 Biosensor for environmental monitoring 8

1.2.1 Biosensor classification 9

1.2.2 Biosensors for ß-agonist detection 11

1.3 Surface plasmon resonance biosensor 16

1.3.1 Advantages of surface plasmon resonance sensor 17

1.3.2 Summary of the previous study in the detection of ß-agonist 17

1.4 Immunoassay format 20

1.4.1 Direct assay 21

1.4.2 Sandwich assay 22

1.4.3 Competitive assay 23

1.4.4 Indirect competitive inhibition assay 23

1.5 Objective and outline of the thesis 25

1.5.1 Objective of the thesis 25

1.5.2 Outline of the thesis 29

1.6 References 31

Chapter 2: Experimental **46**

2.1 Materials and chemicals 46

2.2 Surface Plasmon Resonance (SPR) 47

2.2.1 SPR configuration 47

2.2.2 General principle of SPR 49

2.3 Electrochemical measurements 54

2.4 X-ray Photoelectron Spectroscopy 56

2.5 Scanning Tunneling Microscopy (STM) 58

2.6 Preparation of Au substrates 59

2.7 References 60

Chapter 3: Surface coverage effect on sensitivity of detection 62

3.1 Introduction 62

3.2 Fabrication of the sensor surface 64

3.3 Results and Discussion 66

3.3.1 Characterization of self-assembled monolayer 66

3.3.2 Detection of clenbuterol 71

3.3.3 Kinetics analysis 73

3.3.3.1 Langmuir adsorption isotherm 73

3.3.3.2 Indirect competitive inhibition immunoassay 75

3.4 Summary 77

3.5 References 78

Chapter 4: Effect of alkanethiol molecular structure on sensitivity of SPR sensor 84

4.1 Introduction 84

4.2 Fabrication of the sensor surface 87

4.3 Immunoassay 89

4.4 Results and discussion 89

4.4.1 Characterization of the various alkanethiol monolayers 89

4.4.2 Detection of clenbuterol 92

4.4.3 Kinetic analysis 93

4.5 Summary 95

4.6 References 96

Chapter 5: Highly selective and sensitive detection of ractopamine and salbutamol using SPR sensor 100

5.1 Introduction 100
5.2 Fabrication of the sensor surfaces 102
5.3 Immunoassay 104
5.4 Results and discussion 104
5.4.1 Detection of ß-agonist compounds 104
5.4.2 Quantitative analysis 107
5.4.3 Selectivity study 109
5.5 Summary 111
5.6 References 112
Chapter 6: Summary and conclusion **115**
6.1 Summary and conclusion 115

Chapter 1

Introduction

1.1 Recent environmental challenge

Environmental problems are one of major global challenges faced by human beings beside energy shortage [1]. Pollution, climate change, global warming, deforestation, overpopulation, water conservation, and food borne illnesses are common environmental problems [3–11] in all parts of the world, and the victims in terms of human life and suffering is enormous. World Health Organization (WHO) reported that contaminated food causes to 1.5 billion cases of diarrhea in children each year, resulting in more than three million premature deaths [12]. Those deaths and illnesses are shared by both developed and developing nations. Furthermore, in the United States, the Centers for Disease Control and Prevention (CDC) reported that about 48 millions of US citizen (roughly one in six people in United State) get sick from eating contaminated food every year, as well as 325,000 hospitalizations, and 5,000 deaths [13].

The problems in food safety also create significant burden on the economy [14]. Consumers lost their expenses for medical treatment, legal, and other expenses including the absence at work and school. For miserable consumers, the loss of income due to food borne illness can stimulate the cycle of poverty. The contaminated food causes chronic diseases can be even more damaging when the medical costs and lost wages increase. In developing countries, these foodborne diseases already overburdened to the people and poorly funded by healthcare

systems.

There are several issues in food safety [15–16]:

- The use of chemicals in agricultural and animal husbandry (pesticides, ß-agonists etc)
- Untreated or less treated wastewater
- The presence of sewage and animal manure on crops
- Infrequently of food inspection
- Scarcity of infrastructures to maintain the quality of food
- Less hygiene of water supplies

To answer the major environmental challenges, nanotechnology exploits nanoscale materials offered from the promising solution by new discovery, design, and novel utilization. One of the important uses of nanomaterials in practical application is related to biosensors. Since environmental policy demands assessment and monitoring of the risks in food processing activities, raw materials, and farming [17], biosensors development is becoming important sector and achieve great attention from researchers to ensure the environmental quality such as food safety in all aspects.

1.2 Biosensor for environmental monitoring

Concern about environmental pollution controls manifest into initiative and legislative programs. These actions parallel with the increasing of scientific and social concern in environmental issues [18–21]. The necessity of tools for

environmental monitoring has encouraged the researchers to develop new technologies and methodologies. From this background, biosensors arise as an analytical tool answering the requirement in environmental assessments.

1.2.1 Biosensors classification

Biosensor is subgroup of chemical sensors in which analyte detection is conducted by biological mechanism [22–24]. The International Union of Pure and Applied Chemistry (IUPAC) defines biosensor as a self-contained integrated device that is capable of providing specific quantitative or semi-quantitative analytical information using a biological recognition element (biochemical receptor), which is retained in direct spatial contact with the transduction element [24–25]. When the transducer was separated from analytical system, biosensors could be distinguished from bioassays [26-28]. Up to date, biosensors are being developed in wide applications including drug discovery, medical applications, environmental monitoring, food safety, security, and military [29-40].

According to bioreceptor element involved in the biological recognition process, biosensors are classified as whole-cells of microorganisms, plants or animal tissues, and molecular fragments. Considering the physicochemical transducer used, biosensors can be named as mechanical, optical, and electrochemical transducers. Electrochemical transducer monitors a change in the measured current at a fixed applied bias (amperometric), a change in the measured voltage between the electrodes (potentiometric), and a change in the ability to transport charge (impedimetric). The optical sensors generally measure fluorescence, absorbance and reflectance, and surface plasmon resonance or changes in light reflectivity. On other

hand, mechanical transducers can be divided based on piezoelectric, surface acoustic wave and cantieliver resonance frequency [41].

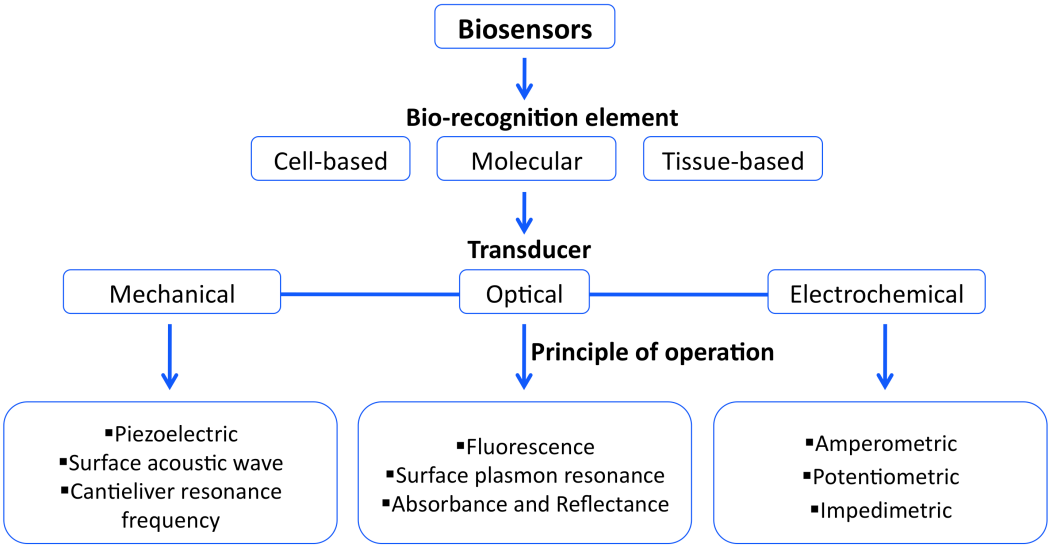

Figure 1.1 Scheme of biosensors classification based on principles of operation [41].

Several advantages offered by biosensors upon conventional analytical techniques are ability to measure pollutants in complex matrices, portability, miniaturization, on-site measurements, and simple preparation [42-44]. Biosensors can be used by authorities and industries for routine assessment of environmental samples because their biological basis is quiet ideal for toxicological measurement [45–47]. However, most of biosensors system cannot compete yet with conventional analytical methods in terms of accuracy and reproducibility. Therefore, biosensors are used for monitoring in environmental samples, while conventional techniques are utilized for only measure the concentrations [48].

1.2.2 Biosensors for ß-agonist detection

Some countries in the world still import food product such as meat from other countries due to limited self-sufficiency. In other hand, the inspection rate to check the safety and quality of imported food product is very limited. Figure 1.2-a shows the self-sufficiency of food product from various countries in the world [49]. Figure 1.2-b also depicts the inspection rate conducted in Japan to check the safety and quality of imported food product [50].

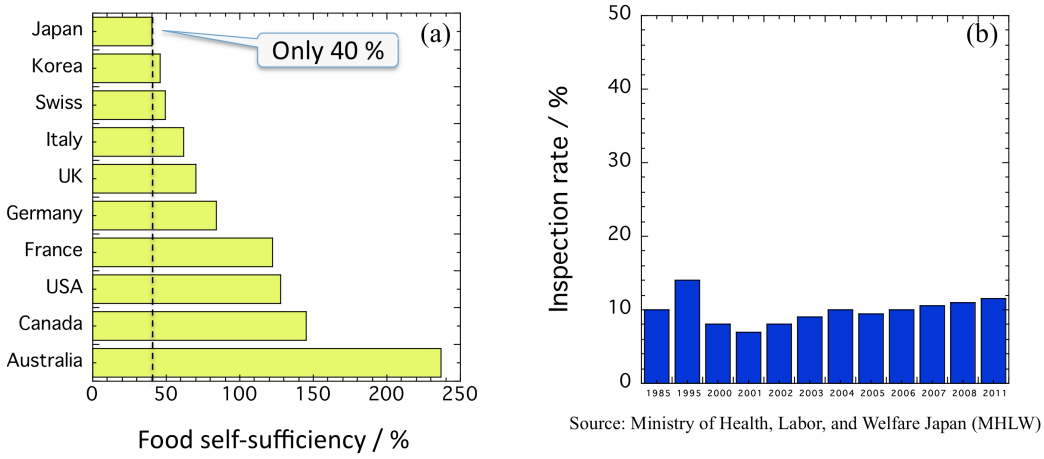

Figure 1.2 (a) Japan food sufficiency compare to other countries [49]; (b) inspection rate for imported food product in Japan [50].

Toxic compounds are found in food product such as beta-adrenergic agonists (ß-agonists). ß-agonists are member of sympathomimetic agents and activate over the beta adrenoceptors [51]. Beta agonist ligands serve as chemical mediators for conveying the nerve impulses to effectors organ in the lungs, heart, and smooth muscle tissue [52]. Based on position in human tissues where the ß-agonists activated, these compounds are divided into [53–54]:

- β1 = dobutamine, isoproterenol, xamoterol, epinephrine.
- β2 = clenbuterol, salbutamol, levosalbutamol, fenoterol, formoterol, isoprotenerol, epinephrine, metaprotenerol, salmeterol, terbutaline, isoetarine, pirbuterol, procaterol, ritodrine.
- β3 = amibegron, mirabegron, solabegron, etc.
- Undetermined β-agonist = ractopamine, arbutamine, cimaterol, zilpaterol, etc.

Among β-Agonists, clenbuterol, ractopamine, and salbutamol are commonly used in animal husbandry (Figure 1.3).

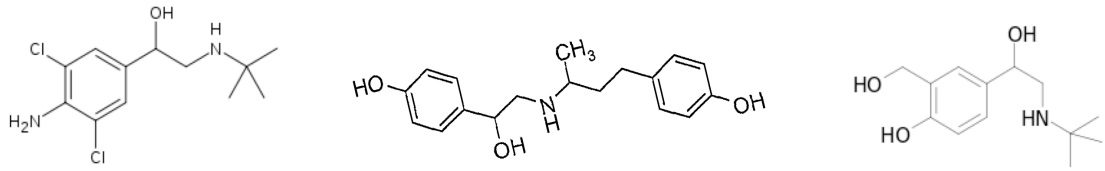

Clenbuterol Ractopamine Salbutamol

Figure 1.3 chemical structures of ß-agonists as target compound

β-Agonists are usually used as drugs for the treatment of respiratory diseases and asthma [51, 52, 55–58]. However, due to their potential roles in reducing animal fat levels and increasing the amount of muscling in livestock, β-agonists are used in animals as growth promoters to increase the daily weight gain [59–66]. β-agonists compounds can be easily stored in human tissues after meat consumption, and result in many serious health problems with symptoms such as palpitations, tremors and tachipnoea [67–69]. Recently, more than 150 countries have strictly banned the use of β-agonists in stockbreeding, including China, Japan and Europe countries, due to

their negative side effects in the human body [54, 70–72]. In addition, it was reported that from 1998 to 2013 more than 1700 people were poisoned by these β-agonists (Sichuan Pork Trade Chamber of Commerce in China).

Recently, the doping issue becomes a massive topic in the world competitions such as World Cup Soccer, Olympics game and Tour de France cycling. In January 2013, World was shocked by the confession of seven times Tour de France champion-Lance Armstrong regarding his usage of banned performance-enhancing drugs throughout much of his cycling career at a broadcast interview with Oprah Winfrey. Also the doping case is still high in the multi even Olympics [73], and interrupt the fairness of the competition (Summer and Winter, see the Figure 1.4). Since then, the attention to this β-adrenergic agonist compound has intensified due to easily uptake and deposit in the human body during daily meat consumption. Therefore it is necessary to develop a reliable detection method with high sensitivity and rapid detection time. Inspection services for food safety are particularly interested in the three main β-agonists, i.e., clenbuterol, ractopamine and salbutamol.

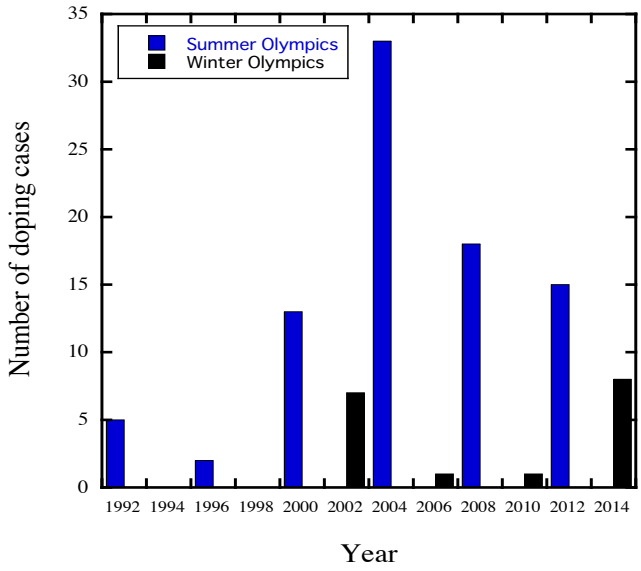

Figure 1.4 Number of doping cases in Olympics games [73]

Up to date, the development of an assay for the detection of ß-agonist compounds have been reported as an alternative to the classical method such as ELISA test [74–75], liquid chromatography [76–77], liquid chromatography/tandem mass spectrometry [78–79], electrophoresis [81–82], and electrochemistry [83].

a. ELISA test [74–75]

ELISA (enzyme-linked immunosorbent assay) is laboratory technique that utilizes color change to identify the analyte. The amount of analyte present in the sample is related to colored end product. ELISA is simple to perform and large number of samples can be managed in one series experiment. However, non-specific bonding of antigen or antibody to the plate leads falsely result, also inaccuracy of color strength for long time assessment.

b. Liquid chromatography [76–77]

Liquid chromatography is analytical method to separate analytes in the sample based on their interaction to the stationary phase and mobile phase. Even though this method is applicable to any soluble compound in liquid phase, it consumes relatively long time in analysis.

c. Liquid chromatography tandem mass spectrometry (LC-MS) [78–79]

LC-MS is liquid chromatography that couple mass spectrometry as a detector. This technique can improve the specificity and reproducibility due to MS analyzer. However, most of chromatographic methods are less appropriate for onsite usage due to time consuming and elaborate sample preparation [80].

d. Electrophoresis [80–81]

Electrophoresis usually employs gel as a media (gel-electrophoresis). This method is used to separate the analyte (DNA, proteins, etc.) based on physical characteristic such as molecular size. Electrophoresis is popular for inexpensive method and very simple to run. But, only high molecular weight analyte can be analyzed by this method; also difficult to be automated.

e. Electrochemistry [83]

In electrochemistry method, electrical current is generated due to chemical reaction occurrence. Electrochemistry is easy to handle, but inaccurate electrode response possible to happen due to long time analysis and quality degradation of electrolyte solution.

Table 1.1 summarizes the sensitivity of β-agonist detection in available commercial methods. Since the maximum residues limit of β-agonists is 10 ppb–50 ppb in most country in the world, the requirement of detection limit in commercial

sensor is at least 0.1 ppb [84–85]. Therefore, the development of practical biosensor to create highly sensitive sensing tools is required.

Table 1.1 Commercial methods for detection of β-agonists [74–83].

Method	Elisa test	LC-FID	LC-MS	Electrophoresis	Electrochemistry
Sensitivity	0.5 – 100 ppb	1-25 ppb	1-100 ppb	0.5-10 ppb	10 ppb
References	Shelver and Smith (J. Agri. Food. Chem., 2004)	E. Shishani et al. (Anal. Chim. Acta, 2003)	Juan et al. (J. Chromatogr. A, 2010)	Ji et al. (Talanta, 2006)	Fan et al. (J. Mol. Liq., 2012)
	Sheu et al. (Anal. Chim. Acta, 2009)	Zhang et al. (J. Chromatogr. Sci., 2004)	Wu et al. (J. Pharmacol. Toxicol. Methods, 2014)	Zhou et al. (J. Chromatogr. B, 2007)	

1.3 Surface plasmon resonance biosensor

Surface plasmon resonance (SPR) is an optical transducer based on surface plasmon phenomena. SPR can measure the refractive index changes occurring at the interface caused by the binding of target analytes with biointerfacial materials (1 mdeg ~ 10 RU ~ 1 ng/cm^2). In the SPR system used in this study, LOD reaches up to 30 pg/cm^2 (0.3 RU). The monitoring of the biomolecules interaction by SPR could be conducted without the need of labeling, and it was by exploiting the interfacial refractive index changes associated with any affinity binding interaction. SPR takes an important role in the research from first introduction in 1990s [86–88] in the characterization of biomaterial, drug discovery interaction based on kinetic study, and various investigations of chemical and biological substances [89–93]. SPR is used to study the protein interaction [94–95], kinetics parameters including association, dissociation, and affinity constants [96–101].

1.3.1 Advantages of surface plasmon resonance sensor

SPR-based biosensor is established used in food industry for screening the drug residues and quantify the vitamins in food products [102–103]. SPR biosensor has several advantages compare to other analytical techniques such as [43, 104–116]:

- High sensitivity
- Label-free detection
- Rapid and real-time analysis (possible to attach the flow channels)
- Immunoassay provides high selectivity.
- Relatively simple procedures
- Low amount of sample solution
- Miniaturization.

1.3.2 Summary of the previous study in the detection of ß-agonist

Interest in the development and application of SPR immunosensors is growing rapidly for decades [117–118]. The most important achievement obtained by SPR based immunosensors is the capability to detect small molecule in complex matrices with highly sensitive and highly specific results [119–123]. It was reported that SPR sensor can be used for the detection of ß-agonist compounds [34, 116, 124–125]. To date, several sensor surfaces fabrications have been introduced as illustrated in Figure 1.5:

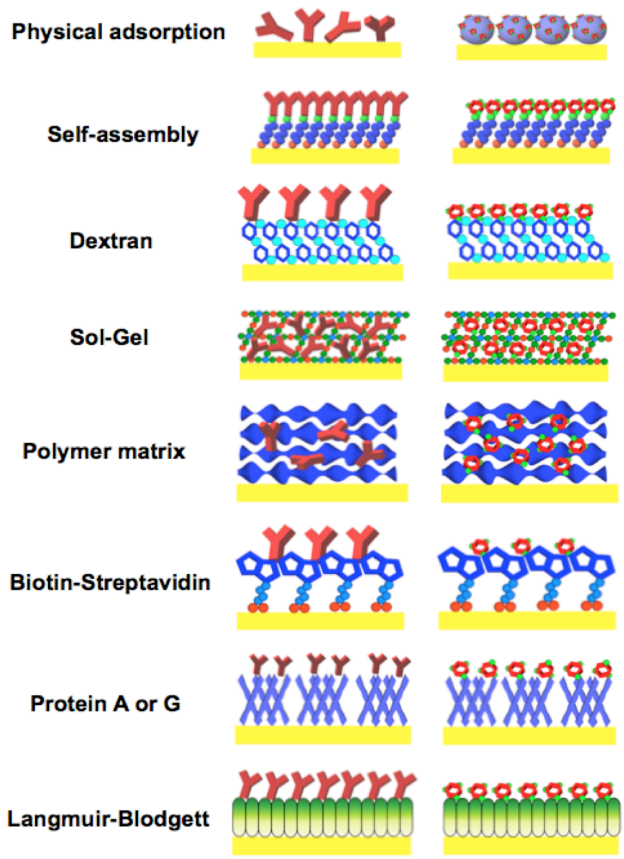

Figure 1.5 Previous studies of sensor surface fabrication method [126].

a. Physical adsorption [119, 127–128]

The adsorption of biological component such as protein conjugate is performed based on electrostatic, hydrophobic, hydrogen binding and Van der Waals interaction. By using the physical adsorption method, immunosensor surface is possible to be regenerated without any chemical modification.

b. Self-assembly [129–132]

Self-assembly is immobilization method of biological component based on covalent binding to the surface. The formation of Au-thiol monolayer is commonly used in the self-assembly method. The formation of monolayer on the Au surface by self-assembly is achieved by simply immersing of Au substrates in a thiol solution or

by the flow of the thiol solution over the gold for several hours.

c. Dextran platform [133–135]

Large surface area with high possibility of biomolecule immobilization can be achieved using carboxymethyl (CM) dextran matrix. Even though nonspecific adsorption is challenged, this method is very popular for interfacial immobilization layers. Sticky surface is achieved after the formation of dextran platform.

d. Sol-gel [136–138]

Sol-gel process is formed at low temperature from inorganic silicate matrices. Then, biological components entrapment can be performed by this sol-gel formation. The degree of native properties of biomolecules is determined during the biomolecules interaction. This method gives advantages such as simple process, retention of the activity, and high loading of biomolecules.

e. Polymer matrix [139–142]

There are two kinds of polymer matrix namely hydrophilic polymers and hydrophobic polymers. Using photo and thermal initiated polymerization, polymer networks are synthesized. Molecularly imprinted polymer (MIP) achieved great attention because its similarity to antibody in the biological activities.

f. Biotin–streptavidin [143–145]

Biotin is important enzymes cofactor with molecular weight of 244 Da that present in various plant and animal product as protein-bound formation. Streptavidin is tetrameric protein with molecular weight of 60 kDa and its tightly binding to biotin. The biotin-streptavidin interaction reveals high reproducibility, larger binding capacity, and chemical resistance.

g. Protein A or G [146–148]

Protein A is a single polypeptide chain with 40-60 kDa of molecular weight and 4-5 IgG of binding domains. Protein G can be achieved from *Streptococcus sp* as cell wall protein with 45-65 kDa of molecular weight and 2-3 of binding domains. By using protein A and G of sensor surface for the immobilization of antibody, SPR based immunosensor can be stable, sterically accessible, and uniformly achieved.

h. Langmuir-Blodgett (LB) film [149–151]

The formation of LB membrane employs the amphiphilic molecules (e.g. fatty acids, phospholipids) located at the air–water interface onto a solid substrate by immersing the substrate into liquid surface covered by monolayer. The difficulties in reproducibility and complexity lead the limitation of LB membrane in SPR immunoassay.

Among these sensor surface fabrication methods mentioned above, self-assembly shows great advantages in surface stability, simple preparation, and highly oriented of monolayer formation.

1.4 Immunoassay format

Considering the biochemical reaction occurrences, immunoassay techniques are divided into two fundamental classifications, namely homogeneous and heterogeneous [43, 152–153]. Different with homogeneous assay where biochemical reaction takes place entirely in the solution part, in heterogeneous immunoassays, the binding interaction of antibody or antigen with target analyte takes place at the interface. Most of the SPR immunoassays exploit heterogeneous formats, because SPR response is selective to surface-bound immunoreactions at transducer surface.

In addition, heterogeneous format also shows further advantages such as rapid detection time, high surface area/volume ratios, and significant signal intensities [152–153].

In heterogeneous format, SPR immunoassays are further classified due to choice methodology of detection as direct assay, sandwich assay, competitive assay, and indirect competitive inhibition assay (Figure 1.6) [43].

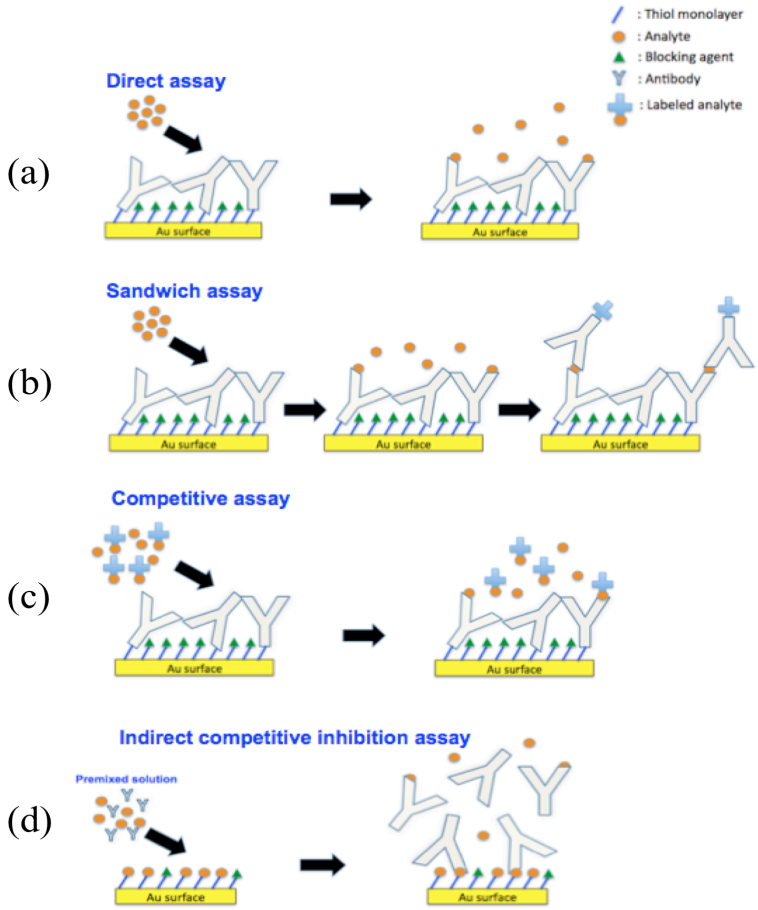

Figure 1.6 Immunoassay format

1.4.1. Direct assay [154–159].

In the direct assay (Figure 1.6-a), sensor surface is constructed with bio-recognition elements (antibodies) on the sensor surface. SPR monitors the resonance

angle change due to the binding interaction between antibody immobilized sensor surface and the analyte. It was reported that concentration of analyte was almost proportional to measured resonance angle changes. This assay is appropriate for large molecule target analyte (MW>10 kDa) due to insufficient refractive index change caused by small molecules. In case of small size analytes as target detection, the direct assay employs labeled-analytes compound based on fluorescence detection.

By using direct assay, the limit of the detection in the previous reports was ranging from 1 ppb–100 ppm. [43, 155–158].

1.4.2. Sandwich assay [160–167]

In the sandwich assay (Figure 1.6-b), the analyte connecting/sandwiching between recognition molecule 1 and recognition molecule 2 with a signaling marker. Here, antibodies usually used as recognition molecule. So, analyte first will bound to the primary antibody immobilized on the surface (Ab1), and then signaling-labeled secondary antibody (Ab2) is bound to the analyte, forming a sandwich-like configuration. Concentration of the analyte is proportional to the signaling intensity of the immunocomplex derived from the label marked with Ab2. Sandwich assay is employed for large molecules detection (>5000 Da) due to simultaneously binding of analyte with two antibodies. For labeling the secondary antibody, chemiluminescence and fluorescence methods are preferable to use [168–169].

1.4.3 Competitive assay [170–179]

In competitive assay format, mixed solution consisting of analyte and labeled-analyte is introduced to the measurement system (Figure 1.6-c). Sensor surface is antibody immobilized on the surface. In case of unlabeled analyte is introduced after the labeled-analyte injection, this procedure known as displacement method [175, 178–179]. Fluorescence or chemiluminescence method is employed to measure the displaced labeled-analyte [176–177].

1.4.4 Indirect competitive inhibition assay [36, 43, 70, 180–186]

Since the most target analytes including ß-agonist compound have a low molecular weight (around 300 Da), all the above immunoassay formats have great challenges. The indirect competitive immunoassay offered the solution by utilizing the immunosurface modified with antigen instead of antibody. Thus, SPR monitors the signal due to the binding heavyweight antibody onto the antigen immobilized on the sensor surface.

Figure 1.6-d shows the scheme of indirect competitive inhibition immunoassay. In this assay, the low molecular weight analyte (antigen) is firstly immobilized on the sensor surface. The immobilization of antigen is carried out by an appropriate monolayer or analyte–carrier proteins (such as BSA or HRP) conjugate. Then, premixed solution (analyte and antibody) is injected to the sensor surface. This process ensures that the signal response of the mass transducer is large, because the antibody, rather than the antigen, is being measured. The measured binding response is inversely proportional to the concentration of analyte in

premixed solution.

Table 1.2 Sensitivity of target compounds using different sensor surface fabrication and immunoassay formats [36, 122–123, 154–159].

Analyte	Application	Assay format	LOD	Fabrication method	References
Methamphetamine	Drug analysis	Direct	20 ppb-100 ppm	Physical adsorption	Miura et al. (Sens. Actuators B. 13-14. 1993)
TNP	Pollutant monitoring		3 ppb		Sakai et al. (Sens. Mater. 15. 2003)
Insulin growth	Cancer diagnosis	Direct	4-100 ppb	Embedding in polymer or membrane	Guidi et al. (Biosens. Bioelectron. 16. 2001)
Hemoglobin	Marker proteins		100ppb-20 ppm		Sonezaki et al. (J. Imm. Method 238. 2000)
TNT	Security control	Direct	200ppb-10 ppm	Sol-gel entrapment	Lan et al. (Chem. Mater. 12. 2000)
Hepatitis B	Medical diagnosis		2-360 ppb		Liang et al. (Anal. Chim. Acta 534. 2005)
NO_2	Environmental monitoring	Direct	100 ppm	Langmuir-Blodgett deposition	Kato et al. (Coll. Surf. A. 198-200. 2002)
Protein G	Marker proteins		2-5 ppb		Oh et al. (Mater. Sci. Eng. C. 24. 2004)
BaP	Endocrine diagnosis	**Indirect competitive inhibition**	**50 ppt**	**Self-assembly monolayer**	Shankaran et al. (Sens. Actuators B. 114. 2006)
DNA	Clinical diagnosis		**50-100 ppt**		Kim et al. (Sens. Actuators B. 115. 2006)
TNT	Security control		**10 ppt -100 ppb**		Kawaguchi et al. (Sens. Actuators B. 133, 2008)

Table 1.2 shows some combination between sensor surface fabrication method and immunoassay format. The achieved number of sensitivity detection was ranging from ppt to ppm level. Considering that future practical demand such as doping screening in sports and custom department for food import products requires high sensitive method up to ppt level, so the combination of self-assembled monolayer in sensor surface fabrication and indirect competitive inhibition method produces relatively high sensitivity in the detection [36, 122–123). Therefore, this combination will be adopted in this study. Furthermore, the kinetics aspect related the sensitivity of the detection and sensor surface control also did not reported yet.

In the indirect competitive inhibition method, typically sigmoid curve is obtained as illustrated in Figure 1.7.

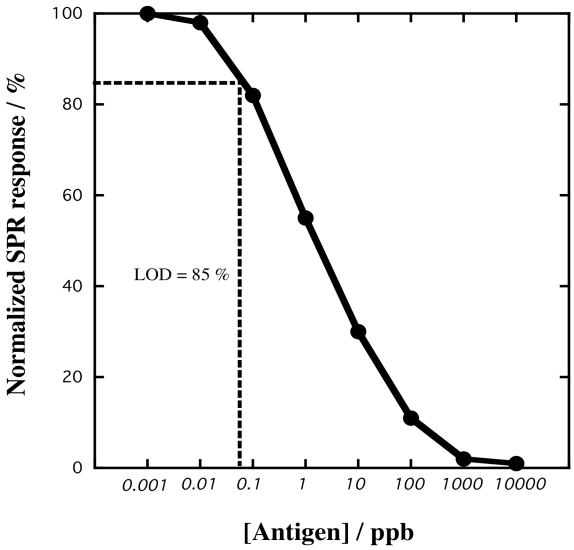

Figure 1.7 SPR sigmoid-type curve for indirect competitive inhibition assay.

From this sigmoid curve, the limit of detection (LOD) value can be achieved. LOD value can be defined as the concentration of the species being measured which gives a minimum detectable difference signal (reduction in activity) that is equal to 2 or 3 standard deviations (S.D.) of the mean response of the blank samples (zero concentration of the inhibitor) [187]. To determine the limit of detection (LOD) value, it is generally corresponds to 85% of residual activity, that is equal to 15% of inhibition [43, 187].

1.5 Objective and outline of the thesis

1.5.1 Objective of the thesis

Recently, the development of analytical methods for environmental assessments and monitoring increasingly demanded in many sectors due to economic, safety reasons, etc. Biosensor utilizes nano-technology attributed with reliability, selectivity, sensitivity, rapid process, and inexpensive. It is promising

devices to answer recent problem in environmental assurance. However, to achieve robust biosensors criteria, the accurate design and control of nano-interface properties is considering as an important factor in the fields of biosensing and surface engineering. The stable integration of a biological recognition element on a transducing substrate surface is the most important step in the creation of a high-functioning biosensor surface. For biosensors development, several works had been reported, such as sensor surfaces immobilization technique, format of the detection method, and data analysis.

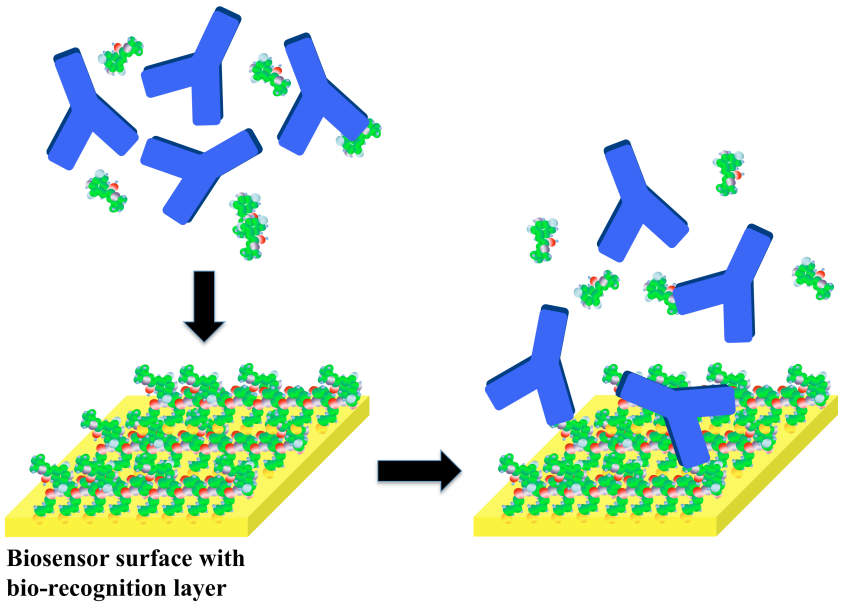

Figure 1.8 Scheme of the bio-recognition element onto Au surface and detection of target analyte.

In biosensors, a bio-receptor molecule is immobilized in a suitable matrix to form a bio-recognition layer, which is then placed in the immediate vicinity of a transducer. Thus, immobilization enables reuse of biomolecules and enhances their

local concentration near the sensor probe. Among the interfacial bio-recognition molecules, self-assembled monolayers (SAMs) achieved great attention due to flexibility, convenient and simplicity of the system. The preparation of SAM is straightforward; the immersion of an appropriate substrate into a solution containing a functionalized alkanethiol or alkylsilane leads to the spontaneous formation of a monolayer. Since the monolayer structure is considered could influence the sensitivity; therefore, researchers direct their efforts to form an ideal monolayer structure that is close-packed and defect-free.

Recently, various compounds for surface fabrication by self-assembly method have been reported. However, the study of stability over multiple sensing usages and control of the molecular structure and distribution at interface in relation with sensitivity of the target compound detection still inadequate. Thus, I investigated the alkanethiols monolayer from the shorter alkyl chain dithiobis succinimidyl propionate (DSP), and various structures of monolayer by dithiobis succinimidyl undecanoate (DSU), carboxy-$(EG)_6$ undecanethiol (CEG_6), and dendrimer alkanethiol (C_2-NTA) compounds.

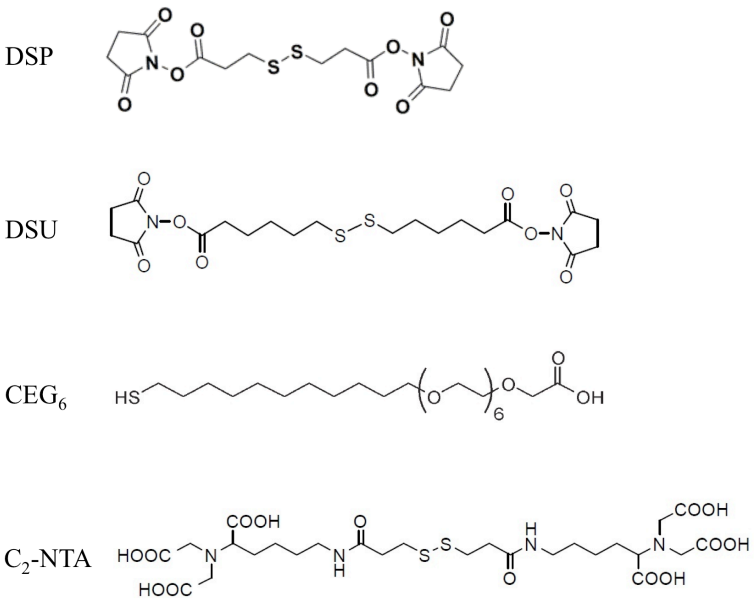

Figure 1.9 Chemical structures of alkanethiol compounds used in this study.

Since alkanethiols with short alkyl chains (DSP) are often shown to adopt a lying-down phase, and changing to upright with the increasing of alkyl thiol density on the surface, the surface concentration of monolayer can significantly affect on the sensitivity of the sensing process. I will, therefore, discuss the relationship between the surface coverage of antigen-immobilized monolayer by varying the DSP solution concentration in the sensor surface fabrication. Moreover, the monolayer structure characteristic of DSU CEG_6, and C_2-NTA were used as underlying structure in the sensor surface fabrication have been discussed to compare the sensing performance in the detection of illegal compound.

In the development of sensor surface for detecting ß-agonists as illegal compounds, some target analytes such as ractopamine and salbutamol do not have a functional group that can form a steady chemical bond to thiol compounds. Thus, the different strategy by immobilization of protein conjugates was conducted onto

alkanethiol monolayer in the sensor surface fabrication process. In advances, the selectivity study of the ß-agonists sensor surface was proposed to confirm the quality of the sensor surface.

Considering that the ß-agonists target compounds (clenbuterol, ractopamine and salbutamol in Figure 1.9) are small molecules (around 300 Da); the immunoassay format of indirect competitive inhibition was employed. By this method, the larger signal is expected because SPR observed the heavyweight antibody instead of lightweight antigen. However, unraveling the kinetic aspects of this assay can be challenging because the antibody competitively binds either to immobilized antigen or antigen in the sample solution. Therefore, the kinetics parameters of the indirect competitive inhibition method have been also examined for understanding their relation with sensing performances.

1.5.2 Outline of the thesis

The main body of the thesis comprises 6 chapters.

Chapter 1 describes present situation of environmental problems and its adverse effects on human beings, also inadequacy of classical methodologies to overcome the environmental assessments and monitoring. The promising surface plasmon resonance (SPR) biosensors with nano-materials development have been introduced to deal with environmental challenges. In addition, the scope and outline of the thesis have been described in this chapter.

In chapter 2 mentions the details of experimental procedures of SPR sensor including the principle of SPR sensor, electrochemistry method, preparation of the sensor substrates. In addition the principle of XPS and STM are also mentioned.

In chapter 3 discusses about monolayer coverage effect on sensitivity of the detection. The fabrication and characterization of the sensor surface were carried out by SPR, cyclic voltammetry reductive desorption, and STM observation. The DSP solution concentration effect on the sensitivity of clenbuterol detection has been discussed. In addition, kinetic study of indirect competitive inhibition method and secondary antibody of the detection are also described.

In chapter 4 studies the various monolayer structures in relation with sensitivity of clenbuterol detection. Different sensor surface fabrications from various alkanethiols monolayer have been described. The detection process of target analyte and kinetics parameters of K_1 and K_2 are discussed.

In chapter 5 describes the sensor interface modification by using protein conjugates. SPR sensor based on an alkanethiol monolayer functionalized on Au surface for highly selective and sensitive detection of ß-agonist compounds (ractopamine and salbutamol) has been studied. The fabrication and characterization of the sensor surfaces have been examined by SPR sensorgram and STM observation. The comparison of kinetic parameters in the detection of ractopamine and salbutamol are also mentioned. In addition, it is proposed the selectivity study of the sensor surface by cross-reactivity and multiple antibody injections.

In chapter 6, the principal results of this study have been summarized and the future prospective of the SPR biosensors by indirect competitive inhibition method with the ability of nano-control interface has been discussed.

1.6 References

[1] A.C. Dillon, Chem. Rev. 110 (2010) 6856–6872.

[2] C. Wolfram, O. Shelef, P. Gertler, J. Econ. Perspective 26 (2012) 119–138.

[3] J.M.A. Ganeva, C. Yao, Y-L. Feng, Talanta 130 (2014) 475–494.

[4] Y. Xu, Environ. Sci. Technol. 45 (2011) 380–385.

[5] C. Hao, L. Xua, C. Xing, H. Kuang, L. Wang, C. Xu, Biosens. Bioelectron. 36 (2012) 174–178.

[6] R. Tang, J.M. Clark, T. Bond, N. Graham, D. Hughes, C. Freeman, Environ. Pollut. 173 (2013) 270–277.

[7] K. Reckmann, I. Traulsen, J. Krieter, J. Environ. Manag. 107 (2012) 102–109.

[8] P. Blowers, D.M. Moline, K.F. Tetrault, R.R. Wheeler, S.L. Tuchawena, Environ. Sci. Technol. 42 (2008) 1301–1307.

[9] B. Zhang, A. Fieldman, Q. Wang, Sens. Actuators B 186 (2013) 597–602.

[10] D. Pimentel, Environ. Dev. Sustain 14 (2012) 151–152.

[11] H.O. Johnson, S.C. Gupta, A.V. Vecchia, F. Zvomuya, J. Environ. Qual. 38 (2009) 1018–1030.

[12] Y.M. Ozer, G. Leavesley, A student guide to health: understanding the facts, trends, and challenges, ABC-CLIO, LLC (2012) California-USA.

[13] Center for Disease Control and Prevention, Tracking and reporting foodborne disease outbreaks in 2013, at www.cdc.gov.

[14] M. Williams, J. Historical Geography 26 (2000) 28–46.

[15] A.J. Lopez-Menendez, R. Perez, B. Moreno, J. Environ. Manag. 145 (2014)

368–373.

[16] WHO Regional Office for Europe, Improved coordination and harmonization of national food safety control services: report on a joint WHO/EURO–FSAI meeting, Dublin, Ireland, 19–20 June 2001.

[17] A. Roehr, K. Luddecke, S. Drusch, M.J. Mueller, R.v. Alvensleben, Food Control 16 (2005) 649–655.

[18] R. Macrory, Modernising environmental justice, Centre for Law and The Environment, Faculty of Law, University College, London-UK.

[19] X. Wang, Y. Cao, X. Zhong, P Gao, J. Environ. Qual. (Technical Report) (2012) 1393–1401.

[20] S.A. Hajkowicz, J. Environ. Manag. 88 (2008) 607–614.

[21] S-Y. Tang, C.W-H. Lo, G.E. Fryxell, J. Environ. Manag. 91 (2010) 2008–2018.

[22] K.R. Rogers, Anal. Chim. Acta 568 (2006) 222–231.

[23] S. Rodriguez-mozaz, M-P. Marco, M.J.L. Alda, Pure Appl. Chem. 76 (2004) 723–752.

[24] S. Rodriguez-Mozaz, M-P. Marco, M.J.L. Alda, D. Barceló, Talanta 65 (2005) 291–297.

[25] International Union of Pure and Applied Chemistry, Electrochemical biosensors: Recommended definitions and classification, at www.iupac.org.

[26] M. Sharpe, J. Environ. Monit. 5 (2003) 109–113.

[27] P. Leonard, S. Hearty, J. Brennan, L. Dunne, J. Quinn, T. Chakraborty, R. O'Kennedy, Enzyme Microb. Technol. 32 (2003) 3–13.

[28] N. Verma, M. Singh, BioMetals. 18 (2005), 121–129.

[29] M.A. Cooper, Nat. Rev. 1 (2002) 515–528.

[30] J. Homola, Chem. Rev. 108(2) (2008) 462–493.

[31] Y. Yanase, T. Hiragun, T. Yanase, T. Kawaguchi, K. Ishii, M. Hide, Allergology Int. 62 (2013) 163–169.

[32] J. Mitchell, Sensors 10 (2010) 7323–7346.

[33] M. Farre, E. Martinez, J. Ramon, A. Navarro, J. Radjenovic, E. Mauriz, L. Lechuga, M.P. Marco, D. Barcelo, Anal. Bioanal. Chem. 388 (2007) 207–214.

[34] X. Lu, H. Zheng, X. Li, X. Yuan, H. Li, L. Deng, H. Zhang, W. Wang, G. Yang, M. Meng, R. Xi, H.Y. Aboul-Enein, Food Chem. 130 (2012) 1061–1065.

[35] M. Petz, Monatsh Chem. 140 (2009) 953–964.

[36] T. Kawaguchi, D.R. Shankaran, S.J. Kim, K. Matsumoto, K. Toko, N. Miura, Sens. Actuators B Chem. 133 (2008) 467–472.

[37] R. Kurita, Y. Yokota, Y. Sato, F. Mizutani, O. Niwa, Anal. Chem. 78 (2006) 5525–5531.

[38] A. Amine, H. Mohammadi, I. Bourais, G. Palleschi, Biosens. Bioelectron. 21(2006) 1405–1423.

[39] H. Bai, R. Wang, B. Hargis, H. Lu, Y. Li, Sensors 12 (2012) 12506–12518.

[40] B. Bohunicky, S.A. Mousa, Nanotech, Sci. Appl. 4 (2011) 1–10.

[41] D.R. Thevenot, K. Toth, R.A. Durst, G.S. Wilson, Pure Appl. Chem. 71 (1999) 2333–2348.

[42] K.R. Rogers, C.L. Gerlach, Environ. Sci. Technol. 30 (1996), 486–491.

[43] D.R. Shankaran, K.V. Gobi, N. Miura, Sens. Actuators B 121 (2007) 158–

177.

[44] B. Bo, X. Zhu, P. Miao, D. Pei, B. Jiang, Y. Lou, Y. Shu, G. Li, Talanta 113 (2013) 36–40.

[45] K. Riedel, G. Kunze, A. Konig, Adv. Biochem. Eng. Biotechnol. 75 (2002) 81–118.

[46] S.F. D'Souza, Biosens. Bioelectron. 16 (2001) 337–353.

[47] J. Davis, D.H. Vaughan, M.F. Cardosi, Enzyme Microb. Technol. 17 (1995), 1030–1035.

[48] Mulchandani, A.S. Bassi, Crit. Rev. Biotechnol. 15 (1995), 105–124.

[49] Ministry of Internal Affairs and Communications Japan, Statistics Bureau (2014), http://www.stat.go.jp/english/data/handbook/index.html.

[50] The Ministry of Health, Labor, and Welfare Japan (2014), http://www.mhlw.go.jp/english/topics/importedfoods/index.html

[51] National Library of Medicine - Medical Subject Headings, Adrenergic beta-agonist, http://www.nlm.nih.gov/cgi/mesh/2011/.

[52] T. Miyashita, C.L. Williams, Neurobio. Learn. Memory. 85 (2006) 116–124.

[53] M. Johnson, J. Allergy. Clin. Immunol. 117 (2006) 18–24.

[54] Wikipedia at http://en.wikipedia.org/wiki/Beta-adrenergic_agonist.

[55] C. Crescenzi, S. Bayoudh, P.A.G. Cormack, T. Klein, K. Ensing, Anal. Chem. 73 (2001) 2171–2177.

[56] S. Liu, Q. Lin, X. Zhang, X. He, X. Xing, W. Lian, J. Huang, Sens. Actuators B 156 (2011) 71–78.

[57] H. Wang, Y. Zhang, H. li, B. Du, H. Ma, D. Wu, Q. Wei, Biosens.

Bioelectron. 49 (2013) 14–19.

[58] X. Yang, F. Wu, D-Z. Chen, H-W. Lin, Sens. Actuators B 192 (2014) 529–535.

[59] E. Shishani, S.C. Chai, S. Jamokha, G. Aznar, M.K. Hoffman, Anal. Chim. Acta 483 (2003) 137–145.

[60] S. Shen, Z. Li, P. He, Electrochem. Comm. 12 (2010) 876–881.

[61] X. Lu, H. Zheng, X.Q. Li, X.X. Yuan, H. Li, L.G. Deng, H. Zhang, W.Z. Wang, [62] G.S. Yang, M. Meng, R.M. Xi, H.Y. Aboul-Enein, Food Chem. 130 (2010) 1061–1065.

[63] Z. Li, Y. Wang, W. Kong, Z. Wang, L. Wang, Z. Fu, Sens. Actuators B 174 (2012) 355–358.

[64] J. Han, H. Gao, W. Wang, Z. Wang, Z. Fu, Biosens. Bioelectron. 48 (2013) 39–42.

[65] M. Regiart, M.A. Fernandez-Baldo, V.G. Spotorno, F.A. Bertolino, J. Raba, Biosens. Bioelectron. 41 (2013) 211–217.

[66] P. Miao, K. Han, H. Sun, J. Yin, J. Zhao, B. Wang, Y. Tang, Appl. Mater. Interface 6 (2014) 8667–8672.

[67] G. Brambilla, T. Cenci, F. Franconi, R. Galarini, A. Macrì, F. Rondoni, M. Strozzie, A. Loizzo, Toxicol. Lett 114 (2000) 47–53.

[68] G. Mazzanti, C. Daniele, G. Boatto, G. Manca, G. Brambilla, A. Loizzo, Toxicology 187 (2003) 91–99.

[69] J. Duan, D. He, W. Wang, Y. Liu, H. Wu, Y. Wang, M. Fu, S. Li, Talanta 115 (2013) 992–998.

[70] M. Liu, B. Ning, L. Qu, Y. Peng, J. Dong, N. Gao, L. Liu, Z. Gao, Sens.

Actuators B 161(2012) 124–130.

[71] W. Xiu-Juan, Z. Feng, D. Fei, L. Wei-Qing, C. Qing-Yu, C. Xiao-Gang, X. Cheng-Bao, J. Chromatogr. A 1278 (2013) 82–88.

[72] M. Sairi, D.W.M. Arrigan, Talanta (2014), http://dx.doi.org/10.1016/ j.talanta.2014.08.060.

[73] International Olympic Committee, Fact sheet: The fight against doping and promotion of athlete's health (2014) Château de Vidy, 1007 Lausanne, Switzerland.

[74] W.L. Shelver, D.J. Smith, J. Agric. Food Chem. 52 (2004)) 2159–2166.

[75] S-Y. Sheu, Y-C. Lei, Y-T. Tai, T-H. Chang, T-F. Kuo, Anal. Chim. Acta 654 (2009) 148–153.

[76] X.Z. Zhang, Y.R. Gan, F.N. Zhao, J. Chromatogr. Sci. 42 (2004) 263–267.

[77] X. Zhang, H. Zhao, Y. Xue, Z. Wu, Y. Zhang, Y. He, X. Li, Z. Yuan, Biosens. Bioelectron. 34 (2012) 112–117.

[78] C. Juan, C. Igualada, F. Moragues, N. León, J. Manes, J. Chromatogr. A 1217 (2010) 6061–6068.

[79] J. Wu, X. Liu, Y. Peng, J. Pharmacol. Toxicol. Methods. 69 (2014) 211–216.

[80] K-C. Lin, C-P. Hong, S-M. Chen, Sens. Actuators B 177 (2012) 428–436.

[81] X. Ji, Z. He, X. Ai, H. Yang, C. Xu, Talanta 70 (2006) 353–357.

[82] J. Zhou, X. Xu, Y. Wang, J. Chromatogr. B 848 (2007) 226–231.

[83] G. Fan, J. Huang, X. Fan, S. Xie, Z. Zheng, Q. Cheng, P. Wang, J. Mol. Liq. 169 (2012) 102–105.

[84] A. Alemanno, G. Capodieci, Europe. J. Risk Reg. 3 (2012) 1–10.

[85] Codex Alimentarius Commision, Maximum Residue Limits for Veterinary Drugs in Foods (2012) at www.codexalimentarius.net.

[86] F. Long, A. Zhu, H. Shi, Sensors 13 (2013) 13928–13948.

[87] Y-H. Liang, C-C. Chang, C-C. Chen, Y. Chu-Su, C-W. Lin, Clin. Biochem. 45 (2012) 1689–1693.

[88] P. Englebienne, A.V. Hoonacker, M. Verhas, Spectroscopy 17 (2003) 255–273.

[89] R.L. Rich, D.G. Myszka, J. Mol. Recog. 18 (2005) 431–478.

[90] D.J. Winzor, Anal. Biochem. 318 (2003) 1–12.

[901] J. Homola, S. Yee, D. Myszka, in: F.S. Ligler, C.A.R. Taitt (Eds.), Surface Plasmon Resonance Biosensors, Elsevier, The Netherlands, 2002, pp. 207–251.

[92] R.J. Green, R.A. Frazier, K.M. Shakesheff, M.C. Davies, C.J. Roberts, S.J.B. Tendler, Biomaterial 21 (2000) 1823– 1835.

[93] J. Homola, S.S. Yee, G. Gauglitz, Sens. Actuators B 54 (1999) 3–15.

[94] K.E. Komolov, I.I. Senin, P.P. Philippov, K.W. Koch, Anal. Chem. 78 (2006) 1228–1234.

[95] A. Ahmad, A. Ramakrishnan, M.A. McLean, A.P. Breau, Biosens. Bioelectron.18 (2003) 399–404.

[96] V. Wintgens, C. Amiel, Langmuir 21 (2005) 11455–11461.

[97] H. Nordin, M. Jungnelius, R. Karlsson, O.P. Karlsson, Anal. Biochem. 340 (2005) 359–368.

[98] G.J. Wegner, A.W. Wark, H.J. Lee, E. Codner, T. Saeki, S. Fang, R.M.

Corn, Anal. Chem. 76 (2004) 5677–5684.

[99] K. Matsumoto, A. Torimaru, S. Ishitobi, T. Sakai, H. Ishikawa, K. Toko, N. Miura, T. Imato, Talanta 68 (2005) 305–311.

[100] L.N. Babol, A. Sternesjo, M. Jagerstad, L. Bjorck, J. Agric. Food Chem. 53 (2005) 5473–5478.

[101] W. Huber, S. Perspicace, J. Kohler, F. Muller, D. Schlatter, Anal. Biochem. 333 (2004) 280–288.

[102] J. Spadavecchia, M.G. Manera, F. Quaranta, P. Siciliano, R. Rella, Biosens. Bioelectron. 21 (2005) 894–900.

[103] W. Haasnoot, K. Olieman, G. Cazemier, R. Verheijen, J. Agric. Food Chem. 49 (2001) 5201–5206.

[104] P.K. Maharana, R. Jha, S. Palei, Sens. Actuators B 190 (2014) 494–501.

[105] J. Martinez-Perdiguero, A. Retolaza, L. Bujanda, S. Merino, Talanta 119 (2014) 492–497.

[106] S.M. Yo, D-K. Kim, S.Y. Lee, Talanta 132 (2015) 112–117.

[107] M. Karkar, M. Chamtouri, J. Moreau, M. Besbes, M. Canva, Sens. Actuators B 191 (2014) 115–121.

[108] K. Nagatomo, T. Kawaguchi, N. Miura, K. Toko, K. Matsumoto, Talanta 79 (2009) 1142–1148.

[109] Z. Jiang, Y. Qin, Z. Peng, S. Chen, S. Chen, C. Dheng, J. Xiang, Biosens. Bioelectron. 62 (2014) 268–273.

[110] C. Puttharugsa, T. Wangkam, N. Huangkambang, O. Gajanandana, O. Himananto, B. Sutapun, R. Amarit, A. Somboonkaew, T. Srikhirin,

Biosens. Bioelectron. 26 (2011) 2341–2346.

[111] S. Suwansa-ard, P. Kanatharana, P. Asawatreratanakul, B. Wongkittisuksa, C. Limsakul, P. Thavarungkul, Biosens. Bioelectron. 24 (2009) 3436–3441.

[112] S.D. Mazumdar, M. Hartmann, P. Kampfer, M. Keusgen, Biosens. Bioelectron. 22 (2007) 2040–2046.

[113] S. Shukla, N.K. Sharma, V. Sajal, Sens. Actuators B 206 (2015) 463–470.

[114] C. Hu, N. Gan, Y. Chen, L. Bi, X. Zhang, L. Song, Talanta 80 (2009) 407–410.

[115] V.A. Briand, V. Thilakarathne, R.M. Kasi, C.V. Kumar, Talanta 99 (2012) 113–118.

[116] B. Guven, F.C. Dudak, I.H. Boyaci, U. Tamer, M. Ozsoz, Analyst 139 (2014) 1141–1147.

[117] R.B.M. Schasfoort, A.J. Tudos, Handbook of surface plasmon resonance, 2008, 1-14, http://www.springer.com/978-0-85404-267-8.

[118] H.N. Daghestani, B.W. Day, Sensors 10 (2010) 9630–9646.

[119] S.J. Daly, G.J. Keating, P.P. Dillon, B.M. Manning, R.O. Kennedy, H.A. Lee, M.R.A. Morgan, J. Agric. Food. Chem. 48 (2000) 5097–5104.

[120] K.V. Gobi, H. Tanaka, Y. Shoyama, N. Miura, Biosens. Bioelectron. 20 (2004) 350–357.

[121] Q. Yu, S. Chen, A.D. Taylor, J. Homola, B. Hock, S. Jiang, Sens. Actuators B 107 (2005) 193–201.

[122] S.J. Kim, K.V. Gobi, R. Harada, D.R. Shankaran, N. Miura, Sens. Actuators B 115 (2006) 349–356.

[123] D.R. Shankaran, K. Matsumoto, K. Toko, N. Miura, Sens. Actuators B 114 (2006) 71–79.

[124] I.M. Traynor, S.R.H. Crooks, J. Bowers, C.T. Elliott, Anal. Chim. Acta 483 (2003) 187–191.

[125] H. Bao, T. Wei, H. Meng, B. Liu, Chem. Lett. 41 (2012) 237–239.

[126] D.R. Shankaran, N. Miura, J. Phys. D: Appl. Phys. 40 (2007) 7187–7200.

[127] G. Sakai, S. Nakata, T. Uda, N. Miura, N. Yamazoe, Electrochim. Acta 44 (1999) 3849–3854.

[128] K.V. Gobi, N. Miura, Sens. Actuators B 103 (2004) 265–271.

[129] F. Frederix, K. Bonroy, W. Laureyn, G. Reekmans, A. Campitelli, W. Dehaen, G. Maes, Langmuir 19 (2003) 4351–4357.

[130] W. Senaratne, L. Andruzzi, C.K. Ober Biomacromolecules 6 (2005) 2427–2448.

[131] J.C. Love, L.A. Estroff, J.K. Kriebel, R.G. Nuzzo, G.M. Whitesides, Chem. Rev. 105 (2005) 1103–1169.

[132] S. Ferretti, S. Paynter, D.A. Russell K.E. Sapsford, Trends Anal. Chem. 19 (2000) 530–540.

[133] G. Ferracci, M. Seagar, C. Joel, R. Miquelis, C. Leveque, Anal. Biochem. 334 (2004) 367–375.

[134] F. Touil, S. Pratt, R. Mutter, B. Chen, J. Phar. Biomed. Anal. 40 (2006) 822–832.

[135] J.S. Mitchell, Y. Wu, C.J. Cook, L. Main, Steroids 71 (2006) 618–631.

[136] V.B. Kandimalla, V .S. Tripathi, H. Ju, Crit. Rev. Anal. Chem. 36 (2006) 73–106.

[137] R. Gupta, N.K. Chaudhury, Biosens.Bioelectron. 22 (2007) 2387–2399.

[138] A. Bronshtein, N. Aharonson, D. Avnir, A. Turniansky, M. Alstein M, Chem. Mater. 9 (1997) 2632–2639.

[139] A. Bossi, F. Bonini, A.P.F. Turner, S.A. Piletsky, Biosens. Bioelectron. 22 (2007) 1131–1137.

[140] J.F. Masson, T.M. Battaglia, Y.C. Kim, A. Prakash, S. Beaudoin, K.S. Booksh Talanta 64 (2004) 716–725.

[141] J. Matsui, K. Akamatsu, N. Hara, D. Miyoshi, H. Nawafune K. Tamaki, N. Sugimoto, Anal.Chem.77 (2005) 4282–85.

[142] Z. Zhang, W. Knoll, R. Foerch, R. Holcomb, D. Roitman, Macromolecules 38 (2005) 1271–1276.

[143] M.H.F. Meyer, M. Hartmann, M. Keusgen, Biosens. Bioelectron. 21 (2006) 1987–1990.

[144] C.D. Kang, S.W. Lee, T.H. Park, S.J. Sim, Enz. Microb. Technol. 39 (2006) 387–390.

[145] O. Lazcka, J.D. Campo, F.X. Munoz, Biosens. Bioelectron. 22 (2007) 1205–1217.

[146] U. Bilitewski, Anal. Chim. Acta 568 (2006) 232–247.

[147] A.H. Schmid, S.E. Stanca, M.S. Thakur, K.R. Thampi, C.R. Suri, Sensors Actuators B 113 (2006) 297–303.

[148] N. Soh, T. Tokuda, T. Watanabe, K. Mishima, T. Imato, T. Masadome, Y. Asano, S. Okutani, O. Niwa, S. Brown, Talanta 60 (2003) 733–745.

[149] K. Kato, C.M. Dooling, K. Shinbo, T.H. Richardson, F. Kaneko, R. Tregonning, M.O. Vysotsky, C.A. Hunter, Collids Surf. A: Physiochem.

Eng. Asp. 198–200 (2002) 811–816.

[150] Y. Hou, C. Tlili, N.J. Renault, A. Zhang, C. Martelet, L. Ponsonnet, A. Errachid, J. Samitier, J. Bausells, Biosens. Bioelectron. 20 (2004) 1126–1133.

[151] F. Davis, S.P.J. Higson, Biosens. Bioelectron. 21 (2005) 1–20.

[152] A.T. Pereira, P. Novo, D.M.F. Prazeres, V. Chu, J.P. Conde, Biomicrofluidics 5 (2011) 1–13.

[153] G. Shan, C. Lipton, S.J. Gee, B.D. Hammock, Immunoassay, biosensors and other nonchromatographic methods, Handbook of Residual Analytical Methods for Agrochemicals, John Wiley & Sons, Ltd. Chichester (2002) 623–679.

[154] B. Cunningham, P. Li, B. Lin, J. Pepper, Sens. Actuators B 81 (2002) 316–328.

[155] M. Salmain, M. Ghasemi, S. Boujday, J. Spadavecchia, C. Techer, F. Val, V. le Moigne, M. Gautier, R. Briandet, C-M. Pradier, Biosens. Bioelectron. 29 (2011) 140–144.

[156] I. Ciani, H. Schulze, D.K. Corrigan, G. Henihan, G. Giraud, J.G. Terry, A.J. Walton, R. Pethig, P. Ghazal, J. Crain, C.J. Campbell, T.T. Bachmann, A.R. Mount, Biosens. Bioelectron. 31 (2012) 413–418.

[157] L. Zhang, Y. Jin, H. Mao, L. Zheng, J. Zhao, Y. Peng, S. Du, Z. Zhang, Biosens. Bioelectron. 58 (2014) 165–171.

[158] H-Y. Lin, C-H. Huang, S-H. Lu, I-T. Kuo, L-K. Chau, Biosens. Bioelectron. 51 (2014) 371–378.

[159] C-Y. Poon, H-M. Chan, H-W. Li, Sens. Actuators B 190 (2014) 737–744.

[160] O. Gul, E. Calay, U. Sezerman, H. Basaga, Y. Gurbuz, Sens. Actuators B 125 (2007) 581–588.

[161] J. Tang, J. Li, J. Kang, L. Zhong, Y. Zhang, Sens. Actuators B 140 (2009) 200–205.

[162] S. Shipovskov, A.M. Saunders, J.S. Nielsen, M.H. Hansen, K.V. Gothelf. E.E. Ferapontova, Biosens. Bioelectron. 37 (2012) 99–106.

[163] J. Zhou, N. Gan, F. Hu, T. Li, H. Zhou, X. Li, L. Zheng, Sens. Actuators B 186 (2013) 300–307.

[164] J. Shen, Y. Li, H. Gu, F. Xia, X. Zuo, Che. Rev. 114 (2014) 7631–7677.

[165] Y. Zhuo, G. Gui, Y. Chai, N. Liao, K. Xiao, R. Yuan, Biosens. Bioelectron. 53 (2014) 459–464.

[166] Q. Yue, T. Shen, L. Wang, S. Xu, H. Li, Q. Xue, Y. Zhang, X. Gu, S. Zhang, J. Liu, Biosens. Bioelectron. 56 (2014) 231–236.

[167] J. Silver, Z. Li, K. Neuman, Biosens. Bioelectron. 63 (2015) 117–123.

[168] C.A.R. Taitt, J.P. Golden, M.J. Feldstein, J.J. Cras, K.E. Hoffman, F.S. Ligler, Biosens. Bioelectron. 14 (2000) 785–794.

[169] K.E. Sapsford, P.T. Charles, C.H. Patterson, F.S. Ligler, Anal. Chem. 74 (2002) 1061–1068.

[170] F. Wang, D. Banerjee, Y. Liu, X. Chen, X. Liu, Analyst 135 (2010) 1839–1854.

[171] L. Bonel, J.C. Vidal, P. Duato, J.R. Castillo, Biosens. Bioelectron. 26 (2011) 3254–3259.

[172] X. Fang, M. Han, G. Lu, Wenwen Tu, Z. Dai, Sens. Actuators B 168 (2012) 271–276.

[173] X. Yang, F. Wu, D-Z. Chen, H-W. Lin, Sens. Actuators B 192 (2014) 529–535.

[174] L-S. Hu, C-C. Fong, L. Zou, W-L. Wong, K-Y. Wong, R.S.S. Wu, M. Yang, Biosens. Bioelectron. 53 (2014) 406–413.

[175] X. Wang, S. Reisberg, N. Serradji, G. Anquetin, M-C. Pham, C-Z. Dhong, W. Wu, B. Piro, Biosens. Bioelectron. 53 (2014) 214–219.

[176] V.I. Chegel, Y.M. Shirshov, E.V. Piletskaya, S.A. Piletsky, Sens. Actuators B 48 (1998) 456–460.

[177] P.T. Charles, J.G. Rangasammy, G.P. Anderson, T.C. Romanoski, A.W. Kusterbeck, Anal. Chim. Acta 525 (2004) 199–204.

[178] I. Vikholm-Lundin, S. Auer, A-C. Hellgren, Sens. Actuators B 156 (2011) 28– 34.

[179] B. Zhang, B. Liu, G. Chen, D. Tang, Biosens. Bioelectron. 53 (2014) 465–471.

[180] N. Miura, M. Sasaki, K.V. Gobi, C. Kataoka, Y. Shoyama, Biosens. Bioelectron. 18 (2003) 953–959.

[181] D.R. Shankaran, K.V. Gobi, T. Sakai, K. Matsumoto, K. Toko, N. Miura, Biosens. Bioelectron. 20 (2005) 1750–1756.

[182] K.E. Sapsford, C.R. Taitt, S. Fertig, M.H. Moore, M.E. Lassman, C.M. Maragos, L.C. Shriver-Lake, Biosens. Bioelectron. 21 (2006) 2298–2305.

[183] S.J. Kim, K.V. Gobi, H. Tanaka, Y. Shoyama, N. Miura, Sens. Actuators B 130 (2008) 281–289.

[184] S. Wang, W. Yong, J. Liu, L. Zhang, Q. Chen, Y. Dong, Biosens. Bioelectron. 57 (2014) 192–198.

[185] C-H. Kim, L-P. Lee, J-R. Min, M-W. Lim, S-H. Jeong, Biosens. Bioelectron. 51 (2014) 426–430.

[186] Suherman, K. Morita, T. Kawaguchi, Biosens. Bioelectron. (2014) http://dx.doi.org/10.1016/j.bios.2014.08.055i.

[187] A. Amine, H. Mohammadi, I. Bourais, G. Palleschi, Biosens. Bioelectron. 21 (2006) 1405–31423.

Chapter 2

Experimental

2.1 Materials and chemicals

Potassium hydroxide, salbutamol sulfate, chloroform and ethanol (99.5%) were obtained from WAKO, Japan, while sodium hydroxide was from Junsei chemical Co., Ltd., Japan. Dithiobis succinimidyl propionate (DSP) and phosphate buffer saline (PBS) were purchased from Sigma Aldrich, USA. Methanol (99%), dithiobis succinimidyl undecanoate (DSU), and dithiobis (C_2-NTA) were obtained from Dojindo, Japan. Carboxy (ethylene glycol)$_6$ undecanethiol (CEG_6), *N*-(3-dimethylaminopropyl)-*N*′-ethylcarbodiimide hydrochloride (EDC) and phosphate-buffered saline (PBS) were purchased from Sigma Aldrich, USA, and *N*-hydroxysuccinimide (NHS) was purchased from FLUKA, Germany. Perchloric acid was purchased from Kanto Chemicals, Japan. Clenbuterol hydrochloride and monoclonal mouse IgG antibody of clenbuterol were ordered from LKT laboratories, Inc., USA and Novus Biologicals, USA, respectively. Ractopamine–bovine serum albumin (RCT-BSA) was purchased from Bioss, Inc., USA. Monoclonal mouse IgG antibody against ractopamine (RCT) was ordered from Acris Antibodies, USA. Salbutamol–horseradish peroxidase (SAL-HRP) was purchased from Aviva System Biology, USA, and polyclonal sheep IgG antibody to salbutamol (SAL) was ordered from GenWay Biotech, Inc., USA. Refractive index matching fluid (refractive index = 1.518) was obtained from Cargille Labs., USA. All chemicals were of reagent or

higher grade, and water (18.2 MΩ cm) from a Millipore system was used in all experiments.

2.2 Surface Plasmon Resonance (SPR)

2.2.1 SPR configuration

SPR is an optical transducer based on surface plasmon phenomena. In principle, SPR measures the dielectric constant change occurring at the interface. There are two important components in the SPR system: a) optical setup for the excitation and interrogation of surface plasmons, b) biomolecular recognition elements immobilized on the sensor surface. The resonance of surface plasmons with evanescent field based on total internal reflection occurs when p-polarized incident light hit an electrically conducting metal layer at the interface of a glass chip. Several techniques were commonly used to couple evanescent wave into surface plasmon polariton (SPP), and these techniques known as the configuration of SPR as mention follows:

a. Otto configuration

In the Otto arrangement (Figure 2.1-a), there is a gap between the prism and the metal surface. The space is filled with a lower refractive index medium such as air. Therefore, the evanescent wave is coupled through the air gap into gold film [1–3]. Otto configuration is useful in the study of SPR in solid phase media.

b. Kretschmann configuration

In the Kretschmann configuration (Figure 2.1-b), the prism is coated with a thin film of the noble metal on the glass chip [4–6]. The sample under investigation

can be coupled to the metal film on the glass surface, enabling a more efficient of plasmon generation.

c. Diffraction grating configuration

The Diffraction grating configuration commonly uses to increase the momentum of an optical wave to be matched of a surface plasmon wave [7]. This configuration can demonstrate narrow or broad spectral responses (from a few nanometers to a few tens of nanometers depending on the metal). Then, the light can be totally absorbed under suitable conditions [8–9]. Diffraction grating configuration can be useful in many different spectral filtering applications.

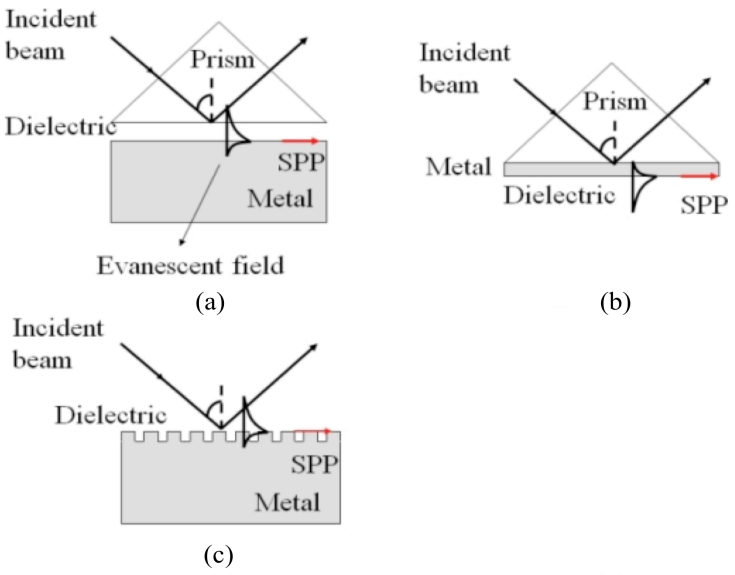

Figure 2.1 Surface plasmon resonance configurations [10]: (a) Otto configuration, (b) Kretschmann configuration, and (c) Diffraction grating.

In practical application, Kretschmann configuration is preferable to use because Otto and diffraction grating configurations require high nano-technology to set-up the dielectric medium gap and diffraction grating surface in nano meter order.

2.2.2 General principle of SPR

Basic principle of SPR sensor is described as follows: when the incident light comes through the SPR prism and hit the backside of the metal layer, the light goes from optically dense media (higher refractive index/RI) to less dense media (lower RI), it is partly reflected and partly refracted. To estimate the refraction angle of the light, Snell's law can be adopted:

$$\frac{n_1}{n_2} = \frac{\sin\theta_2}{\sin\theta_1} \qquad \text{(Eq. 2.1)}$$

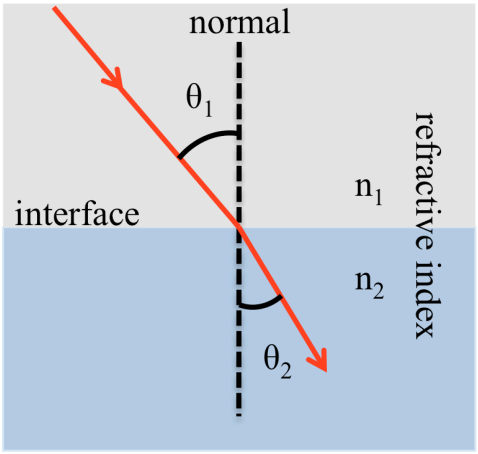

Figure 2.2 Snell's law describing the relationship between the angles of incidence and refraction [11].

At the special angle of incident light (critical angle), total internal reflection (TIR) occurs when all light is reflected back into dense media. In the different condition, when no reflection light occurs (incident light with a particular polarization is perfectly transmitted through a transparent dielectric surface), Brewster's angle is achieved (Figure 2.3). And a component of this light (the

evanescent wave) can propagate into the less dense media to a distance of one wavelength.

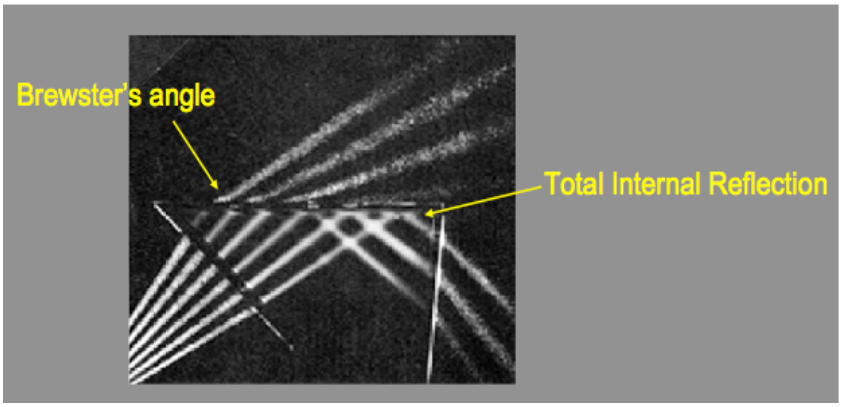

Figure 2.3 Classical method of optic for total internal reflection phenomena [11].

In case of TIR, the evanescent wave (transmitted wave) is generated. This evanescent wave is possible to interact with free electron (plasmon) in the metal film located at the interface between two media. The interaction between an evanescent wave and a surface plasmon in the attenuated total reflection method can be explained using the Fresnel theory, represented by Fresnel's equation to estimate the reflection coefficients and transmission coefficients [12]:

$$r_{II} = \frac{\tan(\theta_i - \theta_t)}{\tan(\theta_i + \theta_t)} \text{ (Parallel reflection)} \qquad \text{(Eq. 2.2)}$$

$$r_{\perp} = -\frac{\sin(\theta_i - \theta_t)}{\sin(\theta_i + \theta_t)} \text{ (Perpendicular reflection)} \qquad \text{(Eq. 2.3)}$$

$$t_{II} = \frac{2\sin\theta_t \cos\theta_i}{\sin(\theta_i + \theta_t)\cos(\theta_i - \theta_t)} \text{ (Parallel transmission)} \qquad \text{(Eq. 2.4)}$$

$$t_{\perp} = \frac{2\sin\theta_t \cos\theta_i}{\sin(\theta_i + \theta_t)} \quad \text{(Perpendicular transmission)} \qquad \text{(Eq. 2.5)}$$

When this surface plasmon wave is resonantly matching to the evanescent wave, the surface plasmon resonance occurs and light energy is lost and the intensity of reflected light decreases. From the plasmon resonance phenomena, the wave vector of evanescent equal to wave vector of surface plasmon (Figure 2.4):

$$k_{eva} = \frac{2\pi}{\lambda} n_{prism} \sin\theta \qquad \text{(Eq. 2.6)}$$

$$k_{sp} = \frac{2\pi}{\lambda} \sqrt{\frac{\varepsilon_{Au} \cdot \varepsilon_{ad-layer}}{\varepsilon_{Au} + \varepsilon_{ad-layer}}} \qquad \text{(Eq. 2.7)}$$

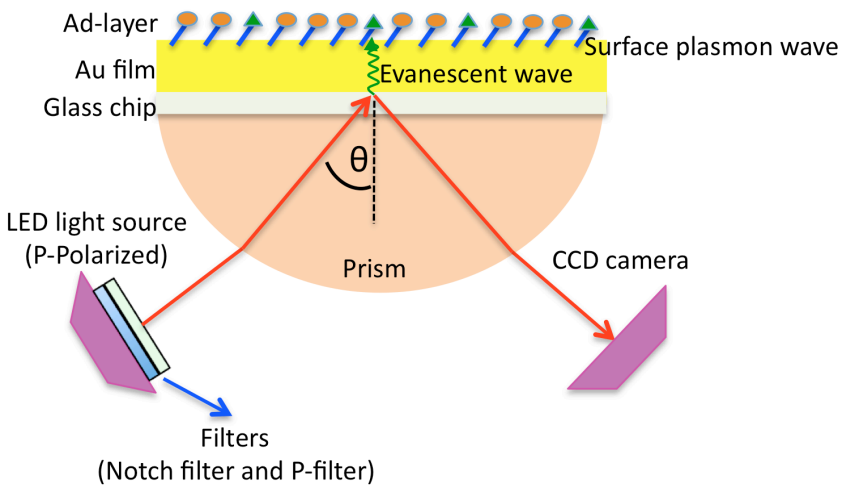

Figure 2.4 Principle of SPR sensing

$$k_{eva} = k_{sp}$$

$$\frac{2\pi}{\lambda} n_{prism} \sin\theta = \frac{2\pi}{\lambda} \sqrt{\frac{\varepsilon_{Au} \cdot \varepsilon_{ad-layer}}{\varepsilon_{Au} + \varepsilon_{ad-layer}}} \qquad \text{(Eq. 2.8)}$$

Thus,

$$\theta = \frac{1}{n_{prism}} \sin^{-1} \sqrt{\frac{\varepsilon_{Au} \cdot \varepsilon_{ad-layer}}{\varepsilon_{Au} + \varepsilon_{ad-layer}}} \qquad \text{(Eq. 2.9)}$$

By inserting number of dielectric constants; $\varepsilon_{Au\text{-}50nm} = 1.25$, $\varepsilon_{methanol} = 32.7$ and refractive index of prism = 1.62, the almost linear linear relation (Figure 2.5) is achieved:

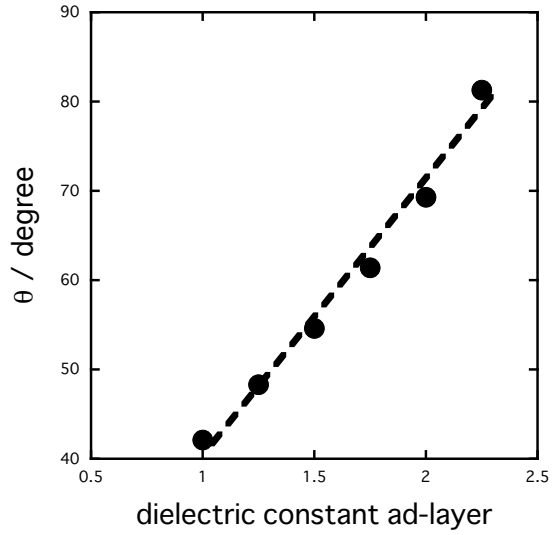

Figure 2.5 Dielectric constant change of ad-layer affected on the resonance angle.

Therefore, the dielectric constants change at the interface directly affects on the resonance angle.

As the analyte binds to the the sensor surface, the refractive index and resonance angle changes strongly correlates to the increase of the mass at the sensor surface. A sensorgram can be obtained in real time by plotting the SPR signal with respect to time when binding between analyte and the immobilized receptor occurs at the sensor surface (Figure 2.6). From the angle difference ($\Delta\theta$), the amount of reacted species is estimated.

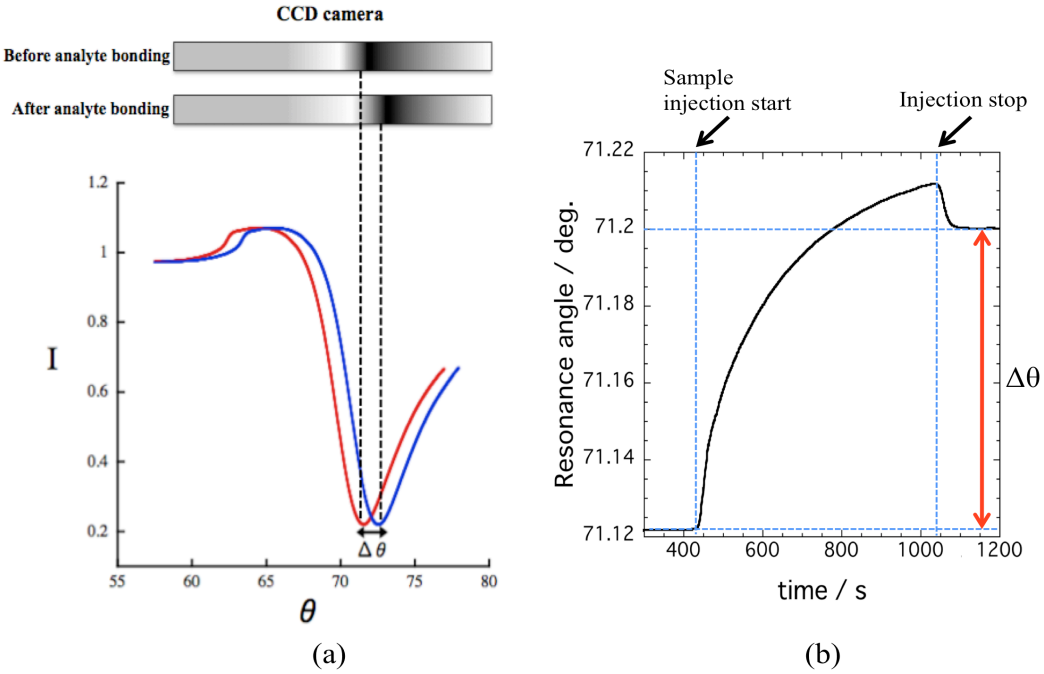

(a) (b)

Figure 2.6 Schematic of SPR detection: (a) CCD camera images before and after the analyte binding, (c) SPR response with respect to time.

In this research, SPR experiments were performed on SPR-670 (Nippon Laser Electronics, Japan) equipped with a fully automated flow system consisting of a plunger pump and an injector (Figure 2.7). The Au-chip is mounted on the semi-cylindrical prism with a refractive index matching liquid. Red light (670 nm) emitted from Ni–Cd laser is reflected at the Au-coated glass plate at attenuated total reflection angles, and the reflected light intensity was recorded using CCD camera.

The reflectance angle, at which the light intensity was minimum (SPR angle), is recorded with time. All the experiments were conducted in an air-conditioned room (25 ^{o}C).

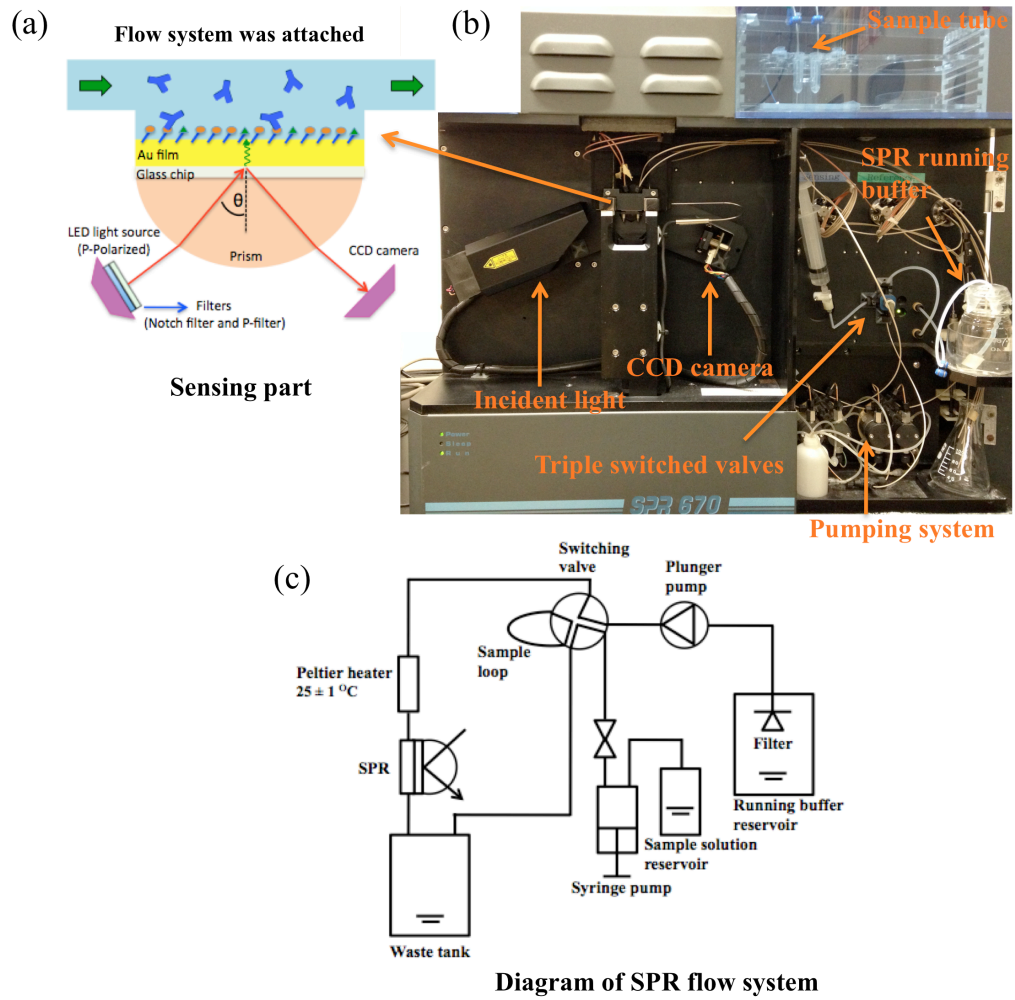

Figure 2.7 SPR 670 from Nippon Laser and Electronics-Japan: (a) sensing part, (b) SPR instrumentation, (c) diagram of SPR flow system.

2.3 Electrochemical measurements

Electrochemistry is the study about chemical changes caused by electrical charges movement between the electrodes (a semiconductor, a solid metal, an ionic

conductor) and the electrolyte [13–14]. The chemical reactions, which take place at the interface, will be monitored by electrochemical method as potential and current changes.

In an electrochemical system, three kinds of electrode are used to perform the experiment including a working electrode, a counter electrode and a reference electrode as shown in Figure 2.8. For monitoring the potential and current of reaction, these electrodes are connected to the potentiostat.

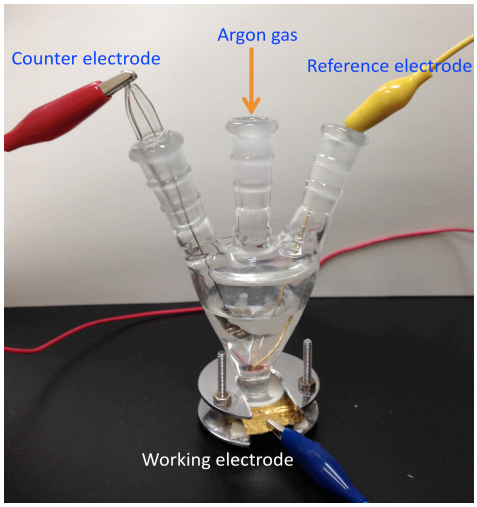

Figure 2.8 Electrochemical cell including Au-chip substrate, platinum wire, and Ag/AgCl (saturated KCl) as working electrode, counter electrode, reference electrode, respectively.

In this study, electrochemical experiments were performed in an electrochemical cell holding using HZ-5000 Automatic Polarization System (Hokuto Denko, Japan). All solutions used were deaerated with 5N Ar in a glove box. Personal computer is used to achieve the data.

2.4 X-ray photoelectron spectroscopy

X-ray photoelectron spectroscopy (XPS) is measurement technique based on the photoelectric effect. Photoelectric effect occurs when X-rays beam strikes to the sample surface, so the core electron of atoms will adsorb the energy [15]. By the energy adsorption, photoelectron emission occurs in case energy of photon ($h\nu$) higher than energy level of the orbital. The binding energy of core electron in atoms is equal to the ionization energy of that electron.

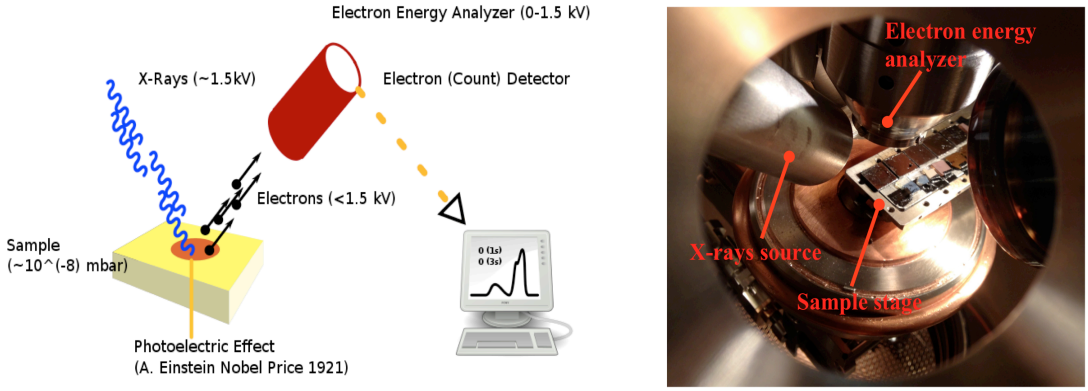

(a) (b)

Figure 2.9 X-ray photoelectron spectroscopy: (a) principle of method, (b) view inside of XPS chamber.

Figure 2.9 shows the principle of XPS method and the view inside the XPS chamber. The binding energy (*Eb*) of the core electron is expressed in the Einstein relationship:

$$h\nu = Eb + Ek + \varphi\ Eb \qquad \text{(Eq. 2.10)}$$

Here, $h\nu$ is X-ray photon energy, *Ek* is the photoelectron kinetic energy; and φ is the work function caused by the analyzer.

When φ can be eliminated, the binding energy is given as:

$Eb = h\nu - Ek$ (Eq. 2.11)

By using the following equation, XPS peak intensity (I) is utilized to estimate the surface composition of the elements:

$I = S \times I_x \times N_n \times \sigma i \times \exp [-d/\lambda_i \cos (\theta)]$ (Eq. 2.12)

Here, S = Machine function

I_x = X-ray intensity

N_n = Number of n atoms per surface area

σ_i = Photoemission cross-section area of atom at i-state

λ_i = Mean of free path length of certain atom n at i-state

θ = Take of angle (angle between detector and the sample)

In normal mode, $\theta = 90$.

The total number of atom at depth d (Å) is estimated from the integration of peak regions. d equal to zero when all atoms located at the surface. In this condition, free path can be ignored.

In this study, intensity of incident X-ray is 300 W. This value is calculated from 30 kV × 10 mA = 300 W. Nn for individual element can be achieved from equation 2.12 by using XPS peak intensity of each element. Thus, Eq. 2.12 can be rewritten as:

$I = \text{Constant x } Nn \times \sigma i$ (Eq. 2.13)

Afterwards, surface composition is directly estimated by the measured intensity.

XPS experiments were conducted using a Rigakudenki model XPS-7000 X-ray photoelectron spectrometer. Monochromatic Mg Kα radiation is operated at 300 W. The angle of take-off is 90^o. For determining the binding energy of elements, Au4f7/2 emission is used as an internal reference.

2.5 Scanning Tunneling Microscope (STM)

The quantum tunneling is basic principle of STM. When the voltage different (a bias) applied between the tip and sample surface, electrons tunnel the vacuum between the tip and surface. Thus, results in current so called tunneling current as function of applied voltage, a tip position, and local density of states of sample [16]. Picoamperometric amplifier can perform amplification of tunneling current.

By monitoring the current as the tip scans across the surface at the constant bias voltage, the STM image is obtained. To maintain the separation between the tip and sample surface, the XYZ positioning of wire tip at a nanometer is performed using piezoelectric controlled scanner (Figure 2.10-b). Since STM method requires sharp tip, clean and stable surfaces, excellent vibration control, and sophisticated electronics, this method could be challenging to the researchers.

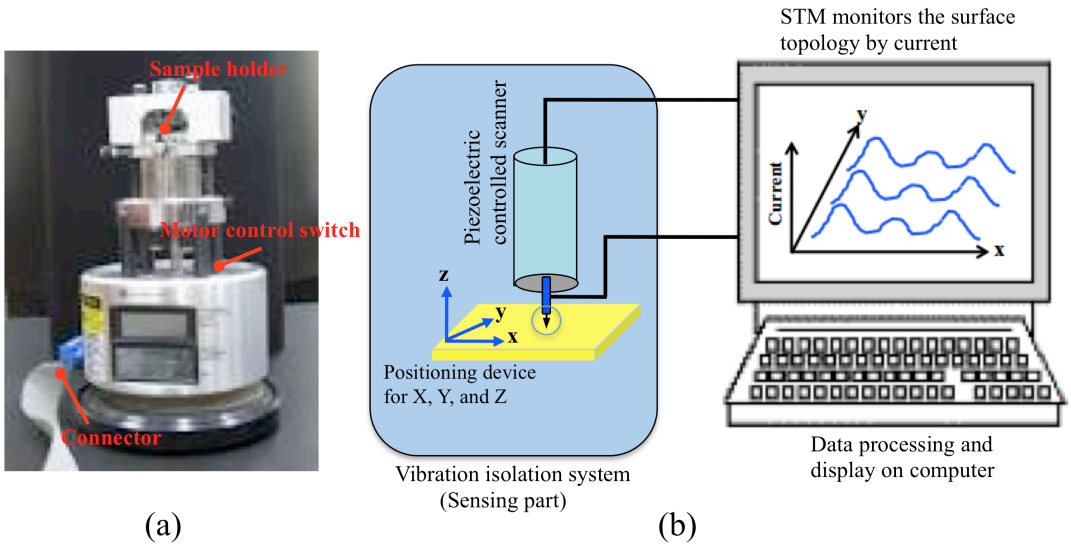

Figure 2.10 Scanning tunneling microscopy: (a) sensing tools, (b) sensing principle.

STM experiments were carried out using a NanoScope STM III (Digital Instruments, USA) operating in the constant current mode (a few hundred picoampere) with the bias voltage typically between 0.5 and 1 V. For imaging, Pt/Ir (80/20) mechanically cut tips (diameter = 0.25 mm, Bruker, USA) were used to scan the surface.

2.6 Preparation of Au substrates

Glass substrates (BK7 type, 20 mm x 13 mm x 0.7 mm^t from Matsunami Glass Ind., Ltd., Japan) were sonicated in soap water (10% Contrad 70 detergent from Fisher). After rinsing with sufficient water, the glass substrates were dried with pure-nitrogen gas. In order to make the surface hydrophilic, the glass substrates were cleaned using plasma at 15 W under 2.0–2.5 Pa. Subsequently Au layer is sputtered onto the glass chips under 2.0–2.5 Pa.

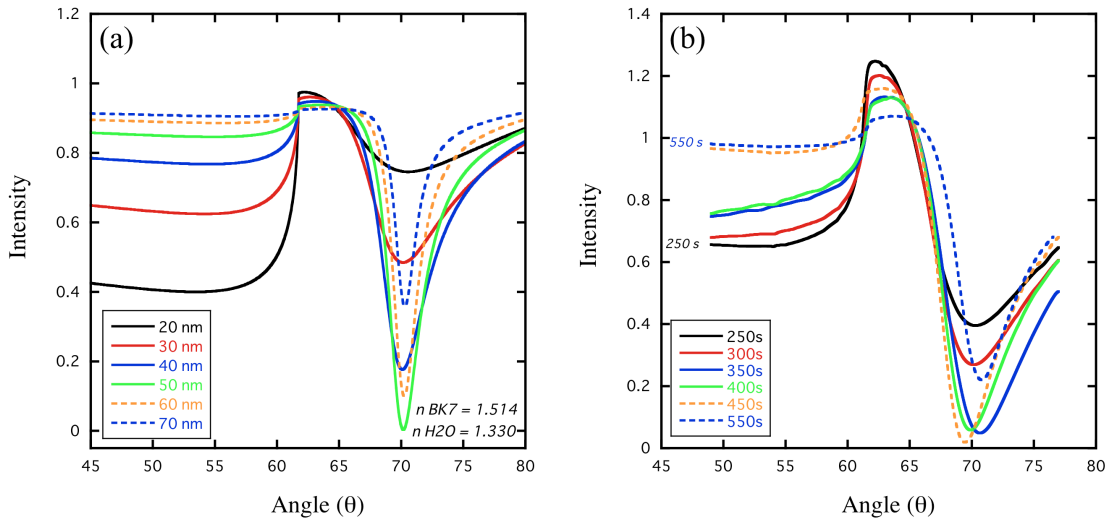

Figure 2.11 SPR angle for various Au thicknesses on glass chip: (a) SPR simulation, (b) Experimental result using sputtering machine of JFC 1600 Auto Fine Coater from JEOL-Japan; note: 1 nm thickness ≈ 10 s deposition.

Considering the SPR simulation (Figure 2.11-a) [17] using several parameters such as incident wavelength at 670 nm, refractive index of water = 1.330 and refractive index of prism = 1.514, and also experimental results (Figure 2.11-b), it was concluded that 50 nm of Au thickness is preferable to use in whole experiment because 50 nm of Au thickness shows the best SPR intensity with sharpest angle respond compare to other thickness.

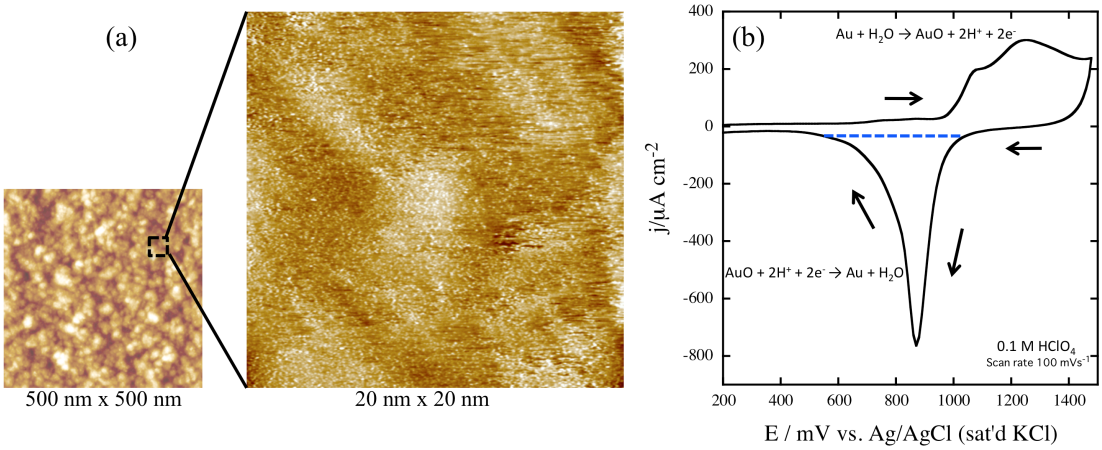

Figure 2.12 Au polycrystalline surface: (a) STM images for of Au surface, (b) cyclic voltammogram for surface roughness calculation.

Surface density of adsorbed species is corrected for the surface roughness of Au-chip (δ = 1.50), which is calculated from the reduction charge density of Au-O in the cyclic voltammogram in 0.1 M sulfuric acid (Figure 2.12). The prepared Au-chips were loaded into the SPR sensing system immediately after excimer ashing pretreatment (172 nm of incident light) for 2 min.

2.7 References

[1] N.H. Salah, D. Jenkins, L. Panina, R. Handy, G. Phan, S. Awan, Smart

Nanosys. Eng. Med. 2 (2012) 10–22.

[2] T. Iwata, Y. Mizutani, Opt. Express 18 (2010) 14480–14487.

[3] E.K. Akowuah, T. Gorman, S. Haxha, Opt. Express 17 (2009) 23511–23521.

[4] A.K. Singh, S.C. Sharma, Opt. Laser Tech. 56 (2014) 256–262.

[5] Y. Mao, Y. Bao, W. Wang, Z. Li, F. Li, L. Niu, Am. J. Anal. Chem. 2 (2011) 589–604.

[6] C. Rhodes, S. Franzen, J. Appl. Phys. 100 (2006) 1–4.

[7] J. Homola, I. Koudela, S.S. Yee, Sens. Actuators B 54 (1999) 16–24.

[8] M.C. Hutley, D. Maystre, Opt. Comm. 19 (1976) 431–436.

[9] L.B. Mashev, E.K. Popov, E.G. Loewen, Appl. Opt. 28 (1989) 2538–2541.

[10] D. Zhang, L. Men, Q. Chen, Sensors 11 (2011) 5360–5382.

[11] Snell's law <http://en.wikipedia.org/wiki/Snell's law>.

[12] Fresnel's theory <www.teknik.uu.se/ftf/education/ftf2/Optics_FresnelsEqns.pdf>.

[13] A.J. Bard**,** L.R Faulkner, Electrochemical Method (Fundamental and Applications), 2nd edition, John Wiley and Sons, Inc. 2001, USA.

[14] Electrochemistry <http://en.wikipedia.org/wiki/Electrochemistry>.

[15] D.J. O'Connor, B.A. Sexton, R.St.C. Smart, Surface Analysis Methods in Materials Science, Springer-Verlag, 1992, Berlin-Germany.

[16] C.J. Chen, Introduction to Scanning Tunneling Microscopy, 2nd edition, Oxford University Press, 2008, New York-USA.

[17] W.N. Hansen, J. Opt. Soc. 58 (3) (1968) 380–390.

Chapter 3

Surface coverage effect on sensitivity of detection

3.1 Introduction

In recent decades, surface plasmon resonance (SPR) sensors have been developed for numerous applications in fields, such as drug discovery, environmental monitoring, food safety, and security [1–12]. SPR is an optical transducer based on surface plasmon phenomena. SPR can measure the refractive index changes occurring at the interface caused by the binding of target analytes with biointerfacial materials (1 mdeg ~ 10 RU ~ 1 ng/cm^2). In my SPR system, the sensitivity can be reached up to 30 pg/cm^2 (0.3 RU). In order to add high selectivity, biochemical recognition elements, such as antibodies, enzymes, proteins, DNA and cells are immobilized on the solid surface of the SPR sensor [13–16]. Biochemical recognition elements can be immobilized by physical adsorption [17–19], by embedding in polymers or membranes [20, 21], by trapping in sol–gels [22, 23], and by using functionalized alkanethiol or functionalized alkylsilane self-assembled monolayer (SAM) [24–26]. Each immobilization approach has advantages. For example, the fabrication of protein-conjugate physically adsorbed on the sensor chip (protein-conjugate/sensor chip) is performed in a single step. With a capacity to store large quantities of the biochemical recognition elements, polymer, membrane, and sol-gel/sensor chips show a large signal response to mass change. Although SAM has the disadvantage of low signal response of mass transducer because immobilization on a

flat surface limits the number of accessible biorecognition elements, its sensitivity and stability are remarkably high.

SAM preparation is very simple; the immersion of metal substrate into thiol solution spontaneously forms the monolayer [27–29]. The monolayer structure is believed could affect on the sensitivity of detection; therefore, researchers concern to obtain an ideal monolayer structure, which is close-packed and defect-free. Analyses by the scanning probe microscope reveal that monolayers consist of ordered and disordered domains [30–34]. Moreover, pinholes and defects are often observed at domain boundaries; analytes and impurities can be adsorbed onto these vacant sites and the mass change due to nonspecific adsorption can significantly affect the sensitivity and selectivity. Thus, the investigation of surface monolayers is continues.

Several academic researchers use a single crystalline metal substrate; however, since polycrystalline metal substrates are used in sensor chips with practical applications, the monolayer structure and coverage on polycrystalline metal substrate in relation with sensing performance is interesting and will be discussed in this research.

Monolayer formation is very sensitive to the cleanliness of the substrate surface. If the surface is partially covered with contaminants, the surface coverage of SAM is low. Thus, the metal substrate requires sufficient cleaning prior to the fabrication of the SAM. In this study, the surface of the metal substrate is cleaned or ashed by irradiation with an excimer light with oxygen, a method that is widely used for cleaning semiconducting wafers. Ozone produced by exciting oxygen using excimer light (λ = 172 nm) oxidizes the contaminants on the metal, thereby cleaning the surface without damaging it.

Here, dithiobis(succinimidyl) propionate (DSP) is used for immobilizing an antigen onto a Au biosensor chip. DSP–a widely used commercially available reagent–has a short alkyl chain, a thiol and a succinimide at its terminal. Thiol terminal of the DSP binds to the Au surface and a biochemical recognition element with an NH_2-terminal can be instantly immobilized, since succinimide group of DSP is replaced by amines in a neutral buffer in a single step. However, since alkanethiols with short alkyl chains are often shown to adopt a lying-down phase [35, 36], the surface coverage of biochemical recognition element can significantly affect the sensitivity of the biosensor. I will, therefore, discuss the relationship between the sensitivity of the sensor and the surface coverage of monolayer.

In this study, I employ the indirect competitive inhibition immunoassay for detecting the small analyte [19, 40–49]. This method ensures that the signal response of the mass transducer is large, because the antibody, rather than the antigen, is being measured. Results from previous reports [9, 16, 26], predict that the surface concentration of immobilized antigen on the sensor surface influences the sensitivity of detection. However, the discussion about kinetics parameters in relation with sensing performance is very rare. Therefore, this study will also discuss the relationship between kinetics of indirect competitive inhibition method and molecular scale structure in the context of sensing performance.

3.2 Fabrication of the sensor surface

One of the most important steps in the biosensing process is the construction of the sensor surface. Figure 3.16 shows the SPR sensorgram of the fabrication

process. Initially, methanol was allowed to flow (5 μL min^{-1}) over the surface of unmodified Au-chip until the resonance angle remained stable. Then, a methanolic solution of DSP was injected over a 40-min period (Figure 3.1-a). The Au-chip is covered with the succinimidyl-terminated propanethiol monolayer during first operation. Subsequently, the running solution was switched from methanol to PBS solution (pH 7.4).

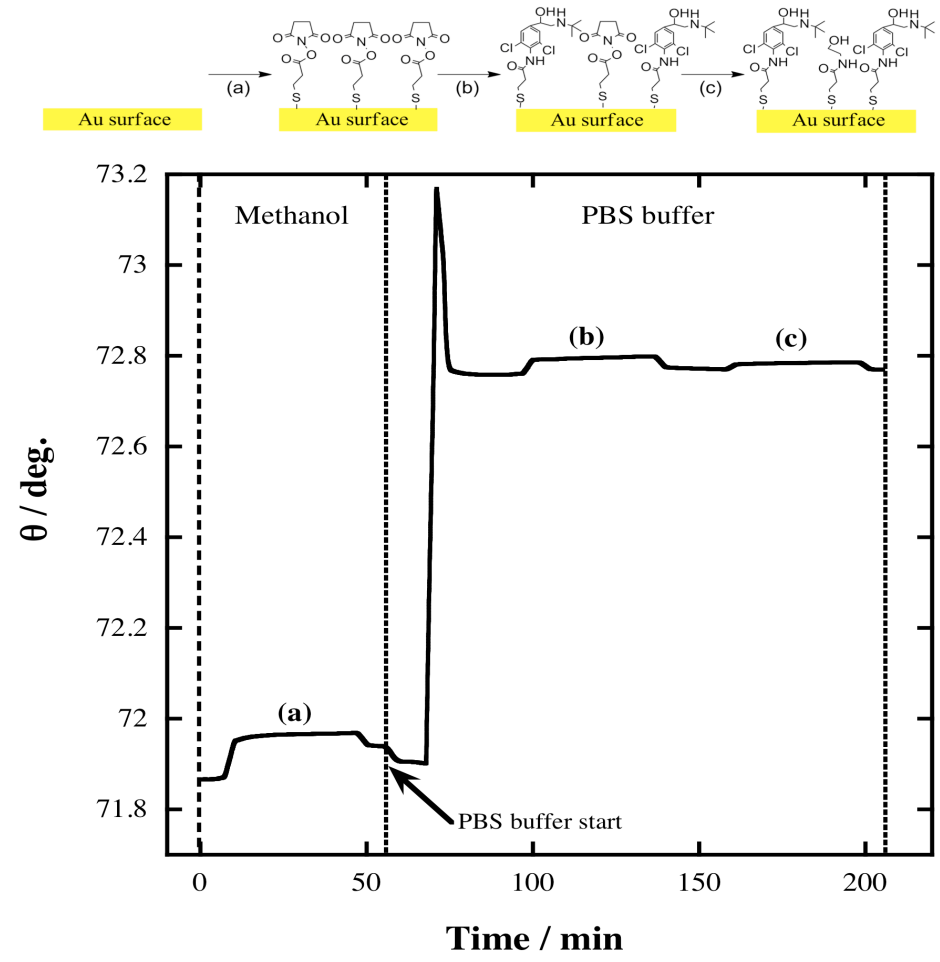

Figure 3.1 SPR sensorgram for fabricating the sensor surface: (a) self-assembly of succinimidyl-terminated propanethiol monolayer, (b) immobilization of clenbuterol by amide coupling reaction, and (c) blocking unreacted *N*-hydroxysuccinimide with ethanolamine.

Since the refractive indices of methanol and PBS solution are different, there was an abrupt shift in the resonance angle. After stabilizing the resonance angle, a solution of clenbuterol (200 μg mL^{-1}) in PBS was injected over a 40-min period (Figure 3.1-b). During this process, the succinimidyl group is replaced by clenbuterol.

Even in the presence of excess clenbuterol, unreacted *N*-hydroxysuccinimide ester groups were retained on the Au-chip. These *N*-hydroxysuccinimide groups were replaced by ethanolamine (a PBS solution containing ethanolamine 1 mg mL^{-1}), i.e., blocking agent, is injected over a 40-min period (Figure 3.1-c). Finally, the sensor surface was used for detecting clenbuterol.

3. 3 Results and discussion

3.3.1 Characterization of self-assembled monolayer

Dependence of the monolayer coverage of succinimidyl-terminated propanethiol on the concentration of DSP solution is examined. Figure 3.2-a shows the SPR sensorgram for the self-assembly of the succinimidyl-terminated propanethiol monolayer on Au-chip.

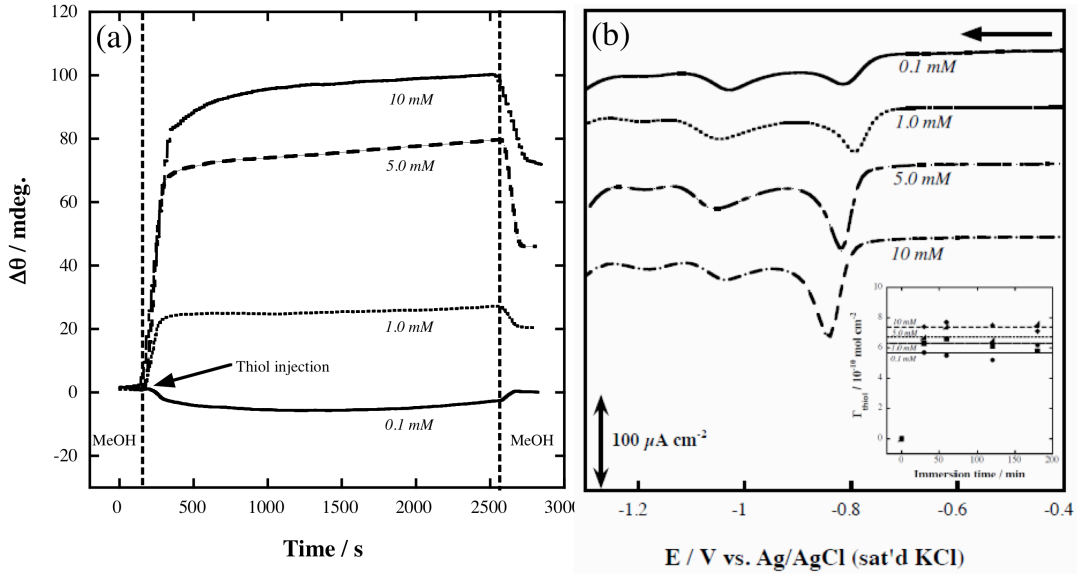

Figure 3.2 (a) SPR sensorgrams for the self-assembly of succinimidyl-terminated propanethiol on Au surface prepared in methanolic solution flowing (5 μL min^{-1}) on the top of Au surface; (b) voltammograms of reductive desorption of succinimidyl-terminated propanethiol monolayer, electrolyte solution was 0.1 M KOH. Sweep rate was 0.1 V s^{-1}. Inset: immersion time dependence on the surface concentrations of succinimidyl-terminated propanethiol monolayer were calculated by reductive desorption. Labeled values are the solution concentration of DSP.

Once a stable baseline is obtained at a flow rate of 5 μL min^{-1}, the methanolic solution of DSP is injected over a 40-min period, following which the running solution is switched back to DSP-free methanol. The initial shift in the resonance angle can be attributed to the difference in the dielectric constant (refractive index) between the interface and the running solution on the inclusion of DSP [50]. As the running solution returns to methanol after 40-min, the shift in the resonance angle decreases (except for DSP concentration of 0.1 mM). Thus, the overall shift in the resonance angle (Δθ) is determined as the difference in resonance angles at t = 0 s and t = 2700 s (at both instances DSP-free methanol is flowing over the chip) to

eliminate the influence of the refractive index of solution. The results indicate that the value of $\Delta\theta$ shows a DSP concentration dependent increase. Since there is no contribution from the refractive index of the solution on the value of $\Delta\theta$, this value directly indicates the dielectric constant of the monolayer. In other words, while the surface concentration of monolayer cannot be estimated from $\Delta\theta$, the shift in the resonance angle can show the dielectric constant difference of the monolayer.

Electrochemical reductive desorption is performed to investigate the structure of monolayer (Figure 3.2-b). Since S–Au bond can be electrochemically cleaved by one-electron reaction [51], the surface concentration of the monolayer can be estimated from the charge density, which is calculated from the integration of reduction current. The reduction current shows three peaks at approximately –0.8 V (from –0.8 V to –0.85 V), –1.04 V and –1.19 V, characteristic of reductive desorption on a polycrystalline Au electrode [52]. By comparing the peak positions in the voltammograms of similar systems reported previously, it is considered that the major peak (at approximately –0.80 V) resulted from the reductive desorption of alkanethiols from the terraces [53], and the peaks at –1.04 V and –1.19 V were due to the desorption of alkanethiols adsorbed on the steps [52, 54, 55] of polycrystalline Au. The intensities of these reduction peaks increase with an increase in either the immersion time or the concentration of DSP (the width of the major peak shrinks). These results indicate that the surface concentration of monolayer increases with increase in the concentration of DSP. The surface concentration of DSP is in the range from 5.1 x 10^{-10} mol cm^{-2} to 7.7 x 10^{-10} mol cm^{-2} (Figure 3.2-b-Inset). With a 30-min immersion time, the surface concentration reaches saturation, a result consistent with the results from SPR studies.

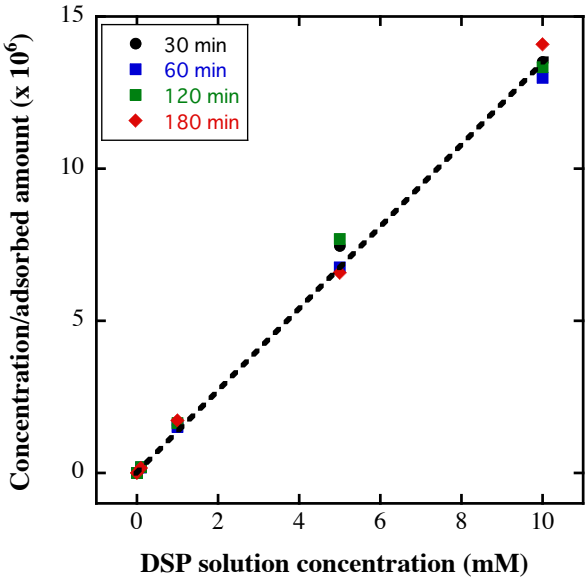

Figure 3.3 Langmuir plot for succinimidyl-terminated propanethiol monolayer on Au surface with variation of immersion time.

According to the Langmuir adsorption isotherm as shown in Figure 3.3 (data taken from Figure 3.2-b-Inset), the Langmuir equilibrium constant (K) and the maximum surface concentration (x^{∞}) of succinimidyl-terminated propanethiol onto Au-surface are estimated to be 1.14 x 10^4 M^{-1} cm^2 and 7.7 10^{-10} mol cm^{-2}. The equilibrium constant K for binding succinimidyl-terminated propanethiol to Au is comparable to that of octadecanethiol (1.08 x 10^4 M^{-1} cm^2 to 1.53 x 10^4 M^{-1} cm^2) and larger than that of octanethiol (1.9 x 10^3 M^{-1} cm^2) [56, 57], suggesting that the strength of the molecular cohesion of succinimidyl-terminated propanethiol is equal to the strength of van der Waals force interactions between long alkyl chains. However, the value of x^{∞} for succinimidyl-terminated propanethiol is lesser than that of alkanethiol monolayer (1.1 x 10^{-9} mol cm^{-2}) [58] because the area occupied by succinimide group is larger than that of methyl group. In addition, the precise surface concentration of DSP could not be determined in this experiment because the local

minimal value (potential of zero charge) is not observed in the differential capacitance curve in potassium hydroxide (0.1 M; data not shown). Therefore, the surface concentration is measured with approximately 30% error [58].

The peak potential of the reductive desorption also provides insights into the monolayer structure. The potential of the major peak is shifted to more negative potential with increase in the concentration of DSP in the range from 1.0 mM to 10 mM. However, there is a discernible shift in the peak potential of the major peak towards more negative values when the concentration of DSP is reduced from 1.0 mM to 0.1 mM. The peak potential is indicative of the permeability of the solvent into the monolayer [59]. When the monolayer is prepared in solution, where the concentration of DSP > 1.0 mM, it is considered that the monolayer density becomes condensed, and the molecular interaction increases with the increase in the concentration of DSP. However, when the monolayer is prepared in 0.1 mM DSP solution, the solvent hardly penetrates inside the monolayer; this phenomena possibly due to the orientation of low density of monolayer, which adopt a lying-down configuration and cover the propanethiol surface [60].

From SPR results, the increase in coverage by clenbuterol correlates with the increase in the concentration of the DSP used to modify the Au-chips. Although the estimated surface concentrations of both clenbuterol and ethanolamine increase with increase in the concentration of DSP, the percentage of coverage by ethanolamine is decreased (Table 3.1). In summary, the surface concentration of monolayer determines the surface composition of clenbuterol and ethanolamine.

Table 3.1 Clenbuterol and ethanolamine coverage on sensor surface.

Method		Clenbuterol	Ethanolamine	Clenbuterol (%)	Ethanolamine (%)	Assumption
SPR	0.1 mM	9.0 ± 3.0 mdeg.	7.1 ± 2.4 mdeg.	55.9	44.1	Dielectric constants/ε are the same.
	1.0 mM	13.4 ± 2.3 mdeg.	8.9 ± 2.8 mdeg.	60.1	39.9	
	5.0 mM	17.6 ± 1.7 mdeg.	11.3 ± 2.9 mdeg.	60.9	39.1	
	10 mM	26.2 ± 5.1 mdeg.	13.5 ± 2.8 mdeg.	66.0	34.0	
XPS	0.1 mM	-	-	30.5	69.5	Depth of thickness coverage are the same
	1.0 mM			30.5	69.5	
	5.0 mM			32.2	67.8	
	10 mM			34.0	66.0	

3.3.2 Detection of clenbuterol

Indirect competitive inhibition immunoassay is employed for detecting clenbuterol [12, 19, 61–64]. SPR senses the change in dielectric constant due to the binding of antibody by the immobilized antigen (clenbuterol) at the interface. A large signal change is typically expected in this assay; however, unraveling the kinetic aspects of this assay [48, 49, 65–68] can be challenging because the Ab competitively binds either to immobilized antigen or antigen in the sample solution. Moreover, several kinetics studies do not consider the two immunoreactions, i.e., during premixing and sensing. Here, I have made an attempt to discuss the kinetics in more detail.

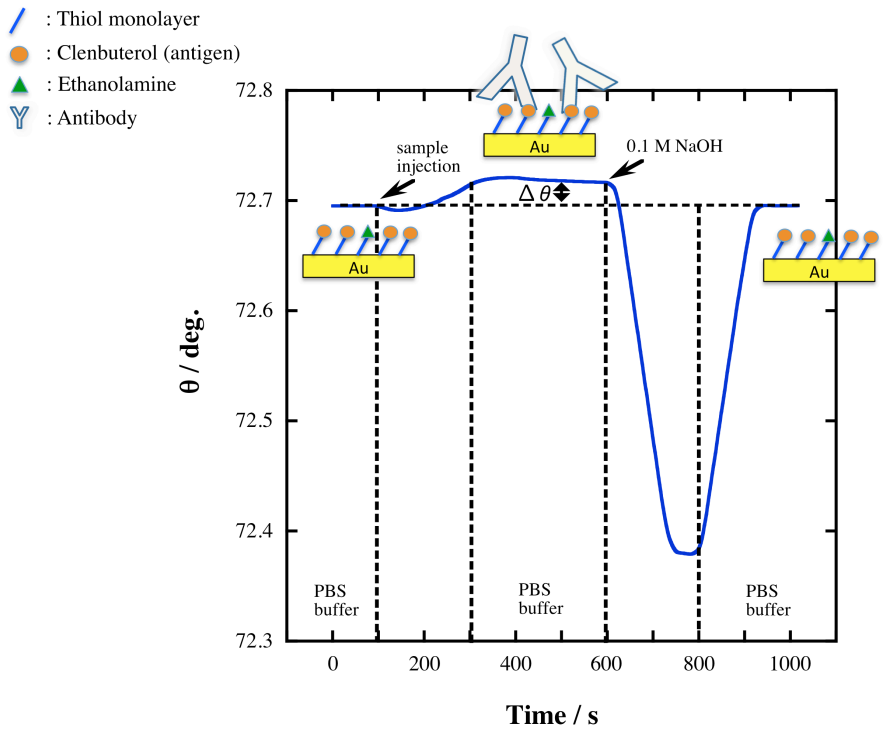

Figure 3.4 SPR sensorgram for the immunoreaction of immobilized clenbuterol with Ab standard solution. PBS (10% ethanol) solution is used as the running solution (100 μL min^{-1}), and 0.1 M NaOH aqueous solution is used for regenerating the sensor surface.

Figure 3.4 shows the representative sensorgram of immunoreaction with Ab. While Ab standard solution flows over the sensor surface for 200 s (from t = 100 s to t = 300 s), the resonance angle shifts gradually to higher values with the binding of Ab by the immobilized antigen onto the sensor surface. Difference in the resonance angle before (t = 100 s) and after (t = 400 s) the binding of Ab to the immobilized antigen is the total resonance angle shift ($\Delta\theta$) of the immunoreaction: this value is used for the concentration dependence curves.

After the immunoreaction, the sensor surface is regenerated by a solution of sodium hydroxide (0.1 M) till the value of the resonance angle returns to the initial

value, indicating that the Ab is detached from the sensor surface. Through such a regeneration process, the sensor surface can be reused for over 100 immunoreactions. One immunoreaction–regeneration cycle takes only 1000 s. Therefore, the same sensor chip is used for evaluating the immunoreaction in various solutions to determine the kinetic parameters. Moreover, <5% error is observed between the results obtained using different sensor chips (N > 3).

3.3.3 Kinetic analysis

3.3.3.1 Langmuir adsorption isotherm

According to reported protocols [48, 49, 67, 68], the affinity constant (K_1) of Ab to the clenbuterol (antigen) immobilized on the sensor surface can be determined using a Langmuir-type adsorption model (Figure 3.5-a).

The Langmuir adsorption isotherm equation for immunoreaction between Ab and the immobilized clenbuterol on the sensor surface (Ss) is given by:

$$Ab + Ss \rightleftharpoons Ab\text{-}Ss \qquad \text{(Eq. 3.1)}$$

$$K_1 = \frac{[Ab - Ss]}{[Ab][Ss]} \qquad \text{(Eq. 3.2)}$$

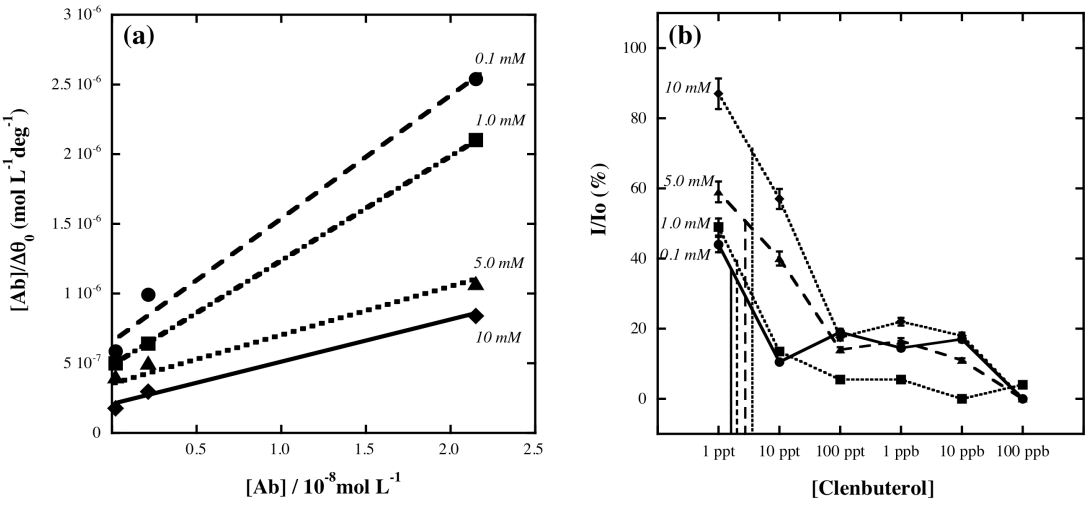

Figure 3.5 (a) Langmuir adsorption isotherm plot for binding clenbuterol antibody (Ab) to clenbuterol immobilized on the sensor surface, and (b) clenbuterol solution concentration dependence by using indirect competitive inhibition immunoassay. Inhibition rate was calculated from the angle shift in presence (I)/absence (I_0) of clenbuterol. In the premixing process, 1 ppm Ab was mixed with series of clenbuterol concentrations. The incubation time was 2 min. Labeled values are the concentration of dithiobis(succinimidyl) propionate (DSP) used in fabricating the sensor surface.

Fundamental equation of Langmuir-type adsorption model is expressed as follows:

$$\frac{[Ab]}{\Delta\theta_0} = \frac{[Ab]}{\Delta\theta_{0,\max}} + \frac{1}{K_1\ \Delta\theta_{0,\max}} \qquad \text{(Eq. 3.3)}$$

Where [Ab] is concentration of the clenbuterol antibody. $\Delta\theta_0$ and $\Delta\theta_{0,max}$ are the total angle shift for a given concentration of Ab standard solution and the maximum angle shift with saturated Ab on the sensor surface, respectively. $\Delta\theta_{0,max}$ and K_1 are determined from the slope and the intercept of the Ab standard solution

concentration dependence as shown in Figure 3.5-a. These parameters are summarized in Table 3.2.

K_1 is observed to increase with increase in the concentration of DSP used in fabricating the sensor surface. This result can be rationalized considering $\Delta\theta_{0,max}$ and the surface composition estimated from SPR results (Table 3.1). Coverage by clenbuterol is approximately 56% when the Au chip is modified with a 0.1 mM DSP solution, where it is 66% for 10 mM DSP. As expected, the reactivity of the sensor surface is proportional to the surface coverage of reactive site (antigen).

3.3.3.2 Indirect competitive inhibition immunoassay

Figure 3.5-b illustrates the clenbuterol concentration dependence by using indirect competitive inhibition immunoassay. During premixing, the following reaction occurs:

$$Ab + Clb \rightleftharpoons Ab\text{-}Clb \qquad \text{(Eq. 3.4)}$$

where Clb is clenbuterol in solution. The affinity constant (K_2) of this immunoreaction is given by:

$$K_2 = \frac{[Ab - Clb]}{[Ab][Clb]} \qquad \text{(Eq. 3.5)}$$

When the sample solution is dispensed onto the sensor surface after the premixing, free-Ab competitively binds to clenbuterol-immobilized sensor surface or clenbuterol (free) in solution, or does not bind at all. Thus, the total concentration of Ab can be defined as follows:

$$\left[Ab_{total}\right] = \left[Ab - Ss\right] + \left[Ab - Clb\right] + \left[Ab\right] \qquad \text{(Eq. 3.6)}$$

By inserting equations (Eq. 3.2) and (Eq. 3.5) to equation (Eq. 3.6), the equation can be rewritten as follows:

$$\frac{1}{[Ab - Ss]} = \frac{1}{[Ab_{total}]} + \frac{1}{[Ab_{total}]\ K_1\ [Ss]} + \frac{K_2}{[Ab_{total}]\ K_1\ [Ss]}[Clb] \qquad \text{(Eq. 3.7)}$$

Because SPR senses the dielectric constant change of [Ab-Ss], so [Ab-Ss] can be represented as $\Delta\theta$. Considering the premixing, the solution concentration of clenbuterol after the incubation is $[Clb] = [Clb]_0 e^{-kt}$ and $\alpha = e^{-kt}$, where k is the reaction rate and t is the period of incubation for the premixing; thus, α is constant of antibody and antigen reaction during the premixed process. The equation (Eq. 3.7), when combined with equation (Eq. 3.4) and considering the premixing, can be rewritten as follows:

$$\frac{1}{\Delta\theta} = \frac{1}{\Delta\theta_0} + \frac{K_2\ \alpha\ [Clb]_0}{[Ab_{total}]\ K_1\ \Delta\theta_{0,\max}} \qquad \text{with } 0 < \alpha < 1 \qquad \text{(Eq. 3.8)}$$

Here, K_1 and $\Delta\theta_{0,max}$ have already been determined (Figure 3.5-a). K_1 can be estimated from the incubation time dependence, and K_2 with constant α is calculated from the slope of equation (Eq. 3.8) (Table 3.2). Note that K_1 is higher than K_2,

irrespective of the concentration of DSP used in fabricating the sensor surface. In other words, Ab prefers to bind to the clenbuterol immobilized on the sensor surface rather than the free clenbuterol in the sample solution.

Table 3.2 Kinetic parameters for detecting clenbuterol by indirect competitive inhibition immunoassay.

[DSP]/mM	$\Delta\theta_{0,max}$ (mdeg.)	K_1 (x 10^8 M^{-1})	*r (correlation coefficient)*	$\alpha.K_2$ (x 10^8 M^{-1})
0.1	10.5	2.19	0.9933	
1.0	11.9	2.72	0.9999	0.65 ± 0.35
5.0	23.1	2.91	0.9985	
10	27.9	4.42	0.9962	

Correlating the sensitivity and kinetic parameter, a high sensitivity of the detection is obtained from a low K_1. With the sensor fabricated in the solution of DSP at 0.1 mM, the limit of detection (LOD) is approximately 3 ppt (3 pg mL^{-1}). These results illustrate that surface coverage of monolayer directly affected on clenbuterol detection. Thus, clenbuterol antibody recognizes the 2-tert-butyl amino-ethanol moiety of clenbuterol. The mechanism of recognition of the antigen by the antibody is intriguing, and studies investigating this are underway.

3.4 Summary

This chapter investigated the relationship between the surface concentration of antigen-immobilized monolayer and the sensing performance of SPR. Since my

target is clenbuterol, a small analyte (Mw = 277), the indirect competitive inhibition immunoassay is employed for its detection. To immobilize clenbuterol onto the sensor surface, succinimidyl-terminated propanethiol monolayer is fabricated on a Au-chip by self-assembly. It is found that the surface concentration and distribution of succinimide group was highly dependent on the concentration of DSP used in self-assembly. The *N*-hydroxysuccinimide group of the succinimidyl-terminated propanethiol was replaced with covalently linked clenbuterol at neutral pH. The sensor surface prepared modified in a high concentration of DSP solution shows a high affinity for clenbuterol antibody. However, the high affinity constant K_1, exhibited by the sensor surface was coupled to a low sensitivity. In contrast, the immunosensor fabricated in the lowest concentration of DSP (0.1 mM) shows a remarkably high sensitivity (LOD = 3 ppt). This is the highest sensitivity reported for detecting clenbuterol. Furthermore, this immunosurface can be regenerated by 0.1 M sodium hydroxide. One immunoreaction–regeneration cycle took only 1000 s, and the same sensor surface could be used for >100 immunoreactions.

3.5 References

[1] J. Homola, Chem. Rev. 108 (2) (2008) 462–493.

[2] J. Mitchell, Sensors 10 (2010) 7323–7346.

[3] J. Homola, Anal. Bioanal. Chem. 377 (2003) 528–539.

[4] M.A. Cooper, Nat. Rev. 1 (2002) 515–528.

[5] H. Bai, R. Wang, B. Hargis, H. Lu, Y. Li, Sensors 12 (2012) 12506–12518.

[6] Y. Yanase, T. Hiragun, T. Yanase, T. Kawaguchi, K. Ishii, M. Hide,

Allergology Int. 62 (2013) 163–169.

[7] R. Kurita, Y. Yokota, Y. Sato, F. Mizutani, O. Niwa, Anal. Chem. 78 (2006) 5525–5531.

[8] M. Farre, E. Martinez, J. Ramon, A. Navarro, J. Radjenovic, E. Mauriz, L. Lechuga, M.P. Marco, D. Barcelo, Anal. Bioanal. Chem. 388 (2007) 207–214.

[9] S.J. Kim, K.V. Gobi, H. Tanaka, Y. Shoyama, N. Miura, Sens. Actuators B 130 (2008) 281–289.

[10] X. Lu, H. Zheng, X. Li, X. Yuan, H. Li, L. Deng, H. Zhang, W. Wang, G.Yang, M. Meng, R. Xi, H.Y. Aboul-Enein, Food Chem. 130 (2012) 1061–1065.

[11] M. Petz, Monatsh Chem. 140 (2009) 953–964.

[12] T. Kawaguchi, D.R. Shankaran, S.J. Kim, K. Matsumoto, K. Toko, N. Miura, Sens. Actuators B 133 (2008) 467–472.

[13] A. Abbas, M.J. Linmas, Q. Cheng, Biosens. Bioelectron. 26 (2011) 1815–1824.

[14] X. Fan, I.M. White, S.I. Shopova, H. Zhu, J.D. Suter, Y. Sun, Anal. Chim. Acta 620 (2008) 8–26.

[15] M. Piliarik, H. Vaisocherova, J. Homola, Surface plasmon resonance biosensing, Avraham Rasooly and Keith E. Herold (eds.), Method in Molecular Biology: Biosensors and Biodetection, vol. 503 © Humana Press, a part of Springer Science & Business Media, LLC 2009. DOI 10.1007/978-1-60327-567-5_5.

[16] M. Kyo, K. Usui-Aoki, H. Koga, Anal. Chem. 77 (2005) 7115–7121.

[17] D.R. Shankaran, N. Miura, J. Phys. D: Appl. Phys. 40 (2007) 7187–7200.

[18] N. Miura, K. Ogata, G. Sakai, T. Uda, N. Yamazoe, Chem. Lett. 26 (1997) 713–714.

[19] D.R. Shankaran, K.V. Gobi, T. Sakai, K. Matsumoto, K. Toko, N. Miura, Biosens. Bioelectron. 20 (2005) 1750–1756.

[20] A. Bossi, F. Bonini, A.P.F. Turner, S.A. Piletsky, Biosens. Bioelectron. 22 (2007) 1131–1137.

[21] K.S. Phillips, J.H. Han, M. Martinez, Z. Wang, D. Carter, Q. Cheng, Anal. Chem. 78 (2006) 506–603.

[22] E.H. Lan, B. Dunn, J.I. Zink, Chem. Mater. 12 (2000) 1874–1878.

[23] R. Liang, J. Qiu, P. Cai, Anal. Chim. Acta 534 (2005) 223–229.

[24] W. Senaratne, L. Andruzzi, C.K. Ober, Biomacromolecules 6 (2005) 2426–2448.

[25] K.V. Gobi, C. Kataoka, N. Miura, Sens. Actuators B 108 (2005) 784–790.

[26] S.S. Mark, N. Sandhyarani, C. Zhu, C. Campagnolo, C.A. Batt, Langmuir 20 (2004) 6808–6817.

[27] D.K. Schwartz, Annu. Rev. Phys. Chem. 52 (2001) 107–137.

[28] J.C. Love, L.A. Estroff, J.K. Kriebel, R.G. Nuzzo, G.M. Whitesides, Chem. Rev. 105 (2005) 1103–1169.

[29] R. Meunier-Prest, G. Legay, S. Raveau, N. Chiffot, E. Finot, Elec. Chim. Acta 55 (2010) 2712–2720.

[30] W. Azzam, L. Al-Momani, Appl. Surf. Sci. 266 (2013) 239–244.

[31] A. Riposan, Y. Li, Y.H. Tan, G. Galli, G. Liu, J. Phys. Chem. A 111 (2007) 12727–12739.

[32] C. Vericat, M.E. Vela, R.C. Salvarezza, Phys. Chem. Chem. Phys. 7 (2005)

3258– 3268.

[33] G.E. Poirier, Langmuir 13 (1997) 2019–2026.

[34] C. Schoenenberber, J. Jorritsma, J.A.M. Sondag-Huethorst, L.G.J. Fokkink, J. Phys. Chem. 99 (1995) 3259–3271.

[35] M.A.D. Millone, H. Hamoudi, L.M. Rodríguez, A. Rubert, G.A. Benitez, M.E. Vela, R.C. Salvarezza, J.E. Gayone, E.A. Sanchez, O. Grizzi, C. Dablemont, V.A. Esaulov, Langmuir 25 (2009) 12945–12953.

[36] V. Chaudhari, H.M.N. Kotresh, S. Srinivasan, V.A. Esaulov, J. Phys. Chem. C 115 (2011) 16518–16523.

[37] J. Pleadin, A. Vulic, N. Persi, D. Milic, N. Vahcic, Food. Technol. Biotechnol. 49 (2011) 517–522.

[38] L.Y. Zhang, B.Y. Chang, T. Dong, P.L. He, W.J. Yang, Z.Y. Wang, J. Chromatogr. Sci. 47 (2009) 324–328.

[39] Y. Zhang, Z. Zhang, Y. Sun, Y. Wei, J. Agric Food Chem. 55 (2007) 4949–4956.

[40] N. Miura, H. Higobashi, G. Sakai, A. Takeyasu, T. Uda, N. Yamazoe, Tech. Digest 4-IMCS (1992) 228–231.

[41] N. Miura, M. Sasaki, G. Sakai, K.V. Gobi, Chem. Lett. 1 (2002) 342–343.

[42] H. Kawazumi, K.V. Gobi, K. Ogino, H. Maeda, N. Miura, Sens. Actuators B 108 (2005) 791–796.

[43] K.V. Gobi, N. Miura, Sens. Actuators B 103 (2004) 265–271.

[44] N. Miura, M. Sasaki, K.V. Gobi, C. Kataoka, Y. Shoyama, Biosens. Bioelectron. 18 (2003) 953–959.

[45] K.V. Gobi, H. Tanaka, Y. Shoyama, N. Miura, Biosens. Bioelectron. 20 (2004)

350–357.

[46] K.V. Gobi, H. Tanaka, Y. Shoyama, N. Miura, Sens. Actuators B 111–112 (2005) 562–571.

[47] S. Kumbhat, D.R. Shankaran, S.J. Kim, K.V. Gobi, V. Joshi, N. Miura, Chem. Lett. 35 (2006) 678–679.

[48] N. Miura, D.R. Shankaran, T. Kawaguchi, K. Matsumoto, K. Toko, Electrochemistry 75 (2007) 13–22.

[49] N. Soh, T. Tokudo, T. Watanabe, K. Mishima, T. Imato, T. Masadome, Y. Asano, S. Okutani, O. Niwa, S. Brown, Talanta 60 (2003) 733–745.

[50] K.D. Kihm, S. Cheon, J.S. Park, H.J. Kim, J.S. Lee, I.T. Kim, H.J. Yi, Opt. Lasers Eng. 50 (2012) 64–73.

[51] M.M. Walczak, D.D. Popenoe, R.S. Deinhammer, B.D. Lamp, C.K. Chung, M.D. Porter, Langmuir 7 (1991) 2687–2693.

[52] K. Shimazu. Y. Hashimoto, T. Kawaguchi, K. Tada, J. Electroanal. Chem. 534 (2002) 163–169.

[53] K. Shimazu. T. Kawaguchi, T. Isomura, J. Am. Chem. Soc. 124 (2002) 652–661.

[54] C.J. Zhong, J. Zak, M.D. Porter, J. Electroanal. Chem. 421 (1997) 9–13.

[55] M.M. Walczak, C.A. Alves, B.D. Lamp, M.D. Porter, J. Electroanal. Chem. 396 (1995) 103–114.

[56] D.S. Karpovich G.J. Blanchard, Langmuir 10 (1994) 3315–3322.

[57] N. Camillone, C.E.D. Chidsey, G. Liu, G. Scoles, J. Chem. Phys. 98 (4) (1993) 3503–3511.

[58] T. Kawaguchi, H. Yasuda, K. Shimazu, Langmuir 16 (2000) 9830–9840.

[59] J.A. Williams, C.B. Gorman, J. Phys. Chem. 111 (2007) 12804–12810.

[60] W.E. Rudzinski, K. Francis, Appl. Surf. Sci. 256 (2010) 5399–5405.

[61] M. Liu, B. Ning, Y. Peng, J. Dong, N. Gao, L. Liu, Z. Gao, Sens. Actuators B 161 (2012) 124–130.

[62] D.R. Shankaran, K. Matsumoto, K. Toko, N. Miura, Sens. Actuators B 114 (2006) 71–79.

[63] K. Matsumoto, A. Torimaru, S. Ishitobi, T. Sakai, H. Ishikawa, K. Toko, N. Miura, T. Imato, Talanta 68 (2005) 305–311.

[64] D.R. Shankaran, K.V. Gobi, K. Matsumoto, K. Toko, Sens. Actuators B 100 (2004) 450–454.

[65] Y. Li, J. Ren, H. Nakajima, B.K. Kim, N. Soh, K. Nakano, T. Imato, Talanta 77 (2008) 473–478.

[66] H. Aizawa, Y. Gokita, J.W. Park, Y. Yoshimi, S. Kurosawa, IEEE Sensors Journal 6 (2006) 1052–1056.

[67] G. Sakai, S. Nakata, T. Uda, N. Miura, N. Yamazoe, Electrochim. Acta 44 (1999) 3849–3854.

[68] G. Sakai, K. Ogata, T. Uda, N. Miura, N. Yamazoe, Sens. Actuators B 49 (1998) 5–12.

Chapter 4

Effect of alkanethiol molecular structure on sensitivity of SPR sensor

4.1 Introduction

Biosensors are analytical devices that measure binding of analytes to surfaces, a binding biomolecules (e.g., DNA, protein, enzyme, and antibody) induce a signal in a physichochemical transducer [1–4]. Several developments in biosensors have been reported, such as fluidic design [5–7], sensor surface immobilization [8–11], advances in detection methods [12–15], and data analysis [15–16]. An ideal biosensor is reliable, selective, sensitive, quick to respond, and inexpensive to fabricate. To achieve an ideal biosensor, accurate design and control of the interfacial chemical reaction are important in biosensing and surface engineering [17]. Among the interfaces with molecular recognition, self-assembled monolayers (SAMs) have received attention because of advantages such as excellent stability and direct integration with biomolecular materials, and the possibility of molecular-level control in applications such as sensors, catalysts [18–20]. SAMs can be easily prepared on metal surfaces, because adsorbates (e.g., thiol and silane) can spontaneously organize into crystalline or semicrystalline structures. Thus, these adsorbates form highly ordered and highly oriented monolayers on surfaces. Known to date, the molecular structure controlling the detection has not been reported yet. Therefore, in this study, I investigated the influence of various molecular structure of monolayer sensor surface that determines sensitivity of an immunoassay. I propose that the sensor surface structure plays an important role in interactions with the target

compound.

In my previous work described at chapter 3 [21], I fabricated a biosensor chip using succinimidyl-terminated propanethiol prepared from dithiobis(succinimidyl propionate) (DSP). I found that the surface coverage of SAM depended on DSP solution concentration used in self-assembly process. Moreover, the surface distribution of antigen immobilized on the surface was strongly correlated with the DSP solution concentration. It concluded that the coverage of immobilized antigen on surface affects the immunoassay sensitivity.

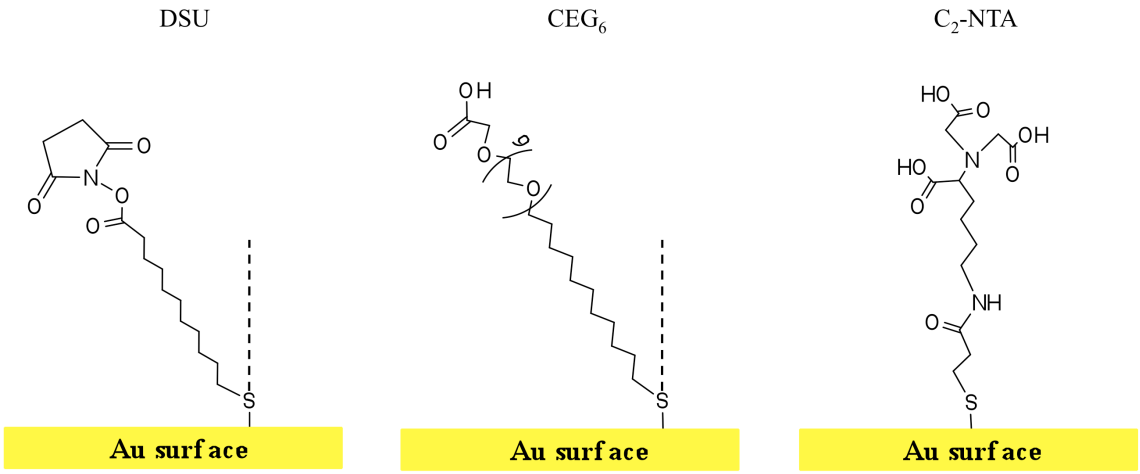

Figure 4.1 Three-dimensional structures of DSU, CEG_6, and C_2-NTA thiols sensor surfaces.

To further explore the key factors controlling sensitivity of detection, three types of alkanethiol structures are examined in this work, as illustrated in Figure 4.1: (1) straight-chain alkanethiol prepared from dithiobis(succinimidyl undecanoate) (DSU), (2) flexible-chain alkanethiol prepared from carboxy-EG_6-undecanethiol (CEG_6), and (3) three-branched alkanethiol (dendrimer alkanethiol, C_2-NTA)

prepared from 3,3′-dithiobis[*N*-(5-amino-5-carboxypentyl)propionamide-*N*,*N*′-diacetic acid]. DSU is a well-known succinimidyl-terminated alkanethiol for biosensors [22–24]. DSU has a long straight alkyl chain and a succinimidyl group in the head group; it forms a highly oriented and concentrated monolayer on Au surfaces [24]. CEG_6 is widely used as a biochemical linker because of its ability to prevent nonspecific adsorption [25–28]. C_2-NTA is of interest to researchers because of its well-defined molecular structure and interesting properties, such as low intrinsic viscosity and solubility higher than analogues linear molecules [29]. Thus, I surmised that these three alkanethiols could covalently immobilize the target analyte in different orientations on the sensor surface.

The target analyte is clenbuterol, which is a controversial substance in sports because of doping. Clenbuterol is a member of the β-adrenergic agonist family, and its primary medical use is as a bronchodilator agent in asthma treatments [30–31]. Farmers illegally use this compound to boost muscle tissue production of their livestock, such as pigs, cows, and turkeys to increase profit. Because doping is a serious issue in global competitions, such as the soccer World Cup, the Olympics, and *Tour de France*, attention to this β-adrenergic agonist compound has intensified because of its easy uptake and deposition in the human body with daily meat consumption. Thus, developing a reliable detection method with high sensitivity and rapid detection time is necessary.

In this study, surface plasmon resonance (SPR) is used to sense clenbuterol because it satisfies the above requirements for practical use. SPR is well known as a highly optical transducer based on surface plasmon phenomena. SPR monitors the dielectric constant change at the interface caused by a binding event of target analyte

and bio-interfacial material. Even though the limit of detection (LOD) for measuring mass change using my SPR sensor is approximately 30 pg/cm^2, the detection of a small-sized target in a short time remains difficult. Therefore, I used an indirect competitive inhibition immunoassay [14]. Compared to other immunoassays, this immunoassay has a better sensitivity for detection of a small analyte, because the mass transducer react to mass change due to binding of an antibody instead of an antigen (a lightweight analyte). However, the mechanism for this enhancement remains unclear. For rapid detection, the sensor monitors the initial process of immunoreaction, which is affected by the concentration of analyte according to the Langmuir equation. Therefore, I also discuss the effect of kinetics on the immunoassay sensitivity.

4.2 Fabrication of the sensor surfaces

Figure 4.2 shows the SPR sensorgram of the fabrication process. Firstly, the thiols monolayer was formed on an Au surface by self-assembly process from 5 mM solution concentration for each thiol with the flow rate of 5μL min^{-1}. Since the DSU solution is diluted in chloroform, so the preparation of DSU monolayer was done by immersion process at outside the SPR system to avoid the damage of the flow system by chloroform.

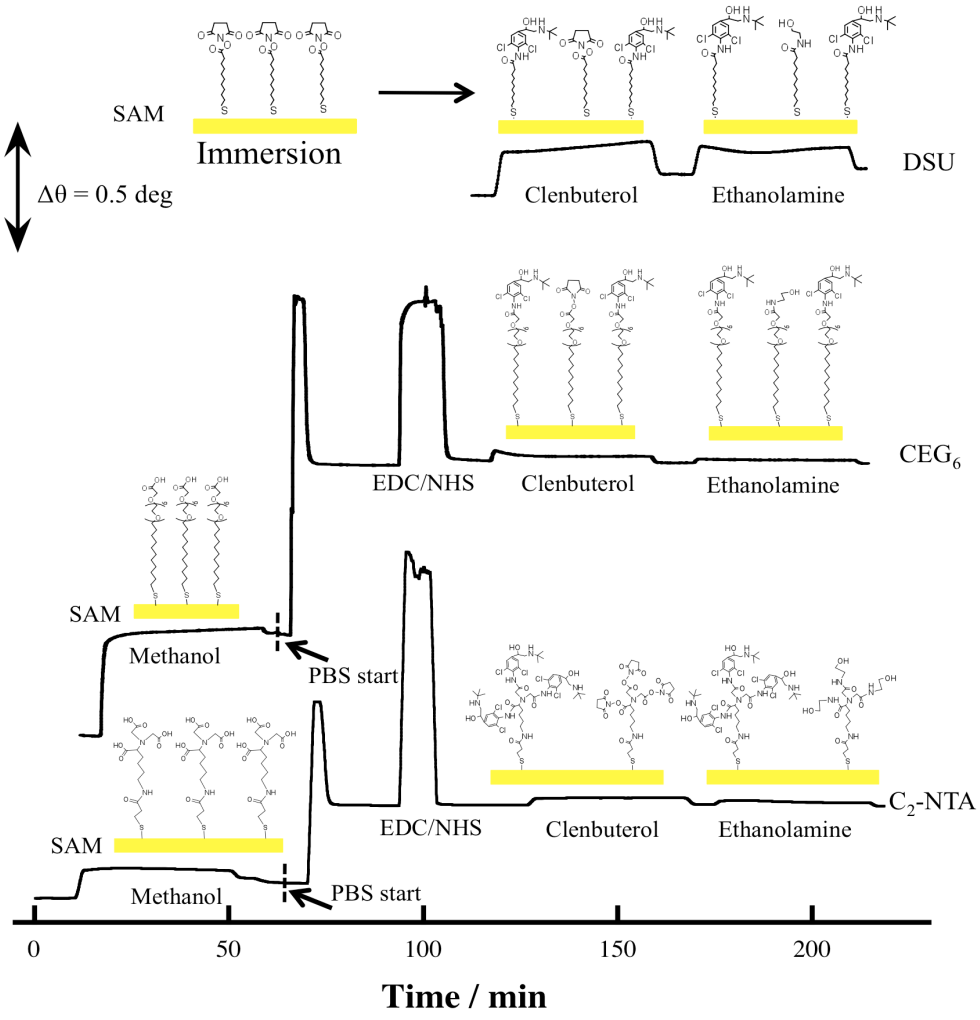

Figure 4.2 SPR sensorgram for fabrication of the sensor surface by using functionalized various thiols monolayer (DSU, C_2-NTA and CEG_6) on Au surface. Flow rate was 5μL min^{-1}.

In order to convert carboxyl group to succinimidyl group, EDC/NHS (0.2M/0.05M) was used. Then, clenbuterol solution (PBS solution containing 1 mg mL^{-1} of clenbuterol) was injected for 40-min (equal to flow rate at 5μL min^{-1}). On this process, succinimidyl group replace to clenbuterol. Although clenbuterol sufficiently flowed over the succinimidyl group terminated propanethiol monolayer on sensor chip, unreacted succinimidyl groups still remained. In order to protect unreacted succinimidyl groups, ethanolamine (PBS solution containing 1 mg mL^{-1},

blocking agent) is injected for 40-min as well. Unreacted succinimidyl groups totally replace to ethanolamine. These sensor surfaces are very stable, because this fabrication is consisted only with covalent bonds (S-Au, S-S, and NHCO) [32] and later on will be used for the detection of target analysis.

4.3 Immunoassay

For detecting clenbuterol, the indirect competitive inhibition method was employed. Some researchers had been reported the assay protocol of this method [32-35]. In this work, the Ab solution (PBS solution containing 1 μg mL^{-1} of monoclonal mouse IgG antibody of clenbuterol) premixed with a sample solution (PBS solution containing clenbuterol) before the injection into the sensing system. As the mixed solution flowed over the sensor surface, the SPR senses the dielectric constant change at the interface due to the binding of the unreacted Ab to clenbuterol-immobilized on the sensor surface. After the detection, Ab is detached from the sensor surface by 0.1 M sodium hydroxide. Thus, the sensor surface was used for the detection of clenbuterol again. Here, I confirm reproducibility by using different sensor chips (N>3), and each plot is averaged within 10% experimental error bars.

4.4 Results and Discussion

4.4.1 Characterization of various alkanethiol monolayers

Electrochemical reductive desorption is performed to investigate the structure of monolayer (Figure 4.3). Since S–Au bond can be electrochemically cleaved by

one-electron reaction; the surface concentration of the monolayer can be estimated from the charge density, which is calculated from the integration of reduction current.

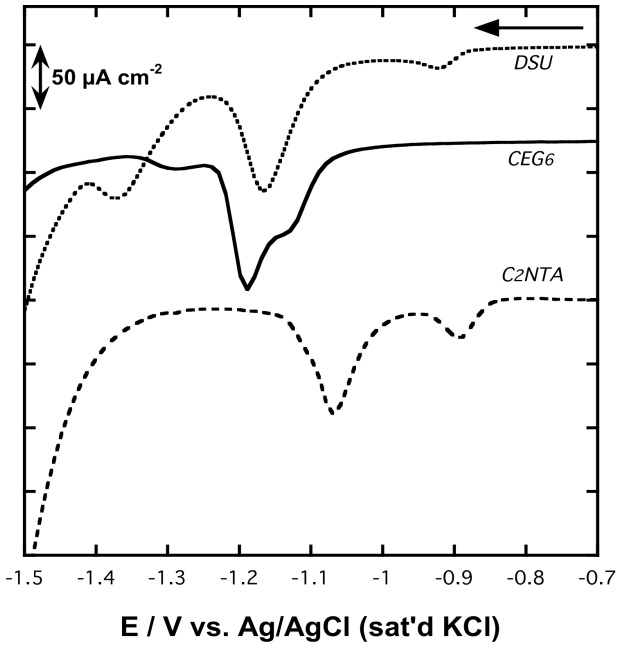

Figure 4.3 Voltammograms of reductive desorption of DSU, CEG_6 and C_2-NTA monolayer. Electrolyte solution was 0.1 M KOH, while sweep rate was 0.1 V s^{-1}.

The reduction current shows several peaks in the range of –0.9 V to –1.35 V. This is the characteristic of reductive desorption on a polycrystalline Au electrode [36]. By comparing the peak positions in the voltammograms of similar systems reported previously, it is considered that peak at approximately –0.90 V resulted from the desorption of alkanethiols from the terraces [37], and the peaks at –1.08 V to –1.37 V were due to the desorption of alkanethiols adsorbed on the steps [38–39] of polycrystalline Au.

The surface concentrations (after considering the roughness factor 1.50) of DSU, CEG_6 and C_2-NTA thiols are 6.6 x 10^{-10} mol cm^{-2}, 8.5 x 10^{-10} mol and 4.6 x 10^{-10} mol cm^{-2} respectively. If I further consider that –30% of error could include in the calculated surface concentration by voltammogram reductive desorption from the double layer electrical charge, so this result is comparable with the results from SPR experiments (see Table 4.1).

Table 4.1 Surface concentrations of various alkanethiols monolayer and immobilized antigen calculated by different methods.

Thiols	**Surface concentration** (x 10^{-10} mol cm^{-2})		
	SPR		**Electrochemistry**
	Thiol	Immobilized Antigen	Thiol
DSU	Immersion	0.7 ± 0.2	6.6 ± 0.4
CEG_6	5.5 ± 0.1	1.0 ± 0.1	8.5 ± 0.5
C_2-NTA	2.6 ± 0.1	1.2 ± 0.1	4.6 ± 0.2

The surface concentrations of immobilized antigens (clenbuterol) to various monolayers were almost the same. Those values mentioned in Table 4.1 are comparable each other at approximately 1.0 x 10^{-10} mol cm^{-2} for DSU, CEG_6 and C_2-NTA, respectively. Therefore, instead of the surface concentration of thiols monolayer, the molecular structure of various thiols on the surface are believed take an important rule in affecting the sensitivity of detection.

4.4.2 Detection of clenbuterol

Figure 4.4 (A-C) shows the representative sensorgram of immunoreaction with Ab for DSU, CEG_6 and C_2-NTA sensor surfaces, respectively. While Ab standard solution flows over the sensor surface for 250 s (from t = 100 s to t = 350 s), the resonance angle shifts gradually to the higher values with the binding of Ab by the immobilized antigen onto the sensor surface. Difference in the resonance angle before (t = 100 s) and after (t = 400 s) the binding of Ab to the immobilized antigen is the total resonance angle shift ($\Delta\theta$) of the immunoreaction: this value is used for calculating the surface concentration.

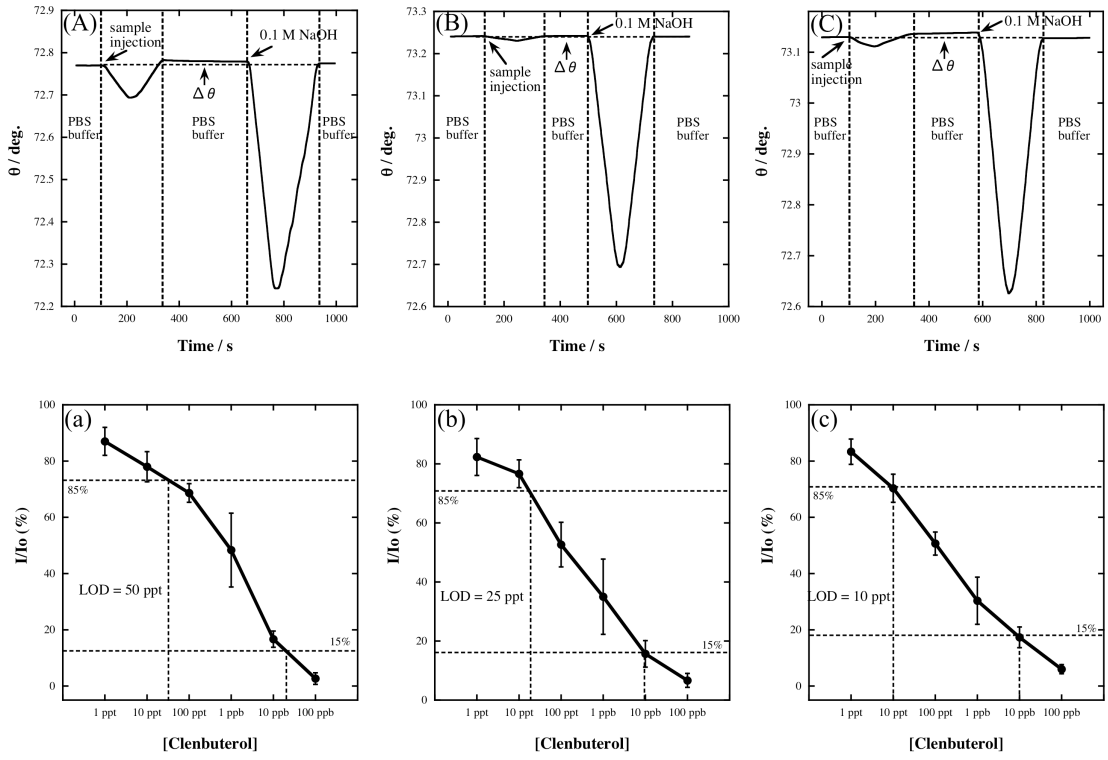

Figure 4.4 SPR sensing format for immunoreaction at (A) DSU, (B) CEG_6 and (C) C_2-NTA sensor surfaces at the flow rate of 100μL min^{-1}. Clenbuterol detection by using indirect competitive inhibition immunoassay on various sensor surfaces: (a)

DSU, (b) CEG_6 and (c) C_2NTA. Inhibition rate was calculated from the angle shift in presence (I)/absence (I_0) of clenbuterol. In the premixing process, 1 ppm Ab was mixed with series of clenbuterol concentrations. The incubation time was 2 min.

After the immunoreaction, the sensor surface is regenerated by a solution of 0.1 M sodium hydroxide till the value of the resonance angle returns to. Through such a regeneration process, the sensor surface can be reused for over 100 immunoreactions. One immunoreaction–regeneration cycle takes only 1000 s.

Indirect competitive inhibition immunoassay is employed for detecting clenbuterol. SPR senses the change in dielectric constant due to the binding of antibody by the immobilized antigen (clenbuterol) at the interface. From the sigmoid curve, it was achieved the limit of the detection (LOD) of clenbuterol by various thiols sensor surface at 50 ppt (DSU), 25 ppt (CEG_6) and 10 ppt (C_2-NTA) respectively (Figure 4.4a-c). Since the surface concentration of immobilized antigens (clenbuterol) were almost the same for any kind of thiols (Table 4.1), the different in molecular structure of monolayer highly affected on sensitivity of detection. From the Figure 4.4, the branched-molecular structure of C_2-NTA sensor surface reveals highest sensitivity at 10 ppt. The kinetic aspect of different molecular structure sensor surface in relation with sensitivity detection will be discussed below.

4.4.3 Kinetic analysis

By following the past works [40-44], the affinity constant K_1 of Ab to the clenbuterol-immobilized sensor surface and the maximum angle shift of the SPR after Ab injection ($\Delta\theta_{0,max}$) were determined using a Langmuir-type adsorption model as mentioned in Chapter 3:

$$\frac{[Ab]}{\Delta\theta_0} = \frac{[Ab]}{\Delta\theta_{0,\max}} + \frac{1}{K_1\ \Delta\theta_{0,\max}} \qquad \text{(Eq. 3.3)}$$

And K_2 as affinity constant of Ab to the free clenbuterol in the solution (Figure 4.5 a and b) following this equation:

$$\frac{1}{\Delta\theta} = \frac{1}{\Delta\theta_0} + \frac{K_2\ \alpha\ [Clb]_0}{[Ab_{total}]\ K_1\ \Delta\theta_{0,\max}} \qquad \text{with } 0 < \alpha < 1 \qquad \text{(Eq. 3.8)}$$

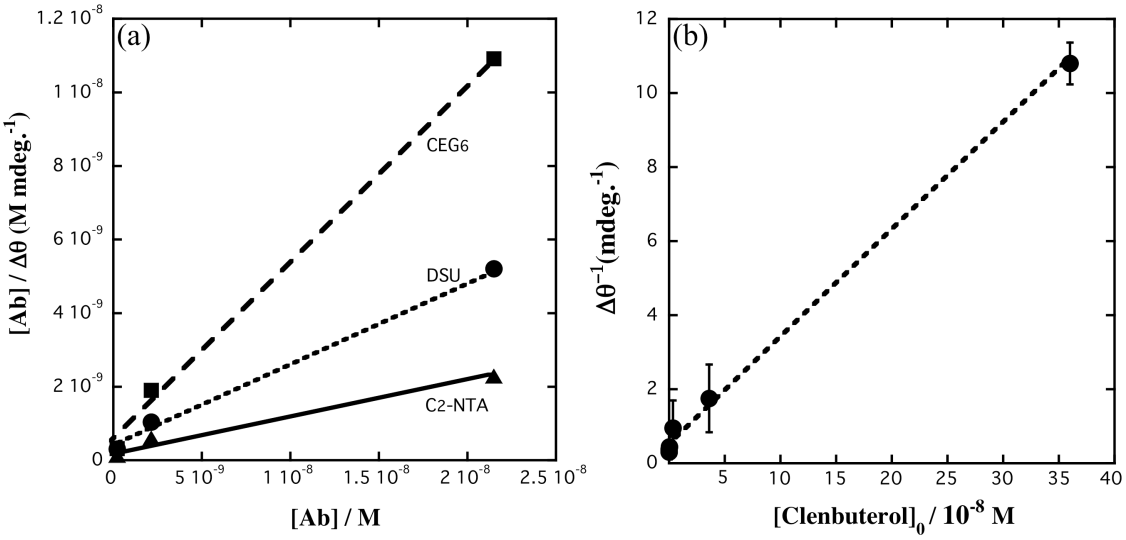

Figure 4.5 (a) Langmuir adsorption isotherm plot for binding of anti-clenbuterol antibody (Ab) to clenbuterol immobilized on the sensor surface, and (b) clenbuterol solution concentration dependence using indirect competitive inhibition immunoassay.

From the kinetics analysis, it is calculated that the affinity constants of antibody to the antigen immobilized to the surface (K_1) were 5.2 x 10^8 M^{-1}, 9.7 x 10^8

M^{-1}, and 4.8 x 10^8 M^{-1} for DSU, CEG_6 and C_2-NTA, respectively. While, affinity constants of antibody to the free antigen in solution ($\alpha.K_2$) was (1.8 ± 0.8) x 10^9 M^{-1}. Considering these kinetic parameters of various thiols sensor surface for the detection of clenbuterol, a lower K_1 of C_2-NTA sensor surface in combination with a higher $\alpha.K_2$ reveals the better sensitivity (10 ppt). This result shows same statement with the previous result in the study of clenbuterol detection using DSP alkanethiol monolayer, that lower K_1 showed the highest sensitivity. The values of K_1 and K_2 are related to the sensor surface structure characteristic. Sensor surface constructed from high orientation DSU monolayer and flexible arm CEG_6 give higher K_1, while branched structure of dendrimer C_2-NTA affect on the lowest K_1 produces higher LOD value. Therefore, molecular structure characteristic of C_2-NTA sensor surface highly affects on sensitivity of detection.

4.5 Summary

This study investigates the affect of various alkanethiols monolayer characteristic to the sensing performance of SPR. To immobilize clenbuterol onto the sensor surface, succinimidyl-terminated various alkanethiols monolayer were fabricated on an Au-chip by self-assembly. EDC/NHS is used to activated the carboxylates terminal (CEG_6 and C_2-NTA) became succinimidyl group. Then, *N*-hydroxysuccinimide group of the succinimidyl-terminated alkanethiols were replaced with covalently linked clenbuterol at neutral pH.

It was found that the sensitivity of the detection of clenbuterol target analyte highly dependent on the characteristic of sensor surface. The sensor surface prepared

by dendrimer C_2-NTA showed a highest sensitivity (LOD = 10 ppt). The characteristic of regular-branched molecule with different orientation of dendrimer is corresponding with C_2-NTA high sensitivity value, reflected on low K_1 and high K_2.

However, the higher affinity constants K_1 coupled with lower K_2 exhibited by the DSU and CEG_6 sensor surfaces were coupled to a lower sensitivity of detection (50 ppt and 25 ppt for DSU and CEG surfaces, respectively). This immunosurface is very stable and can be regenerated by 0.1 M sodium hydroxide for >100 times of usage. Furthermore, the detection process also very rapid since one immunoreaction–regeneration cycle took only 1000 s.

4.6 References

(1) X. Fan, I.M. White, S.I. Shopova, H. Zhu, Anal. Chim. Acta 620 (2008) 8–26.

(2) S.B. VanEngelenburg, A.E. Palmer, Curr. Opin. Chem. Biol. 12 (2008) 60–65.

(3) A. Villaverde, FEBS Letters 554 (2003) 167–172.

(4) A.K. Trilling, J. Beekwilder, H. Zuilhof, Analyst 138 (2013) 1619–1627.

(5) A.R. Wheeler, S. Chah, R.J. Whelan, R.N. Zare, Sens. Actuators B 98 (2004) 208–214.

(6) C.C.L. Loureiro, A.M.N. Lima, H. Neff, J. Phys.: Conference Series 85 (2007) 1–8.

(7) C.J. Huang, W. Knoll, A. Sessitsch, J. Dostalek, Talanta 122 (2014) 166–171.

(8) W. Putzbach, N.J. Ronkainen, Sensors 13 (2013) 4811–4840.

(9) M. Joshi, N. Kale, V.R. Rao, S. Mukherji, Biosens. Biolelectron. 22 (2007) 2429–2435.

(10) C.W. Chiu, X. He, H. Liang, Acta 94 (2013) 42–48.

(11) S. Yeo, C. Choi, C.W. Jang, S. Lee, Y.M. Jhon, Appl. Phys. Lett. 102 (2013) 073106.

(12) J. Pribyl, M. Hepel, J. Halamek, P. Skladal, Sens. Actuators B 91 (2003) 333–341.

(13) M. Liu, B. Ning, L. Qu, Y. Peng, J. Dong, N. Gao, L. Liu, Z. Ghao, Sens. Actuators B 161 (2012) 124–130.

(14) D.R. Shankaran, K.V. Gobi, N. Miura, Sens. Actuators B 121 (2007) 158–177.

(15) X.D. Hoa, A.G. Kirk, M. Tabrizian, Biosens. Biolelectron. 23 (2007) 151–160.

(16) M.G. Manera, E.F. Vila, J.M.G. Martin, A.G. Martin, R. Rella, Biosens. Biolelectron. 58 (2014) 114–120.

(17) P. Koegler, A. Clayton, H. Thissen, G.N.C. Santos, P. Kingshott, Adv. Drug Delivery Rev. 64 (2012) 1820–1839.

(18) N.K. Chaki, K. Vijayamohanan, Biosens. Biolelectron. 17 (2002) 1–12.

(19) S.K. Arya, P.R. Solanki, M. Datta, B.D. Malhotra, Biosens. Biolelectron. 24 (2009) 2810–2817

(20) V. Chaudhari, H.M.N. Kotresh, S. Srinivasan, V.A. Esaulov, J. Phys. Chem. C 115 (2011) 16518–16523.

(21) Suherman, K. Morita, T. Kawaguchi, manuscript under preparation.

(22) N.M. Grubor, R. Shinar, R. Jankowiak, M.D. Porter, G.J. Small, Biosens. Biolelectron. 19 (2004) 547–556.

(23) M.D. Porter, R.J. Lipert, L.M. Siperko, G. Wang, R. Narayanan, Chem. Soc. Rev. 37 (2008) 1001–1011.

(24) J.M. Encarnacao, L. Rosa, R. Rodrigues, L. Pedro, F.A. da Silva, J. Goncalves, G.N.M. Ferreira, J. Biotechnol. 132 (2007) 142–148.

(25) Y. Zhang, Y. Chen, G. Jin, Sens. Actuators B 159 (2011) 121–125.

(26) K. Nagatomo, T. Kawaguchi, N. Miura, K. Toko, K. Matsumoto, Talanta 79 (2009) 1142–1148.

(27) T. Kawaguchi, D.R. Shankaran, S.J. Kim, K.V. Gobi, K. Matsumoto, K. Toko, N. Miura, Talanta 72 (2007) 554–560.

(28) X. Lou, L. He, Sens. Actuators B 129 (2008) 225–230.

(29) S.M. Grayson, J.M.J. Frechet, Chem. Rev. 101 (2001) 3819–3867.

(30) C. Juan, C. Igualada, F. Moragues, N. leon, J. Manes, J. Chromatogr. A 1217 (2010) 6061–6068.

(31) C. Li, Y-L. Wu, T. Yang, Y. Zhang, W-G. Huang-Fu, J. Chromatogr. A 1217 (2010) 7873–7877.

(32) T. Kawaguchi, D.R. Shankaran, S.J. Kim, K. Matsumoto, K. Toko, N. Miura, Sens. Actuators B 133 (2008) 467–472.

(33) M. Liu, B. Ning, Y. Peng, J. Dong, N. Gao, L. Liu, Z. Gao, Sens. Actuators B 161 (2012) 124–130.

(34) D.R. Shankaran, K. Matsumoto, K. Toko, N. Miura, Sens. Actuators B 114 (2006) 71–79.

(35) K. Matsumoto, A. Torimaru, S. Ishitobi, T. Sakai, H. Ishikawa, K. Toko, N. Miura, T. Imato, Talanta 68 (2005) 305–311.

(36) K. Shimazu, T. Kawaguchi, T. Isomura, J. Am. Chem. Soc. 124 (2002) 652–661.

(37) K. Shimazu, Y. Hashimoto, T. Kawaguchi, K. Tada, J. Electroanal. Chem. 523 (2002) 163–169.

(38) C.J. Zhong, J. Zak, M.D. Porter, J. Electroanal. Chem. 421 (1997) 9–13.

(39) M.M. Walczak, C.A. Alves, B.D. Lamp, M.D. Porter, J. Electroanal. Chem. 396 (1995) 103–114.

(40) Y. Li, J. Ren, H. Nakajima, B.K. Kim, N. Soh, K Nakano, T. Imato, Talanta 77 (2008) 473–478.

(41) H. Aizawa, Y. Gokita, J.W. Park, Y. Yoshimi, S. Kurosawa, IEEE Sensors Journal 6 (2006) 1052–1056.

(42) N. Soh, T. Tokudo, T. Watanabe, K. Mishima, T. Imato, T. Masadome, Y. Asano, S. Okutani, O. Niwa, S. Brown, Talanta 60 (2003) 733–745.

(43) G. Sakai, S. Nakata, T. Uda, N. Miura, N. Yamazoe, Electrochim. Acta 44 (1999) 3849–3854.

(44) G. Sakai, K. Ogata, T. Uda, N. Miura, N. Yamazoe, Sens. Actuators B Chem. 49 (1998) 5–12.

Chapter 5

Highly selective and sensitive detection of ractopamine and salbutamol using SPR sensor

5.1 Introduction

β-Agonists are usually used as drugs for the treatment of respiratory diseases and asthma [1]. However, due to their potential roles in reducing animal fat levels and increasing the amount of muscling in livestock, β-agonists were used in animals as growth promoters to increase the daily weight gain [2]. Due to their stable properties, β-agonists compounds can be easily stored in human tissues after meat consumption, and result in many serious health problems with symptoms such as palpitations, tremors and tachipnoea [3]. Furthermore, more than 150 countries have strictly banned the use of β-agonists in stockbreeding, including China, Japan and Europe, due to their negative side effects in the human body [4].

Inspection services for food safety are particularly interested in the three main β-agonists, i.e., clenbuterol, ractopamine and salbutamol. Thus, ractopamine and salbutamol are the targets of this study. However, they have similar chemical structures (i.e., they are phenyl ethanolamine compounds) [5] and almost the same molecular weight (230–300 Da). In the past studies, analytical methods using high-performance liquid chromatography [6], liquid chromatography/tandem mass spectrometry [7–10] and gas chromatography–mass spectrometry [11] have been reported for determining β-agonists residues. Although these chromatographic approaches can provide satisfactory reproducibility, they are time consuming, require

high sensitivity and less appropriate for onsite usage due to elaborate sample preparation [5].

Biosensors are effective technology for detecting chemical and biological analytes. Among biosensors, optical biosensors based on surface plasmon resonance (SPR) provide high sensitivity without using molecular labels. Thus, the sample preparation time can be minimized. To date, SPR biosensors have been reported in various applications such as medical diagnostics, drug discovery, environmental monitoring, food safety and homeland security [12–19]. SPR can be used as a mass transducer and monitor the dielectric constant as the resonance angle shift. In my SPR system, the limit of detection (LOD) for the resonance angle shift is 0.03 mdeg (0.3 RU). Thus, a mass change of 0.03 ng cm^{-2} due to the adsorption of a protein can be detected. Among the mass transducers, the SPR sensors show the highest sensitivity. To add selectivity to the highly sensitive SPR sensor, immunoassay is usually used. Recently, various methods of immunosensor surface fabrication have been reported. In my previous study, clenbuterol equipped with an amine group was directly immobilized onto a succinimidyl propanethiol monolayer on the sensor surface by amide coupling reaction. However, ractopamine and salbutamol do not have a functional group that can form a steady chemical bond to thiol compounds. Thus, I choose to immobilize the ractopamine–bovine serum albumin (RCT–BSA) conjugate and the salbutamol–horseradish peroxidase (SAL–HRP) conjugate onto a succinimidyl propanethiol monolayer. For the immobilization of the protein conjugate, the physical adsorption method has been proposed [20, 21]. This method exploits the hydrophobic interaction between proteins and the Au surface. However, this interaction is weak, and therefore, the surface could be regenerated up to 30

times by using glycosine–HCl solution [20]. I propose here an immunosensor surface consisting of self-assembled alkanethiol monolayer on a Au chip for highly sensitive and selective detection of ractopamine and salbutamol. Succinimidyl-terminated propanethiol monolayer is easily prepared from dithiobis(succinimidyl) propionate (DSP) by self-assembly process. Subsequently, protein conjugates can be instantly immobilized by replacing the succinimidyl group with an NH_2 group of a protein in a neutral buffer in a single-step reaction. This study discusses the structure of protein conjugates immobilized sensor surfaces by using scanning tunneling microscopy (STM) observation. Moreover, I propose the selectivity test procedures for multiple target detection in indirect competitive inhibition immunoassay.

5.2 Fabrication of the sensor surfaces

Figure 5.1 shows SPR sensorgram of the fabrication of the sensor surfaces. First, self-assembly of alkanethiol monolayer is conducted by injecting 5 mM DSP methanolic solution over the surface of an unmodified Au chip for 40min at a flow rate of 5 $\mu L \cdot min^{-1}$ immediately after the resonance angle became stable during the flowing of methanol running solution (Figure 5.31(i)). With this self-assembly process, the Au surface completely covered by a succinimidyl-terminated propanethiol monolayer. Second, the SPR running solution is switched from methanol to PBS (pH 7.4). The change of the SPR running solution caused an abrupt shift up of the resonance angle due to the refractive index difference between methanol and PBS solution. After the resonance angle became stable again, protein conjugates (PBS solution containing 50 ppm of ractopamine–BSA or salbutamol–

HRP conjugates) were injected for 40min (Figure 5.1(ii)). With this process, the succinimide group is replaced to provide β-agonist protein conjugates.

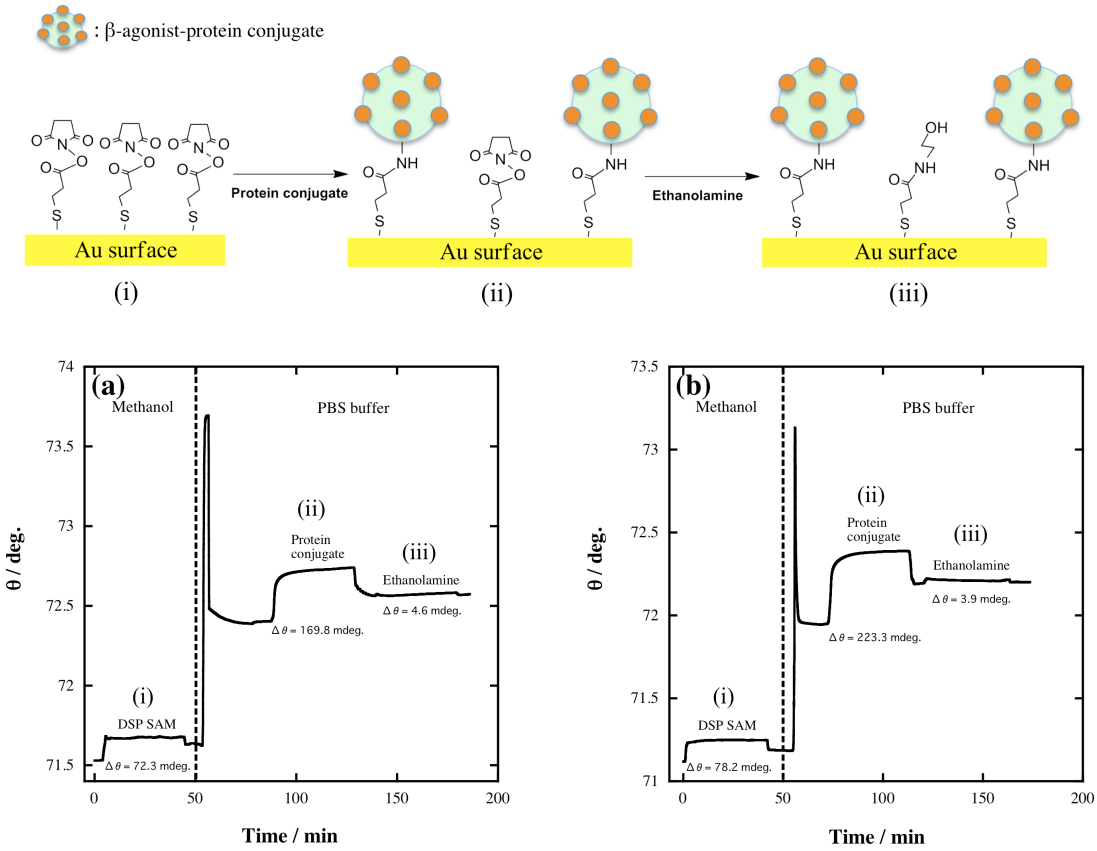

Figure 5.1 SPR sensorgram of the fabrication of the sensor surface at the flow rate of 5μL min^{-1}: (i) self-assembly of the succinimidyl-terminated propanethiol monolayer, (ii) immobilization of the β-agonistprotein conjugates (ractopamine–BSA and salbutamol–HRP), and (iii) blocking of the unreacted succinimidyl-terminated propanethiol with ethanolamine.

Although protein conjugates sufficiently flowed over the succinimidyl-terminated propanethiol monolayer on the sensor chip, unreacted succinimide groups remained. To prevent the occurrence of nonspecific adsorption, ethanolamine (PBS solution containing 1 $mg{\cdot}mL^{-1}$, blocking agent) is injected for 40min to protect the

remaining succinimide groups (Figure 5.1(iii)). Unreacted succinimide groups are completely blocked by ethanolamine. Then, the sensor surface is used for detecting β-agonist compounds.

5.3 Immunoassay

The immunoassay format of indirect competitive inhibition is employed for detecting β-agonist compounds, as previously described [22–24]. As an optical transducer, SPR observes the dielectric constant changes due to the adsorption of heavyweight antibodies instead of lightweight antigens (β-agonists) at the interface. Thus, larger signal responses are expected in this immunoassay.

In this study, the Ab solution (PBS solution containing 1 $\mu g \cdot mL^{-1}$of Ab) is first premixed with a sample solution (PBS solution containing β-agonist compounds) before injection into the sensing system. As the mixed solution flows over the sensor surface, the SPR senses the dielectric constant changes due to the binding of unreacted Ab to the antigen immobilized on the sensor surface. After detection, Ab was removed from the sensor surface by using 0.1 M sodium hydroxide. Hence, the sensor surface is again used for the detection. Moreover, I confirmed the reproducibility by using different sensor chips (N>3), and each plot was averaged within 10% experimental error bars.

5. 4 Results and Discussion

5.4.1 Detection of β-agonist compounds

Figure 5.2 shows the representative sensorgrams of the immunoreaction with anti-ractopamine antibody (a) and anti-salbutamol antibody (b) to the sensor surface.

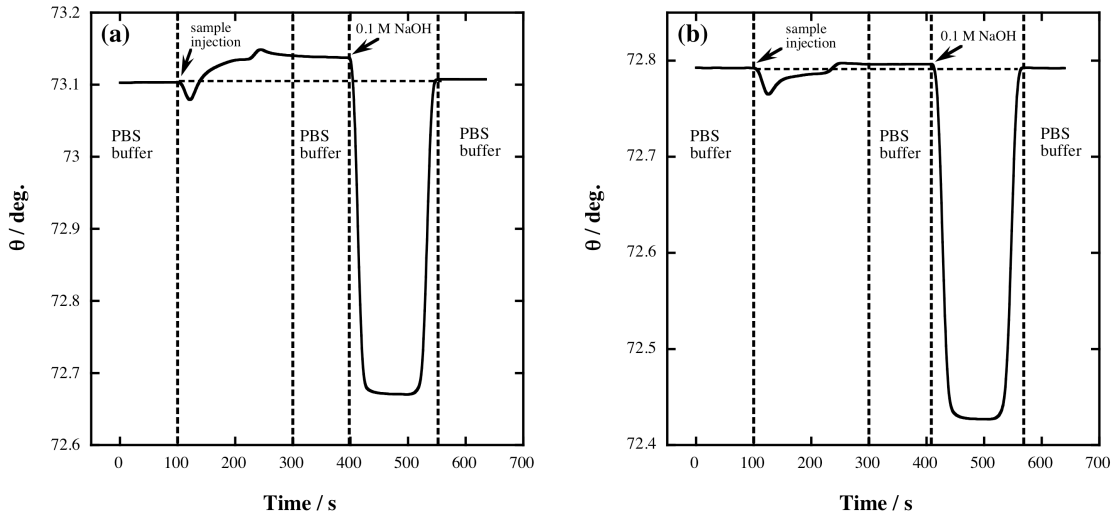

Figure 5.2 SPR sensorgrams of the detection of (a) ractopamine and (b) salbutamol. The flow rate was 100 μL·min^{-1}, PBS (10% ethanol) solution was used as the running solution, and 0.1 M NaOH aqueous solution was used to regenerate the sensor surface.

First, since the sample solution is injected into the SPR system, the resonance angle gradually increases due to the adsorption of Ab onto the sensor surface, and after 200 s, it stabilized. The resonance angle difference between 100 s and 300 s, which was determined as the total angle shift ($\Delta\theta$) of the immunoreaction, is used to calculate the amount of adsorbed species. From the SPR experiments, $\Delta\theta_0$ for 1 μg·mL^{-1} RCT and 1 μg·mL^{-1} SAL were determined as 32.3 ± 1.6 and 5.7 ± 0.1 mdeg, respectively. The lower value obtained for SAL Ab indicated that it has low affinity to the sensor surface. After the immunoreaction, sensor surface is

regenerated using 0.1 M sodium hydroxide. By this regeneration process, the resonance angle returned to its initial value, thus indicating that only Ab was completely detached from the sensor surface. It is also found that the sensor surface could be used for detection more than 100 times without any damage, even though the repetition time of the protein conjugate physically immobilized sensor surface was limited to 30 times. One immunosensing-regeneration cycle requires only 600 s. Thus, the immunoreaction was repeatedly conducted using the same sensor surface for multiple sensing.

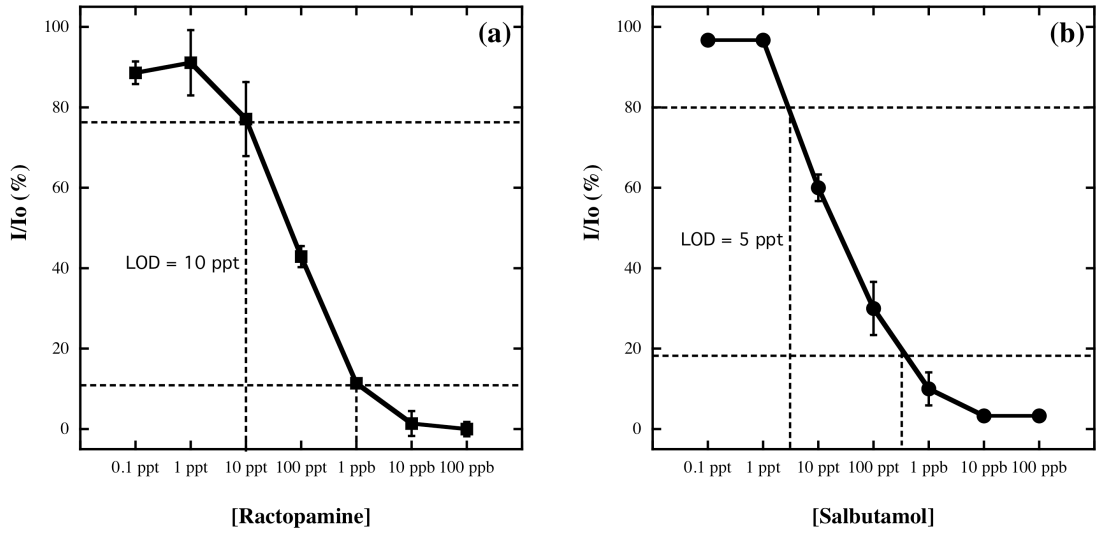

Figure 5.3 Sigmoid curves of β-agonists solution concentration dependence obtained using the indirect competitive inhibition immunoassay. The inhibition rate was calculated from the angle shift in the presence (I)/absence (I_0) of β-agonists. In the premixing process, β-agonists Ab was mixed with a series of antigen concentrations. The incubation time was 2 min.

The detection of β-agonist target compounds is performed by indirect competitive inhibition immunoassay. Figure 5.3 shows the β-agonists solution

concentration dependence on the detection process. From the sigmoid-type curve, the calculated LOD was 5–10 ppt (pg·mL^{-1}). Moreover, this result is comparable to a previous study on the detection of clenbuterol by using alkanethiol monolayer functionalized on a Au surface, which yielded LOD values of 3–7 ppt [25].

5.4.2 Quantitative analysis

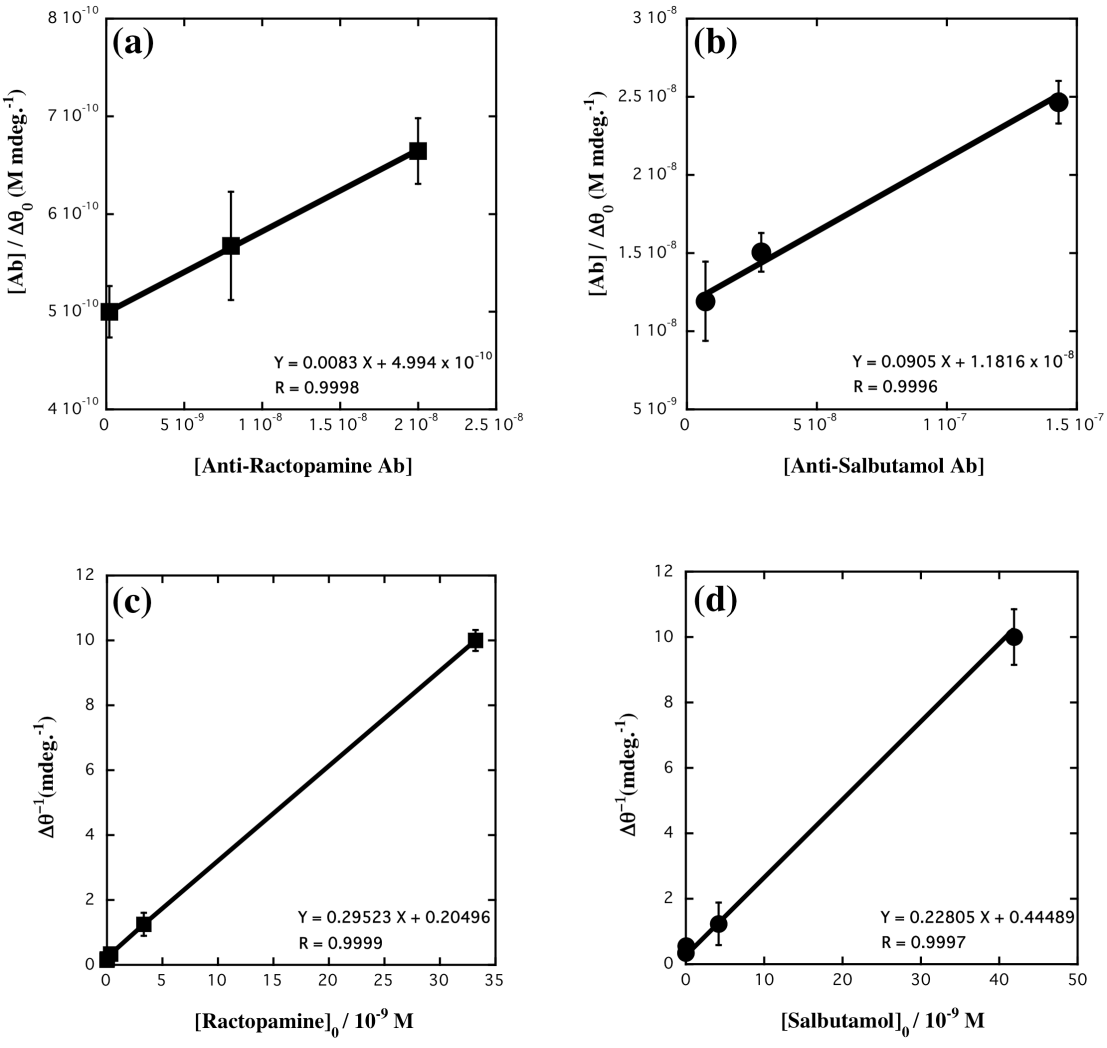

Figure 5.4 Kinetic study of the β-agonists detection. Ab concentration dependence for (a) ractopamine and (b) salbutamol. Antigen concentration dependences for (c) ractopamine and (d) salbutamol.

By following the kinetic analysis reported in past studies [23–24, 26–27], the affinity constant of Ab to the β-agonist (antigen)-immobilized sensor surface (K_1) and the maximum angle shift of the SPR after Ab injection ($\Delta\theta_{0,max}$) are determined using a Langmuir-type adsorption model (Figure 5.4 a and b). For determining $\Delta\theta_{0,max}$, K_1, and K_2 the kinetic equations mentioned in Chapter 3 are followed:

$$\frac{[Ab]}{\Delta\theta_0} = \frac{[Ab]}{\Delta\theta_{0,\max}} + \frac{1}{K_1\,\Delta\theta_{0,\max}} \qquad \text{(Eq. 3.3)}$$

$$\frac{1}{\Delta\theta} = \frac{1}{\Delta\theta_0} + \frac{K_2\,\alpha\,[Clb]_0}{[Ab_{total}]\,K_1\,\Delta\theta_{0,\max}} \qquad \text{with } 0 < \alpha < 1 \qquad \text{(Eq. 3.8)}$$

K_1 and $\Delta\theta_{0,max}$ are calculated as $1.7 \times 10^7\,M^{-1}$ and 120.2 mdeg for RCT and $0.8 \times 10^7\,M^{-1}$ and 11.4 mdeg for SAL, respectively. From the comparison of K_1 for RCT and SAL, the lower K_1 of SAL reveals its higher sensitivity (5 ppt) than that of RCT (10 ppt). Therefore, it can be concluded that lower K_1 corresponds to the higher sensitivity.

The values of K_2 with constant α for RCT and SAL are also estimated as $1.2 \times 10^{10}\,M^{-1}$ and $2.9 \times 10^9\,M^{-1}$, respectively (Figure 5.4 c and d). Here, the values of $\alpha.K_2$ were higher than K_1 for both RCT and SAL. It is known that antibodies preferentially bind free β-agonists in solution than β-agonists immobilized on sensor surfaces, and this resulted in lower K_1. In addition, although the kinetic analyses provided $K_1<K_2$, the sensitivity of the sensor surface was high (i.e., 5–10 ppt) in detecting β-agonist compounds. In summary, high sensitivity in detecting β-agonists

is related to low affinity constant of Ab to antigen immobilized on the sensor surface (K_1).

5.4.3 Selectivity study

To evaluate the selectivity of the sensor surface in multiple targets detection, I use cross-reactivity and multiple Ab injection experiments (Ab matrices test). For the cross-reactivity study, I compare the total resonance angle shifts of single antibody injection and mixed antibodies injection (target Ab in the presence of interfering Abs).

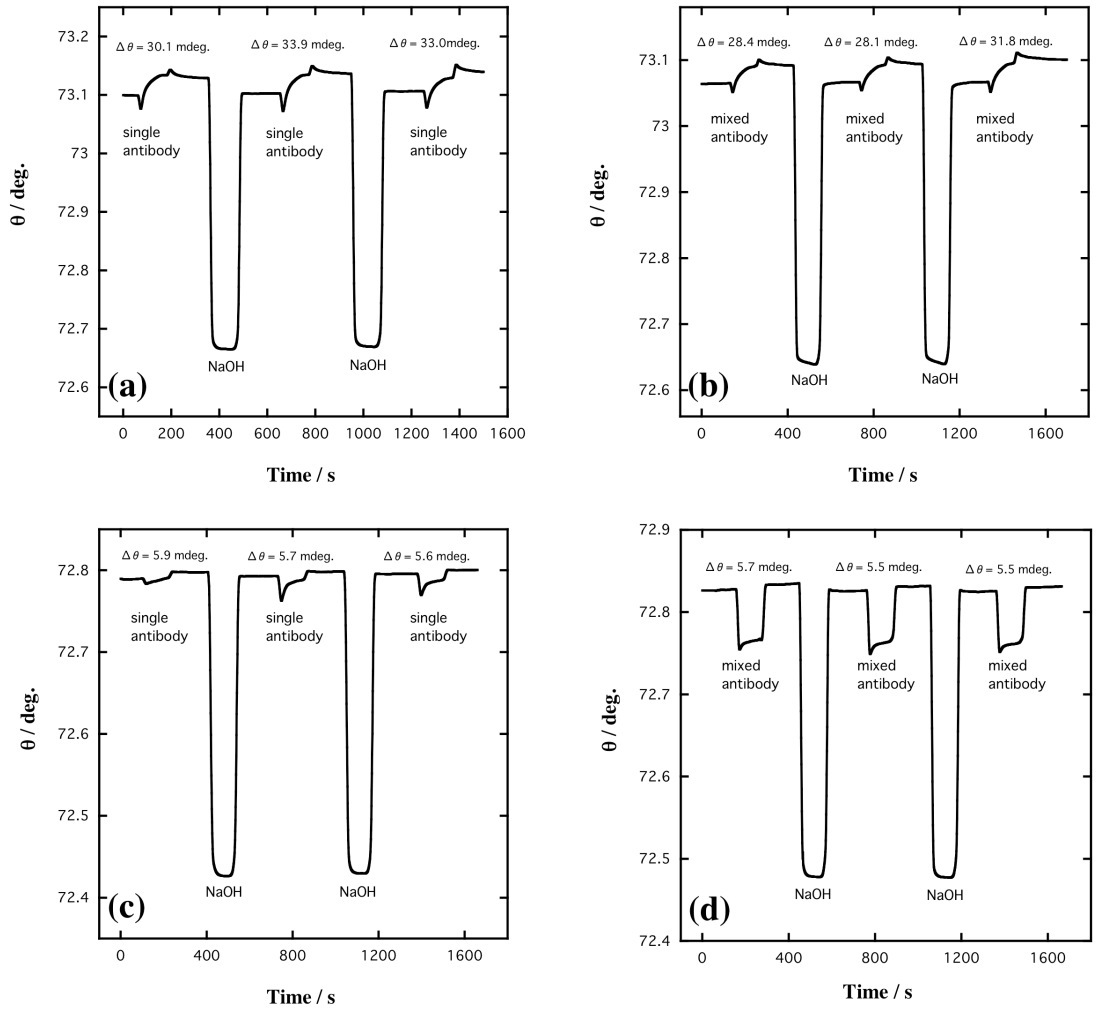

Figure 5.5 Selectivity study of β-agonist antibodies: RCT sensor surface against RCT Ab in the (a) absence and (b) presence of SAL Ab and CLB Ab; SAL sensor surface against SAL Ab in the (c) absence and (d) presence of RCT Ab and CLB Ab. The flow rate was 100μL min^{-1}.

Figure 5.5 (a-d) shows the effect of Ab matrices on the target analyte. For the RCT-based sensor surface, the cross-reactivity provided a confidence level of 91%, which was estimated from $\Delta\theta$ of 32.3 ± 1.6 mdeg and 29.4 ± 1.7 mdeg for single and mixed Ab injection (RCT Ab in the presence of CLB Ab and SAL Ab), respectively (Figure 5.5 a-b). For the SAL-based sensor surface, the selectivity study yielded 97% of confidence level, which was calculated from $\Delta\theta$ of 5.7 ± 0.1 mdeg and 5.5 ± 0.1 mdeg for single and mixed Ab injection, respectively (Figure 5.5 c-d). These results indicate the good selectivity of the sensor surfaces against similar β-agonists Ab.

In addition, I confirmed the selectivity study by injecting multiple Abs on the sensor surface (i.e., RCT, SAL, and CLB Ab injection to the RCT and SAL sensor surfaces (Figure 5.6). I find that the RCT sensor surface clearly distinguished between RCT Ab and other Abs (i.e., CLB and SAL) during the SPR injection with approximately 90% of confidence level. The same result is achieved from the SAL sensor surface selectivity test.

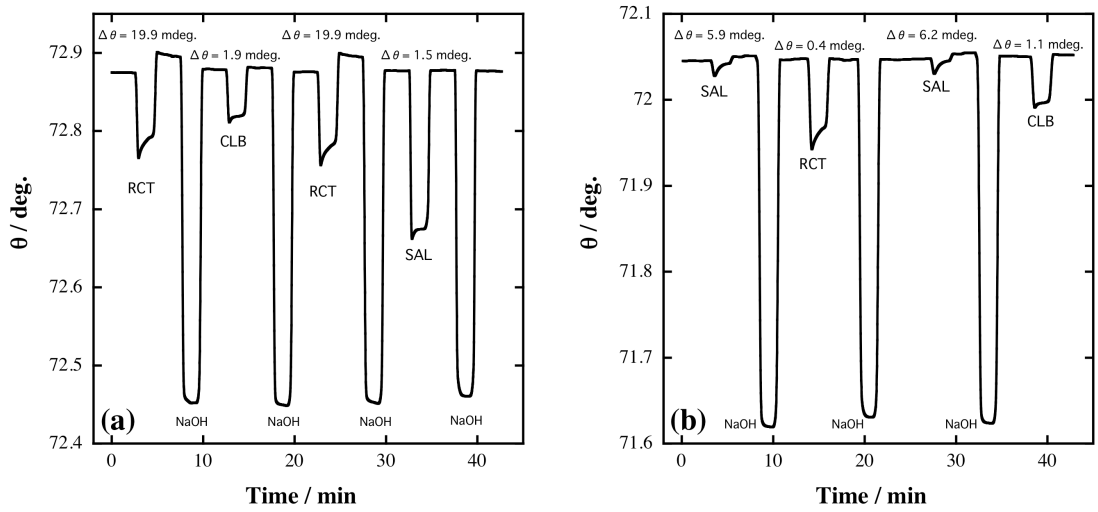

Figure 5.6 Selectivity studies of β-agonist sensor surfaces by multiple antibodies injection on: (a) RCT sensor surface and (b) SAL sensor surface. Flow rate was 100μL min^{-1}.

5.5 Summary

In this study, β-agonist protein conjugates covalently immobilized sensor surfaces are fabricated for detecting ractopamine and salbutamol. To covalently immobilize β-agonist protein conjugates onto the sensor surface, a succinimidyl-terminated propanethiol monolayer is used as a linker molecule. The indirect competitive inhibition immunoassay is used for β-agonists detection. It is found that the lowest LOD was 5–10 ppt, which indicated a remarkably high sensitivity compared to the results of past studies. Furthermore, this immunosurface could be regenerated by using 0.1 M sodium hydroxide. One immunosensing-regeneration cycle required only 600 s, and the same surface could be used for >100 immunoreactions even though the sensor surface fabricated using physical adsorption could be reused up to 30 times.

From the SPR responses, it is also found that one RCT–BSA conjugate reacted to one RCT Ab in 1 $\mu g \cdot mL^{-1}$ RCT Ab solution, while one SAL–HRP conjugate is associated with 0.07 SAL Ab. Consequently, SAL Ab shows a low affinity constant, K_1. From the kinetic analysis, a low K_1 reveals a high sensitivity of the detection process.

For multiple targets detection, I conduct a test using Ab analog matrices. It was found that the fabricated systems have a good selectivity at >90% of confidence level for specific Ab. Therefore, I conclude that the fabricated immunosensor surfaces are highly selective and sensitive.

5.6 References

[1] C. Crescenzi, S. Bayoudh, P.A.G. Cormack, T. Klein, K. Ensing, Anal. Chem. 73 (2001) 2171–2177.

[2] G. Brambilla, T. Cenci, F. Franconi, R. Galarini, A. Macrì, F. Rondoni, M. Strozzie, A. Loizzo, Toxicol. Lett. 114, (2000) 47–53.

[3] E. Shishani, S.C. Chai, S. Jamokha, G. Aznar, M.K. Hoffman, Anal. Chim. Acta 483 (2003) 137–145.

[4] M. Liu, B. Ning, L. Qu, Y. Peng, J. Dong, N. Gao, L. Liu, Z. Gao, Sens. Actuators B 161 (2012) 124–130.

[5] K-C. Lin, C-P. Hong, S-M. Chen, Sens. Actuators B 177 (2013) 428–436.

[6] X.Y. Zhang, Y.R. Gan, F.N. Zhao, J. Chromatogr. Sci. 42 (2004) 263–267.

[7] J-P. Antignac, P. Marchand, B. Le Bizec, F. Andre, J. Chromatogr., B: Anal. Technol. Biomed. Life Sci. (2002) 59–66.

[8] C. Li, Y-L. Wu, T. Yang, Y. Zhang, W-G. Huang-Fu, J. Chromatogr. A. 1217 (2010) 7873–7877.

[9] C. Juan, C. Igualada, F. Moragues, N. León, J. Manes, J. Chromatogr. A 1217 (2010) 6061–6068.

[10] J. Wu, X. Liu, Y. Peng, J. Pharmacol. Toxicol. Methods. 69 (2014) 211–216.

[11] L. He, Y. Su, Z. Zeng, Y. Liu, X. Huang, Anim. Sci. Technol. 132 (2007) 316–323.

[12] M.A. Cooper, Nat. Rev. 1 (2002) 515–528.

[13] M. Farré, E. Martinéz, J. Ramón, A. Navarro, J. Radjenovic, E. Mauriz, L. Lechuga, M.P. Marco, D. Barcelo, Anal. Bioanal. Chem. 388 (2007) 207–214.

[14] D.R. Shankaran, K.V. Gobi, N. Miura, Sens. Actuators B 121 (2007) 158–177.

[15] T. Kawaguchi, D.R. Shankaran, S.J. Kim, K. Matsumoto, K. Toko, N. Miura, Sens. Actuators B 133 (2008) 467–472.

[16] J. Homola, Chem. Rev. 108 (2) (2008) 462–493.

[17] M. Petz, Monatsh Chem. 140 (2009) 953–964.

[18] M. Piliarik, L. Parova, J. Homola, Biosens. Bioelectron. 24 (2009) 1399–1404.

[19] O. Torun, I.H. Boyaci, E. Temur, U. Tamer, Biosens. Bioelectron. 37 (2012) 53–60.

[20] K.V. Gobi, S.J. Kim, H. Tanaka, Y. Shoyama, N. Miura, Sens. Actuators B 123 (2007) 583–593.

[21] D-H. Tsai, F.W. DelRio, A.M. Keene, K.M. Tyner, R.I. MacKuspie, T.J. Cho, M.R. Zachariah, V.A. Hackley, Langmuir 27 (2011) 2464–2477.

[22] N. Soh, T. Tokudo, T. Watanabe, K. Mishima, T. Imato, T. Masadome, Y. Asano, S. Okutani, O. Niwa, S. Brown, Talanta 60 (2003) 733–745.

[23] S. Kumbhat, D.R. Shankaran, S.J. Kim, K.V. Gobi, V. Joshi, N. Miura, Chem. Lett. 235 (2006) 678–679.

[24] N. Miura, D.R. Shankaran, T. Kawaguchi, K. Matsumoto, K. Toko, Electrochemistry 75 (2007) 13–22.

[25] Suherman, K. Morita, T. Kawaguchi, 2014, in preparation.

[26] G. Sakai, K.Ogata, T. Uda, N. Miura, N. Yamazoe, Sens. Actuators B 49 (1998) 5–12.

[27] G. Sakai, S. Nakata, T. Uda, N. Miura, N. Yamazoe, Electrochim. Acta 44 (1999) 3849–3854.

Chapter 6

6.1 Summary and conclusion

The presence of potentially hazardous chemicals (e.g. pesticides, antibiotics, mycotoxins, precursors, infectious substances, etc.) in food products for human consumption remains a major concern in the world community due to its serious problems such as health consequences. Among these kinds of chemical substances, the family of β-adrenergic agonists (β-agonist) is found, which includes compounds such as clenbuterol, ractopamine, and salbutamol. These drugs are originally assigned for the treatment of respiratory illness due to its function as bronchodilator agent. However, because this compound promotes muscle growth and lipid degradation, farmers use these anabolic substances to achieve higher livestock production in order to increase the profit gain.

Recently illegal abuse of β-agonists for growth promoting purposes has been widely reported. Consequently, β-agonists have been banned for feeding animals all over the world. Therefore, the detection of these compounds present in food that could represent a risk to human health has taken great relevance. In this point of view, biosensors development becoming important topic that requires great attention from researchers to ensure the environmental quality such as food safety in all aspects. The promising surface plasmon resonance (SPR) biosensors with nano-materials development have been introduced to deal with environmental challenges. The knowledge about parameters controlling the stability, sensitivity and selectivity of sensor surface has been discussed.

In chapter 3, the surface concentration and succinimidyl group is significantly dependent on the concentration of dithiobis(succinimidyl) propionate (DSP) uses in fabricating the monolayer. Thus, the surface distribution and concentration of immobilized-antigen will be influenced as well. Consequently, high coverage of clenbuterol showed high affinity for clenbuterol antibody. However, the high affinity constant exhibited by the sensor surface is coupled with a low sensitivity. By contrast, lowest concentration of DSP solution (0.1 mM) uses in fabricating the immunosurface shows a detection sensitivity of 3 ppt–the highest reported sensitivity for clenbuterol.

In chapter 4, three types of alkanethiol compounds are used to examine the sensing performance in the detection of clenbuterol in order to get the best sensor surface for practical application. A dendrimer C_2-NTA sensor surface with lowest surface concentration (4.6×10^{-10} mol cm^{-2}) of thiol monolayer reveals highest sensitivity in the detection of clenbuterol than DSU and CEG_6 sensor surfaces (6.6×10^{-10} mol cm^{-2} and 8.5×10^{-10} mol), represented by limit of the detection (LOD) value at 10 ppt. Since the immobilized antigen to different thiols monolayer is almost the same (approximately 1.0×10^{-10} mol cm^{-2} for DSU, CEG_6 and C_2-NTA, respectively), the molecular structure of monolayers takes an important role in sensitivity of detection rather than surface concentration of monolayers. In the kinetics study, K_1 was 5.2×10^8, 9.7×10^8, and 4.8×10^8 M^{-1} for DSU, CEG_6 and C_2-NTA, respectively; and K_2 was $(18.1 \pm 7.9) \times 10^8$ M^{-1}. Correlating these kinetic parameters for the various thiol sensor surfaces to the detection of clenbuterol, a lower K_1 leads to better sensitivity (10 ppt). This result agrees with the finding of my

previous study of clenbuterol detection using a DSP alkanethiol monolayer (Chapter 3), in which a lower K_I corresponded to the highest sensitivity.

In chapter 5, the ractopamine–bovine serum albumin (RCT–BSA) and the salbutamol–horseradish peroxidase (SAL–HRP) conjugates are immobilized onto a succinimidyl propanethiol monolayer for sensor surface fabrication. The lowest detection limits for ractopamine and salbutamol were 10 ppt (10 $pg \cdot mL^{-1}$) and 5 ppt (5 $pg \cdot mL^{-1}$), respectively. In the kinetic study of the indirect competitive immunosensing inhibition, the affinity constant (K_I) of salbutamol antibody is smaller than the K_I of ractopamine antibody. Compare to a previous study of clenbuterol detection, it is concluded that the high K_I was coupled with low sensitivity. In the selectivity study, both immunosensor surfaces of ractopamine and salbutamol provided >90% of confidence level for the specific detection of β-agonist compounds. The fabrication of highly selective and sensitive sensor surfaces for detecting β-agonist compounds is confirmed. Furthermore, since the immunosurface can be regenerated by 0.1 M sodium hydroxide and one immunoreaction–regeneration takes only 1000 s, the same sensor surface could be reused for performing over 100 rapid immunoreaction.

From the experimental results on development of SPR biosensors through nano-control interface, the following points are concluded:

- Immunosensing of β-agonist compounds (clenbuterol, ractopamine, and salbutamol) is achieved using surface plasmon resonance.
- Surface concentration and orientation of succinimide group is significantly dependent on the concentration of dithiobis(succinimidyl) propionate

(DSP) used in fabricating the monolayer.

- Molecular structure of alkanethiol sensor surfaces determines sensitivity of an immunoassay.
- The best LOD is ranging from 3-10 ppt.
- One immunosensing-regeneration cycle requires only 1000 s.
- The same sensor surface could be used for >100 immunoreactions.
- From the kinetic analysis, a low affinity constant K_1 reveals a high sensitivity of the detection process.

Finally, the development of surface plasmon resonance biosensor using self-assembled monolayer for illegal compounds detection could open the further chances to answer the environmental issues.